University of Basel

Master Project

Towards a heralded multi-qubit parity measurement for superconducting qubits

Author:
Patrick Hümbeli
In the Group of Prof. C. Bruder

Supervisor:
Dr. Simon Nigg

August 22, 2016

Acknowledgements

I want to thank Prof. Christoph Bruder for giving me the opportunity of doing my Master Thesis in his group at the University of Basel and all his interest and trust in my project. I also wish to thank my supervisor Dr. Simon Nigg for providing a highly interesting topic for my project, for all his support, explanations and his patience with all my questions. I am glad that his door always has been open. I give a special thanks for all my colleagues and friends from the Department of Physics at the University Basel for creating a pleasant working atmosphere.

Contents

1 Introduction

Circuit quantum electrodynamics (cQED) has established itself to be a promising candidate for quantum information processing. Superconducting qubits can be coupled to a cavity to entangle the qubit states with the bosonic state of the cavity. Govia et al. [2] propose a high fidelity qubit parity measurement that is supposed to be a quantum non-demolition measurement (QND). When we first simulated the system that was proposed, we obtained qubit dephasing, which was induced by the measurement, and a significant decrease in the measurement fidelity for imperfect detection. In this project we try to understand the back-action of the measurement on the qubit states, identify the origin of the dephasing and quantify it. Furthermore we show how imperfect detection influences the measurement outcome and in the end we propose a way to improve the qubit coherence and measurement fidelity. Sections 1.1 to 1.5 are taken from my Master Projektarbeit [18]. For a better understanding of the rest of this thesis we will briefly review them.

1.1 Parity measurement and error correction

This section is a short discussion about the usefulness of parity measurement in quantum information processing. For illustration we use a simple example for the detection stage of quantum error correction (QEC). The unavoidable presence of noise in quantum systems leads to errors that have to be corrected. The origin of noise in quantum systems is manifold and especially the measurement can cause decoherence and other errors. To protect quantum information against noise there are QEC codes which encode the quantum state in a special way to make it resilient against noise. To recover the original state, it has to be decoded by the quantum error correction code again. [5]
One of the simplest QEC codes is the repetition code. The qubit states are represented in Z-basis where the following relations hold:

$$\sigma^z|0\rangle = -|0\rangle \tag{1}$$

$$\sigma^z|1\rangle = +|1\rangle \tag{2}$$

In the repetition code a logical qubit state $|0\rangle_L$ or $|1\rangle_L$ that contains the informations to be processed is represented by a multi qubit state. A way this code might look like is

$$|0\rangle_L = |0\rangle^{\otimes N}, \tag{3}$$

$$|1\rangle_L = |1\rangle^{\otimes N}, \tag{4}$$

where N is the number of physical qubits to encode the logical qubit.
The power of quantum computing comes from the usage of superpostions of qubit states that have for example the form

$$|\psi\rangle = a|0\rangle_L + b|1\rangle_L. \tag{5}$$

A qubit flip is a possible error that can be corrected with the repetition code. Because of their finite relaxation time and environmental influence quantum bits can spontaneously flip from $|0\rangle$ to $|1\rangle$ or vice versa. A way to find such a flip is to measure every qubit. But in this case one would destroy the superposition state because the measurement would project the superposition $|\psi\rangle$ onto the subspace that has been measured. To avoid this, one can use multiple parity measurements instead to extract only the required information, i.e. the location of the qubit flip. The operator $\sigma_i^z\sigma_{i+1}^z$ with $i, i+1 \in [1, N-1]$ measures the parity of the neighbouring qubits i and $i+1$: Since the eigenvalues of σ^z corresponding to $|0\rangle$ and $|1\rangle$ are 1 or -1 the eigenvalue of $\sigma_i^z\sigma_{i+1}^z$ is always 1 if the two neighbouring qubits are in the same state and therefore they have even parity. If they are not in the same state, $\sigma_i^z\sigma_{i+1}^z$ has the eigenvalue -1 and they have odd parity. The advantage of this method is that with it, one gains only enough information to compare the qubits. For example for even parity we can not distinguish whether the neighbouring qubits are both up or down. Therefore the measurement of $\sigma_i^z\sigma_{i+1}^z$ projects the state onto a subspace of given parity and preserves the superposition of Eq. (5).
In the following example the function of such a correction can be easily understood. We start with an initial state $|\psi\rangle = a|0\rangle_L + b|1\rangle_L$ and choose the number of physical qubits to be $N = 4$,

$$|\psi\rangle = a|0000\rangle + b|1111\rangle. \tag{6}$$

If an error occurs and for example the second qubit flips $|\psi\rangle$ changes to

$$|\psi\rangle = a|0100\rangle + b|1011\rangle. \tag{7}$$

The flipped qubit can be detected by measuring $\sigma_i^z \sigma_{i+1}^z$ on every pair of nearest neighbour qubits in this state.

$$\sigma_1^z \sigma_2^z (a|0100\rangle + b|1011\rangle) = -|\psi\rangle \tag{8}$$
$$\sigma_2^z \sigma_3^z (a|0100\rangle + b|1011\rangle) = -|\psi\rangle \tag{9}$$
$$\sigma_3^z \sigma_4^z (a|0100\rangle + b|1011\rangle) = +|\psi\rangle \tag{10}$$

The eigenvalues of $\sigma_1^z \sigma_2^z$ and $\sigma_2^z \sigma_3^z$ are -1 and the eigenvalue of $\sigma_3^z \sigma_4^z$ is $+1$. Therefore the error can be localized because eigenvalue -1 stands for odd parity. So qubit 1 and 2 and qubit 2 and 3 are different. But qubit 3 and 4 are equal. So it has to be qubit 2 that flipped.

One has to keep in mind that this was just an easy example of what parity measurement is useful for and this simple example is just a special case of what is known as "stabilizer QEC". [12] Parity measurements are a part of many promising QEC codes and there are many other applications for this kind of measurement. Other possible errors that can occur in qubit systems are phase flips in σ^z and σ^y direction. An error in z-direction will cause the error $|0\rangle \leftrightarrow |0\rangle$ and $|1\rangle \leftrightarrow -|1\rangle$. And due to the fact that $\sigma^x \sigma^y = i\sigma^y$, a σ^y error is a qubit flip and a phase flip at the same time. A possible quantum error correction code was developed by Shore [11] where 9 qubits are needed to encode a logical qubit. This code is sufficient to correct for a single qubit flip, a single phase flip or for both at the same time. An other more formal description of how many qubits are needed at least to successfully correct single errors, was made by Hamming for classical error correction and is known as the quantum Hamming Bound. It can also be applied on quantum error correction which was shown done by Gottesman. [12] If we encode a logical qubit in N physical qubits, if j errors occur, there are $\binom{N}{j}$ possible locations where the errors can occur. Every of these physical qubits can encounter 3 possible errors (X, Y or Z) which leads to the total number of errors that can occur,

$$\sum_{j=0}^{N} \binom{N}{j} 3^j. \tag{11}$$

All these errors must fit into the 2^N-dimensional subspace of the physical qubits where we have to keep 2 dimensions free for the actual logical qubit. This leads to the inequality

$$\sum_{j=0}^{N} \binom{N}{j} 3^j \leq 2^{N-1}. \tag{12}$$

If only one error occurs at a time the inequality reads

$$(1 + 3N) \leq 2^{N-1} \tag{13}$$

and we can see that it is fulfilled for $N \geq 5$. This means there is no code which encodes one logical qubit in fewer than five physical qubits such that it is protected against all possible single qubit error.

1.2 Scalable two and four qubit measurements

In the publications "High-fidelity qubit measurement with a microwave photon counter" [1] and "Scalable two and four qubit measurement" [2] Govia et al. proposed a promising way of multi qubit parity measurement. Section 1.2 will summarise the main concept of their proposal.

1.2.1 A short review of the Jaynes-Cummings model

The system that was proposed by Govia et al. [2] can be described with the Jaynes-Cummings model and its dispersive regime. The Jaynes-Cummings Hamiltonian has the form

$$H = \frac{\omega_Q}{2}\sigma^z + \omega_C a^\dagger a + g(a\sigma^+ + a^\dagger\sigma^-).$$

It describes the dipolar interaction of a two-level-system (in this case a qubit) with the electromagnetic field of a cavity. σ^z is the Pauli operator in the eigenbasis of the qubit. a and $a^\dagger$ are the photon annihilation and creation operators of the cavity mode. σ^+ and σ^- are the raising and lowering operators of the qubit. ω_Q is the frequency of the qubit, ω_C is the cavity frequency and g is the coupling strength between the qubit and the cavity.
The dispersive regime where $|\delta| = |\omega_Q - \omega_C|$ and $|\delta| \gg g$ is of interest, because in this regime the single photon energy exchange between the qubit an the cavity field is suppressed in consequence of energy conservation. But higher order processes of virtual photon exchange lead to energy shifts in the qubit and the cavity. In the dispersive regime the Jaynes-Cummings Hamiltonian takes the form

$$H_{disp} = \omega_C a^\dagger a + \frac{\omega_Q + \chi}{2}\sigma^z + \chi a^\dagger a\sigma^z, \tag{14}$$

where $\chi = \frac{g^2}{\omega_Q - \omega_C}$ is the dispersive shift. In this limit, one can obtain (the second term on the right hand side) a shift of the qubit frequency by χ, the so called cavity (single-mode) Lamb shift. And much more important the third term on the right hand side can be interpreted as a qubit state dependent cavity frequency shift. Therefore the qubit state can become entangled with the cavity state. This fact can be used to measure the qubit by measuring the cavity.
This expression can be generalized to an N qubit system which is the starting point of the publication by Govia et al. [2]

$$H = \omega_C a^\dagger a + \sum_{n=1}^{N}\left(\chi_n a^\dagger a + \frac{\omega_n + \chi_n}{2}\right)\sigma_n^z \tag{15}$$

1.3 Proposal of Govia et al.

The parity measurement setup that was proposed by Govia et al. [2] is illustrated in Fig. 1. The superconducting qubits Q_i are coupled to a driven cavity which can be read out with a Josephson Photomultiplier (JPM). The JPM is better known as a phase qubit or a current biased Josephson junction. The parity measurement is split into three stages. The driving stage, the measurement stage and the reset stage. The main interest of this project are the second and the third stage, the measurement and the reset. But for a better understanding it is also necessary to go through the main points of the drive stage.

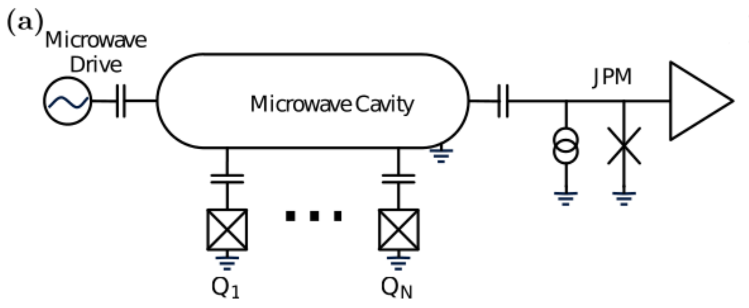

Figure 1: N qubits coupled to a driven cavity that can be read out by a Josephson Photomultiplier (JPM). (picture taken from [2]

)

1.3.1 Drive stage

The goal of this stage is to entangle the qubit state with the cavity. By driving the cavity with $H_D = A(t)(a^\dagger + a)$ the Hamiltonian takes the form

$$H = A(t)(a^\dagger + a) + \omega_C a^\dagger a + \sum_{n=1}^{N} \left(\chi_{Q_n} a^\dagger a + \frac{\omega_{Q_n} + \chi_{Q_n}}{2} \right) \sigma_n^z, \tag{16}$$

with the drive amplitude $A(t) = a_0 \cos(\omega_D t)$. For simplicity one can reduce the whole system of qubits coupled to a cavity to a system where the cavity has qubit dependent shifts. The reduced cavity Hamiltonian,

$$H_C = A(t)(a^\dagger + a) + \tilde{\omega}_C a^\dagger a \tag{17}$$

can be seen as a single mode oscillator with a rescaled resonance frequency $\tilde{\omega}_C = \omega_C + \tilde{\chi}_Q$, where $\tilde{\chi}_Q$ is a qubit state dependent dispersive shift which depends on the number of qubits coupled to the cavity and the states in which the qubits are. For a single qubit coupled to the cavity $\tilde{\chi}_Q = s\chi_Q$ with $s = \pm 1$ representing the eigenvalue of σ^z. Since the publication of Govia et al. [2] is about parity measurement, there have to be at least two qubits coupled to the cavity. Extending this model with a second qubit with the same dispersive shift χ_Q, the total dispersive shift on the cavity is $\tilde{\chi}_Q = \pm 2\chi_Q$ for even qubit parity and $\tilde{\chi}_Q = 0$ for odd qubit parity as illustrated in Figure 2.
By driving the cavity at the frequency ω_D one obtains two different cavity state evolutions depending on the qubit parity. The odd qubit parity state leads to the cavity state $|\alpha_O\rangle$ and the even parity state to $|\alpha_E\rangle$. Applying a drive of the form $A(t) = a_0 \cos(\omega_D t)$ will lead to the cavity amplitudes (Derivation can be found in Appendices Section 10.1.)

$$|\alpha_E|^2 = \left(\frac{a_0}{\Delta_D} \right)^2 \frac{1 - \cos(\Delta_D t)}{2} \tag{18}$$

and

$$|\alpha_O|^2 = \left(\frac{a_0}{2} t \right)^2, \tag{19}$$

with $\Delta_D = \tilde{\omega}_C - \omega_D$. The cavity is put in a high amplitude coherent state if the qubit parity is odd. If it is even the cavity is periodically oscillating back into the vacuum state. Setting the drive equal to the bare cavity frequency $\omega_D = \omega_C$ leads to $\Delta_D = 2\chi_Q$. In this case $\alpha_E = 0$ for $t = \pi/\chi_Q$. Therefore the state of the system takes the form $P_{odd}|\psi\rangle|\alpha\rangle + P_{even}|\psi\rangle|0\rangle$. Where P_{odd} and P_{even} are the projection operators on the odd and the even qubit subspaces. This can later be used to distinguish the even or odd parity states by measuring the cavity at the time $t = \pi/\chi_Q$. If there are photons that can be detected the qubits have odd parity and if the cavity is dark the qubits are in even parity.
In the $N > 2$ qubits case we can no longer perform parity measurement with a single frequency cavity drive, because the degeneracy of the cavity frequency shifts splits. For a system with four qubits the odd parity produces dispersive shifts of $\tilde{\chi}_Q = \pm 2\chi_Q$ and the even parity gives $\tilde{\chi}_Q = \pm 4\chi_Q$ and $\tilde{\chi}_Q = 0$. This is illustrated in Figure 2.

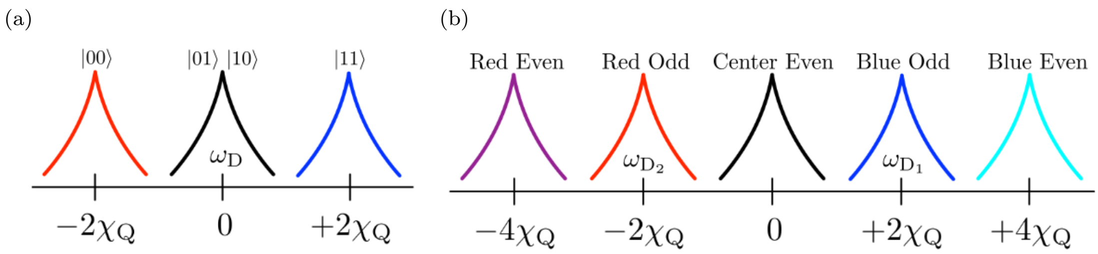

Figure 2: Qubit dispersive shifts for 2 and 4 qubits: (a) 2 qubit dispersive shift. (b) 4 qubit dispersive shift. Red Even corresponds to $|0000\rangle$, Red Odd to $|0001\rangle$, Center Even to $|0011\rangle$, Blue Odd to $|0111\rangle$ and Blue Even to $|1111\rangle$. Each with every possible permutation of the state. [2]

So the drive amplitude in the N qubit case takes the form

$$A(t) = a_0 \sum_i \cos(\omega_{D_i} t), \tag{20}$$

where $\omega_{D_i} = \omega_C + \tilde{\chi}_{Q_i}$ are the dispersively shifted cavity frequencies for the odd-parity subspaces. There are several other ways to entangle qubit states with cavity states as in for example [13].

1.3.2 Measurement stage

After the desired entangled state has been prepared in the drive stage, the drive amplitude $A(t)$ is switched off. At this point we want to measure the cavity occupation to distinguish whether the qubits are in an even or odd parity state. Govia et al. propose in their publication [1] to measure the cavity occupation by a Josephson junction that is biased with a current I_b which is also known under the name of "phase qubit".

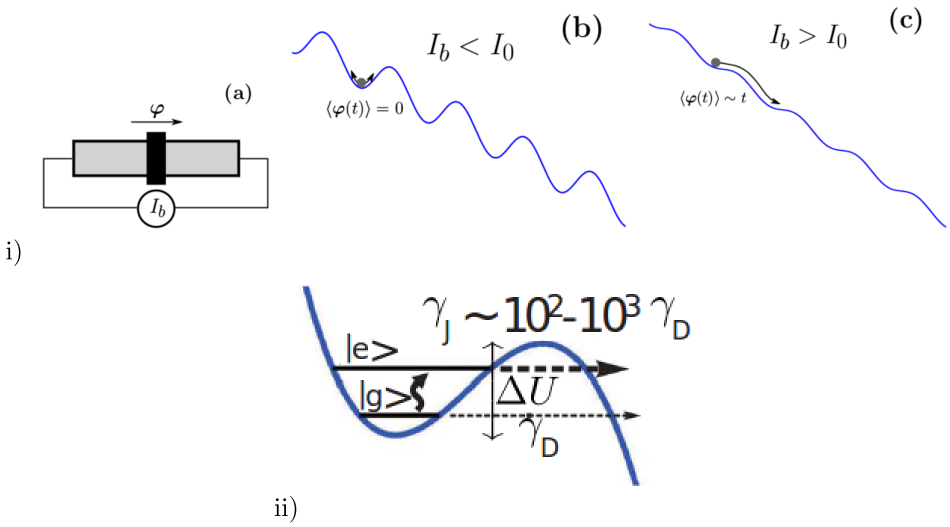

Figure 3: i): (a) A current biased Josephson junction with the superconducting phase difference φ and the bias current I_b. (b) and (c) show the potential energy dependent on the bias current I_b compared to the critical current I_0 [3]
ii): Magnified potential energy in the regime $I_b < I_0$ during the measurement. The energy gap between $|g\rangle$ and $|e\rangle$ can be tuned by the bias current I_b [1]

For the measurement the phase qubit is driven in the regime $I_b < I_0$. The bias current also tunes the energy separation of the ground $|1\rangle$ and the first excited state $|2\rangle$. Their energy gap is tuned on resonance to the cavity frequency ω_C so the coupling strength is maximal and a photon can be absorbed from the junction to get excited into the state $|2\rangle$. If the phase qubit is correctly tuned, the probability to tunnel to the continuum is much bigger if the qubit is excited. For simplicity we neglect the tunnel amplitude γ_D completely. The tunnelling to the continuum finally produces a large and easily measurable voltage of order $2\Delta/e$ where Δ is the superconducting gap and e is the charge of an electron [1]. For the rest of this project we refer to this detector as the Josephson Photon Multiplier (JPM) as proposed in Ref. [1].

1.3.3 Reset stage

In the reset stage the cavity is removed to the vacuum state to disentangle the qubit states from the cavity states. This can be achieved through cavity decay or by actively resetting the cavity. The cavity decay has a too long time scale which is not viable for effective quantum information processing and the active resetting can lead to errors because the cavity can be perturbed by the back action of the JPM measurement. Since a coherent state $|\alpha\rangle$ is an eigenstate of the annihilation operator and α is its eigenvalue we should be able to gain information about the phase of the cavity through the cavity decay via the JPM if the cavity state after the photon decay is still coherent. Given that we are not able to gain information about the cavity phase and amplitude that are contained in α through the photon detection via the JPM, the cavity is not a perfectly coherent state anymore after the measurement. Furthermore there is no existing displacement operator $D(\beta)$ that maps the cavity exactly back to vacuum. Govia et al. proposed that there might be a different decay operator that describes the mechanism of the cavity decay through the JPM more accurate. Their proposal was an approximation of the cavity-JPM dynamics by the operator $B = \sum_{n=0}^{\infty} |n-1\rangle\langle n|$. [1], [14] In Appendix 10.10 is a short discussion about this new operator. And we could show that the loss of coherency is much bigger if we approximate the cavity-JPM interaction with the effective decay rate κ_{eff} and this new B-operator than in the actual full-system numerics. Furthermore the effect is negligibly small and for the rest of this thesis we will use the normal annihilation operator a for the effective model where we neglect any loss of coherence. A much more important and subtle effect of the coupling of the cavity to the qubits is that different parity subspaces lead to different phases in the cavity. So if the time evolution starts in an initial state of the form $|\psi\rangle = |\text{qubit}\rangle \otimes |\text{cavity}\rangle$ through the time evolution the qubit and the cavity subspace will not be separable anymore because the cavity gets entangled with the parity subspaces and we will end up with a state of the form $|\psi\rangle = |q_1\rangle \otimes |c_1\rangle + |q_2\rangle \otimes |c_2\rangle + \cdots$, where $|q_1\rangle$ and $|c_i\rangle$ are different qubit and cavity states. So we will reset the cavity to vacuum after the measurement to disentangle the qubits from the cavity.

1.4 Simulation of the System

As a first step in this project we numerically solved the master equation of the whole qubit-cavity-JPM system during the measurement stage. This means that the Hamiltonian contains the terms for the qubits dispersively coupled to the cavity and for the cavity coupled to the JPM by Jaynes-Cummings interaction. The whole system is illustrated in Figure 4.

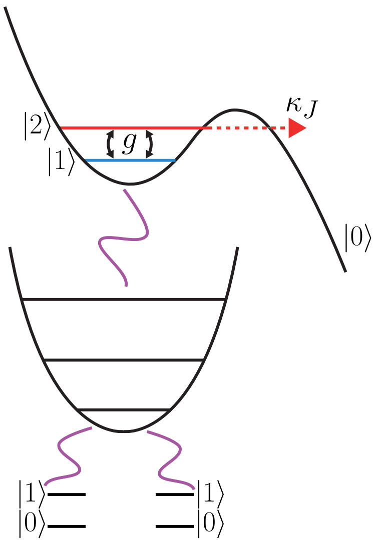

Figure 4: Full system: Two qubits coupled dispersively to the cavity, which is coupled to the JPM via Jaynes-Cummings-Interaction. [2]

For the rest of this thesis we will neglect all decay channels other than the decay of the JPM from its excited state $|2\rangle$ to its continuum state $|0\rangle$. In reality there will be imperfections as for instance an imperfect cavity that looses photons directly to its environment and qubits that can spontaneously decay from their excited state to the ground state. But in a real system it will be necessary to improve these parts of the system against errors but the decay channel κ_J of the JPM will always be necessary to extract information from our system. Therefore it is crucial to understand this decay channel and the back-action of such a measurement on the system.

For two qubits the Hamiltonian has the form

$$H = (\chi_{Q_1}\sigma_1^z + \chi_{Q_2}\sigma_2^z)a^\dagger a + g(a|1\rangle\langle 2| + a^\dagger|2\rangle\langle 1|) + \omega_1|1\rangle\langle 1| + \omega_2|2\rangle\langle 2| + \omega_C a^\dagger a. \tag{21}$$

Where χ_{Q_i} are again the dispersive shifts of the qubits, $a^\dagger$ and a the ladder operators of the cavity, $|1\rangle$ and $|2\rangle$ the ground and the excited state of the JPM and g is the coupling of the cavity with the JPM. Here, the measurement of a photon can be regarded as a decay of the excited state of the JPM $|2\rangle$ to a continuum which is represented by the state $|0\rangle$ with the decay rate κ_J. To start in the most simple system we assume that there is no thermal excitation from the continuum back to the state $|2\rangle$. The master equation then has the form

$$\dot{\rho} = [H, \rho] + \kappa_J D\left[|2\rangle\langle 0|\right]. \tag{22}$$

with the Lindblad dissipator

$$D\left[O\right]\rho = \frac{1}{2}\left(2O\rho O^\dagger - O^\dagger O\rho - \rho O^\dagger O\right). \tag{23}$$

If we solve this system numerically shows it shows that the measurement leads to intra-parity subspace dephasing. This means that we get a phase between the same parity states. In Figure 5 one can see that the expectation value $\langle\sigma_1^x \otimes \sigma_2^x\rangle$, which quantifies the intra-parity subspace coherence for two qubits, decays fast in time and does not return to one again. This means during the measurement something happened that affected the qubit coherence.

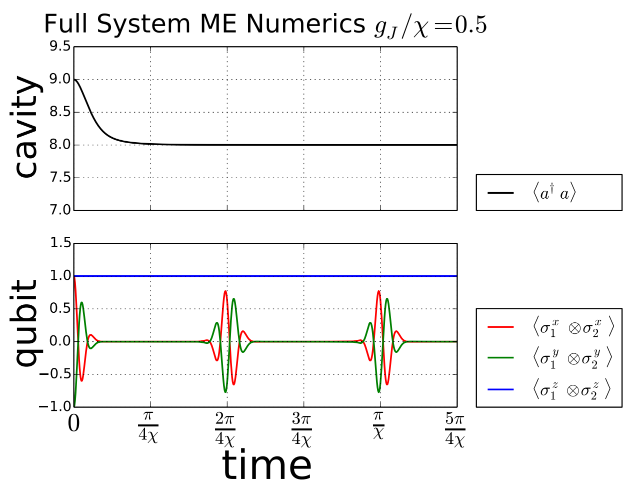

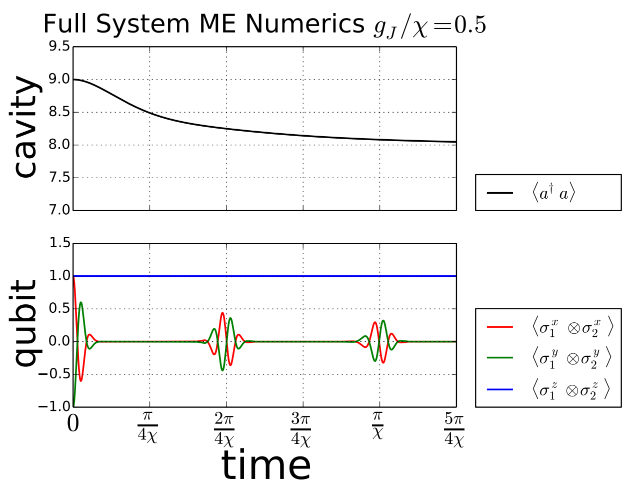

Figure 5: Cavity decay and dephasing of the full system with different cavity decay rate at fixed $\alpha = 3$ and $\kappa/g_J = 100$;
(a) For $g_J/\chi = 2.0$ the cavity decay is fast compared to the revival frequency and the first and the second revival are equal height.
(b) For $g_J/\chi = 0.5$ the cavity decay is slow compared to the revival frequency and the qubit revivals decrease so they are not equal height.

For simplicity we chose $\chi_1 = \chi_2 = \chi$ and the qubit is initially in the even state $|\psi_O\rangle = 1/\sqrt{2}\,(|00\rangle + |11\rangle)$. The cavity amplitude is $\alpha = 3$. The value $\kappa_J/g_J = 100$ represents that the excited JPM decays fast compared to the coupling strength of the cavity to the JPM. The parameter χ is responsible for the frequency of the revival which occur at multiples of $t_{\mathrm{rev}} = \pi/2\chi$. If $g_J > \chi$ and $\kappa_J \gg g_J$ the photon decays before the first revival occurs and after the decay the qubit decoherence stops. If $g_J < \chi$ and $\kappa_J \gg g_J$ the photon decay takes on average longer than the first revival and one can see that the qubit decoheres further after the first revival.
Investigating these numerical results we come to three main conclusions that will be further discussed in this project:

- The measurement leads to an intra-parity subspace dephasing. Which can directly be seen through the decay of the expectation value $\langle\sigma_1^x \otimes \sigma_2^x\rangle$ and its maxima not returning to one. We later also refer to this returning maxima as revival of the coherence.
- The decay of the cavity stops after the loss of one photon which is a consequence of the JPM decaying to the state $|0\rangle$ and not having the possibility to return into its initial state $|1\rangle$ which can physically be understood that on a time scale that is much longer than the photon decay, the phase of the JPM is trapped in the continuum state $|0\rangle$.
- The decay of the revival stops after the decay of the photon.

- We can see that the expectation value $\langle\sigma_1^z \otimes \sigma_2^z\rangle$ does not change during the measurement. So the parity measurement itself is not affected by the dephasing of the qubits and is therefore QND.

At last we have to keep in mind using here an even initial state does not exactly represent the real problem. In the measurement stage (Section 1.3.1) we have seen that in the even parity case for two qubits the cavity is oscillating back to the vacuum state. So we would not be able to measure a photon in this case because the cavity is empty. But to simplify the problem we used $\chi_1 = \chi_2 = \chi$. This would lead to a trivial time evolution of the odd qubit parity state. Since we are mainly interested in the measurement stage we can neglect the driving stage at this point and focus on the dephasing caused by the measurement. Later we generalize to the $N > 2$ qubit case, where the odd parity states are not expected to evolve trivially even for $\chi_1 = \chi_2 = \chi$.
In Fig. 6 the cavity amplitudes and phases are plotted for different times in the rotating frame of the bare cavity frequency ω_C. Initially the qubit and the cavity states are separable and can be written as a product state $|\text{qubit}\rangle \otimes |\text{cavity}\rangle$. After the time evolution begins the cavity starts to split in two different states with different phases that are entangled with one of the two given qubit states $|00\rangle$ and $|11\rangle$. Later in this work we will describe this behaviour more exactly. At the moment it primarily visualizes why the qubits show the revival behaviour and why the X and Y expectation values go to zero between the revival times. The cavity states only overlap again at multiples of the revival time $t_{\text{rev}} = \pi/2\chi$ and the expectation value

$$\langle\sigma_1^x \otimes \sigma_2^x\rangle = \langle\psi|\sigma_1^x \otimes \sigma_2^x|\psi\rangle = (\langle 11| \otimes \langle\alpha_1| + \langle 00| \otimes \langle\alpha_2|)(\sigma_1^x \otimes \sigma_2^x)(|11\rangle \otimes |\alpha_1\rangle + |00\rangle \otimes |\alpha_2\rangle) \tag{24}$$

depends on the overlap of the cavity states $\langle\alpha_1|\alpha_2\rangle$ which is close to zero, except at the revival times t_{rev} when the cavity states overlap again.

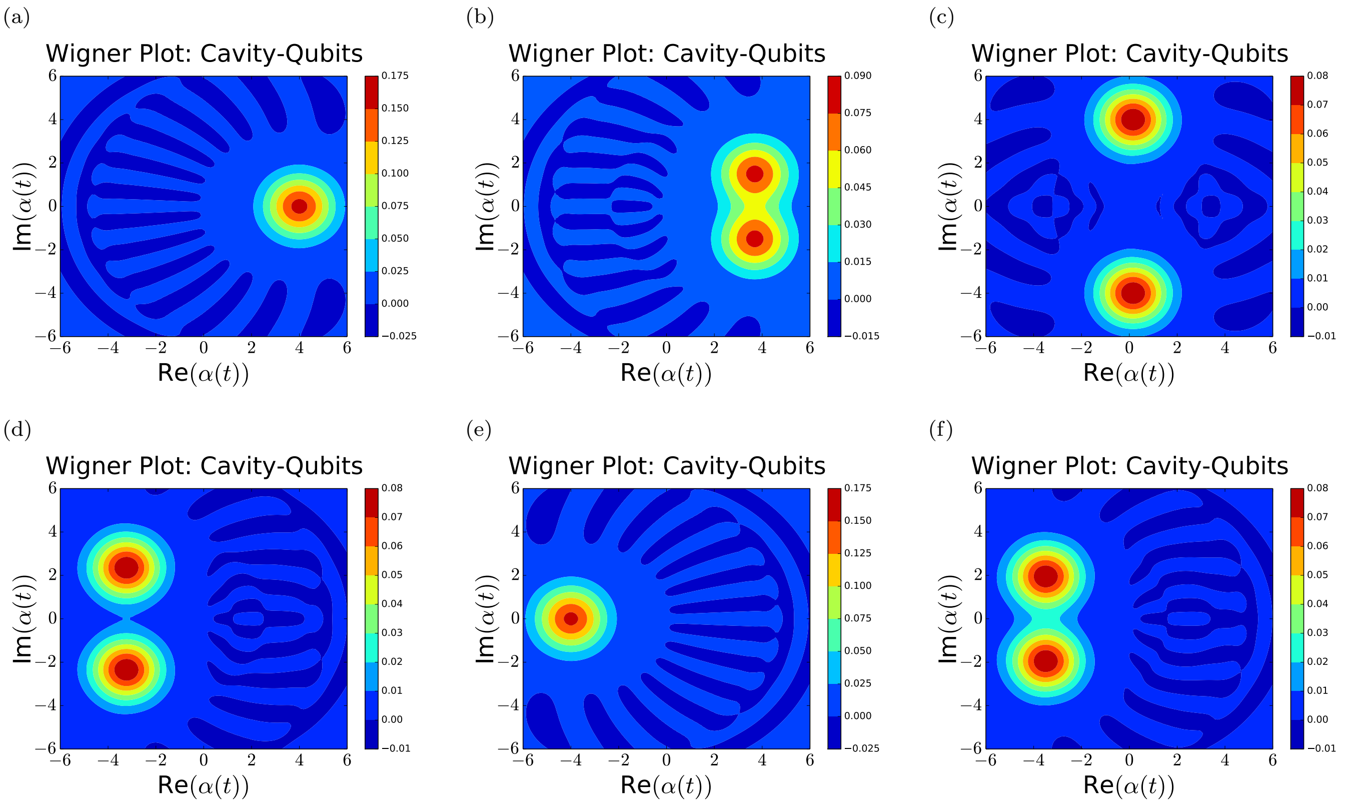

Figure 6: Wigner function of a cavity coupled dispersively to the qubit state $1/\sqrt{2}(|00\rangle + |11\rangle)$. The initial state of the cavity is $|\alpha\rangle$ with the amplitude $\alpha = 4$.
(a) initial state at $t = 0$, (b) cavity states start separating after start, (c) At $t = \pi/4\chi$ the states are maximally separated (d) before the first revival the cavity states start overlapping again, (e) at the revival $t = \pi/2\chi$ the cavity states overlap again perfectly (f) after the revival they separate again.

1.5 The property of Quantum Non-Demolition

Govia et al. propose this parity measurement to be quantum non-demolition (QND) [2] which is necessary for effective quantum information processing. Otherwise the measurement would change the state or even destroy it and following measurements would be negatively influenced by the measurement.

T. C. Ralph et al. give a definition for QND measurement [4]:

"1. The measurement result should be correctly correlated with the state of the input. For example, if the input state is an eigenstate of the observable being measured, then in an ideal QND measure- ment the measurement outcome corresponding to this eigenstate should occur with certainty.
2. The measurement should not alter the observable being measured. For example, an eigenstate should be left in the same eigenstate by the measurement.
3. Repeated measurements should give the same result. In other words, the QND measurement should be a good quantum state preparation device, and should output the eigenstate corresponding to the measurement result."

QND roughly means that a measurement will lead repeatedly to the same result. In the qubit parity measurement it means that if one measures an even parity state, one would repeatedly get the same result. So far the proposal of Govia et al. [2] seems to be right because the expectation value $\langle \sigma_1^z \sigma_2^z \rangle$ does not change over time. But in the simulations one can see that there is a decay in the expectation value of $\sigma_1^x \sigma_2^x$ which is a consequence of an intra-parity subspace dephasing caused by the measurement. The decay in the expectation value $\langle \sigma_1^x \sigma_2^x \rangle$ in the simulation is an expression of a randomization of the relative phase between components of the same parity subspace. Importantly QND measurement is not sufficient for QEC because a perturbation of the state during the measurement, even if the parity measurement is unaffected, will lead to errors in quantum information processing. This is why we demand a stronger form of QNDness. We need eigenstate preserving QND (EP-QND) measurement. [6] The parity observable $Q = Q_+ - Q_-$ applied on an even parity qubit state $|\text{even}\rangle = 1/\sqrt{2}(|11\rangle + |00\rangle)$ always leads to the measurement outcome +1. This is a consequence of the QNDness of the measurement. But since the subspace $|\text{even}\rangle$ of our measurement Q has a higher dimension than 1 it is still possible to have intra subspace rotations and this is what our simulations show. The initial state has changed from $1/\sqrt{2}(|11\rangle + |00\rangle$ to $1/\sqrt{2}(|11\rangle + e^{i\phi_2}|00\rangle$. Therefore the state gained some intra parity subspace phase which do not affect the measurement outcome but the state itself.
The aim of this work will be to extend the measurement procedure of Govia et al. [1] to achieve EP-QND, where the parity states are unaffected by the measurement $Q|\text{even}\rangle = +|\text{even}\rangle$ and $Q|\text{odd}\rangle = -|\text{odd}\rangle$. This will be crucial for further measurements and use of the qubits in a quantum information process and it will not be sufficient to measure parity properly while corrupting the state in an other way.
An important point about the measurement via the JPM is, that the measurement scheme implies that the only information that is extracted by the photon decay is whether the cavity is bright or not. And there is no phase information available through the JPM. But just because there is no detection of the phase does not mean that the information is not contained in the photon. Therefore the measurement via the JPM seems to extract more information than needed from the system and therefore there is not only a projection of the full state on its parity subspace. Also the phase information is projected onto the state. Elucidating the effect that this additional information has on the measurement, will be part of this thesis.

1.6 Content of this Master thesis

To gain a better understanding of the system that Govia et al. proposed [2], we will investigate it step by step. In a first section we will analyse a system where qubits are coupled to a cavity with and without photon decay to develop some intuition about the back-action of the photon decay. In a second step we derive an effective model for a cavity coupled to the JPM which will allow us to make analytic progress. Since in the end we will be interested in single photon detection and the back-action of such a single measurement on the system, we change to the quantum trajectory picture and describe our system with this approach. To gain some intuition about the differences of the master equation and the quantum trajectory pictures we study qubits that are coupled to cavities with and without leakage in both pictures. We will describe and compare them. And after that we will numerically solve the whole system in the quantum trajectory picture and compare these numerical results with our analytical models that have been developed for the qubit-cavity and the cavity-JPM subsystems. After that we are able to describe the back-action of the measurement on our system, we will investigate the last stage of Govias protocol [2], the reset stage. Since the measurement back-action has a big influence on the initial state, we will also propose a way to improve the fidelity of such a measurement and reduce the corruption of the initial state through the back-action, by dynamically decoupling the dispersive part of the Hamiltonian.

2 Analysis of the qubit-cavity interaction

In this section we would like to investigate how the qubits and the cavity interact and how the cavity decay influences the qubit coherence. This section already was part of the Master Projektarbeit [18]. For reasons of completeness and readability it will be reviewed here.

2.1 Time evolution without cavity decay

First we look at the time evolution of a qubit state coupled to a cavity without any loss of photons. This system is a vast simplification and not really physical but it will be the first step to understand intra subspace dephasing. The Hamiltonian in equation (16) can be simplified by putting it into a rotating frame of the bare qubit and cavity frequencies. In the appendices section 10.2 is a brief repetition for rotating frames and unitairy transformation.
The non trivial part of the time evolution is caused by the dispersive Hamiltonian

$$H = \sum_n^N \chi_{Q_n} a^\dagger a \sigma_n^z. \tag{25}$$

2.1.1 Single Qubit

In the first part we are interested in the evolution of a single qubit state and later we will generalize it to N qubits. The single qubit state coupled to a cavity $|\psi\rangle = |\alpha\rangle(a|0\rangle + b|1\rangle)$ evolves the following way:

$$e^{-iHt}|\psi\rangle = e^{-\chi a^\dagger a \sigma^z t}|\alpha\rangle(a|0\rangle + b|1\rangle) = e^{-|\alpha|^2/2}\sum_{n=0}^{\infty}\frac{\alpha^n}{\sqrt{n!}}e^{-i\chi\sigma_z\hat{n}t}|n\rangle(a|0\rangle + b|1\rangle), \tag{26}$$

with the number operator $a^\dagger a = \hat{n}$. Further calculations lead to

$$= e^{-|\alpha|^2/2}\sum_{n=0}^{\infty}\left\{\frac{\alpha^n e^{+i\chi nt}}{\sqrt{n!}}|n\rangle a|0\rangle + \frac{\alpha^n e^{-i\chi nt}}{\sqrt{n!}}|n\rangle b|1\rangle\right\} = e^{-|\alpha|^2/2}\sum_{n=0}^{\infty}\left\{\frac{(\alpha e^{+i\chi t})^n}{\sqrt{n!}}|n\rangle a|0\rangle + \frac{(\alpha e^{-i\chi t})^n}{\sqrt{n!}}|n\rangle b|1\rangle\right\} \tag{27}$$

$$= a|\alpha e^{+i\chi t}\rangle|0\rangle + b|\alpha e^{-i\chi t}\rangle|1\rangle. \tag{28}$$

The relations $\sigma_z|0\rangle = -|0\rangle$, $\sigma_z|1\rangle = +|1\rangle$ still hold.
So in this example one can easily see, that for $t = 2\pi/\chi$ we are back in the initial state again. As expected there is no inter subspace dephasing in the case the cavity does not loose any photons at all.

2.1.2 N Qubits

In this section N qubit states will be investigated with the same model of a perfectly lossless cavity. In the N-qubit even parity state we have basis states of the form: $|00000\cdots\rangle$, $|11000\cdots\rangle$ and so on until we have the even state, where all qubits are in the "up" state $|11111\cdots\rangle$. All these basis states will evolve differently except they are permutations of each other. Therefore

$$e^{-\chi\sigma_z a^\dagger at}|\alpha\rangle|00000\cdots\rangle = |\alpha e^{-i\chi Nt}\rangle|00000\cdots\rangle \tag{29}$$

$$e^{-\chi\sigma_z a^\dagger at}|\alpha\rangle|11000\cdots\rangle = |\alpha e^{-i\chi(N-4)t}\rangle|11000\cdots\rangle \tag{30}$$

$$\vdots$$

$$e^{-\chi\sigma_z a^\dagger a t}|\alpha\rangle|11111\cdots\rangle = |\alpha e^{+i\chi N t}\rangle|11111\cdots\rangle. \tag{31}$$

So we have the following conditions for our driving time t:

$$e^{\pm iN\chi t} \stackrel{!}{=} 1 \Rightarrow t = \frac{2\pi}{N\chi} \tag{32}$$
$$e^{\pm i(N-4)\chi t} \stackrel{!}{=} 1 \Rightarrow t = \frac{2\pi}{(N-4)\chi} \tag{33}$$
$$\vdots$$
$$e^{\pm i4\chi t} \stackrel{!}{=} 1 \Rightarrow t = \frac{\pi}{2\chi} \tag{34}$$

If there are the same amount of qubits in the up and the down state the phase completely chancels and the cavity does not rotate at all (in the rotating frame of the bare cavity frequency ω_C). For even N there is a time $t_D = \frac{\pi}{2\chi}$ after which all the phases vanish and the relation $e^{-iHt_D}|\psi\rangle = |\psi\rangle$ holds. The evolution of the odd parity states is similar. It will also lead to a driving time t where the cavity returns into its initial state. The qubit coherence is once again not affected by the cavity. So it can be said that its origin is in the extraction of photons out of the cavity

2.2 Time evolution with cavity decay

For a better understanding of the dephasing caused by the measurement, respectively photon decay, we investigate the following system. It consists of two qubits in some initial state $|\psi\rangle_0 = c_{11}|11\rangle + c_{00}|00\rangle + c_{01}|01\rangle + c_{10}|10\rangle$ coupled to a cavity that has a non-zero decay rate κ.
The Hamiltonian in this case is the dispersive Hamiltonian. In a rotating frame with the bare qubit frequencies it reduces to

$$H = \omega_C a^\dagger a + (\chi_1\sigma_1^z + \chi_2\sigma_2^z)a^\dagger a. \tag{35}$$

The master equation in our simplified case has the form

$$\dot\rho = -i\big[H,\rho\big] + \kappa D\left[a\right]\rho. \tag{36}$$

where $D\left[O\right]\rho = \frac{1}{2}(2O\rho O^\dagger - O^\dagger O\rho - \rho O^\dagger O)$ is the Lindblad dissipator. Because the Hamiltonian is diagonal in the qubit subspace, we can write it in the following way:

$$H = H_1|11\rangle\langle 11| + H_2|00\rangle\langle 00| + H_3|10\rangle\langle 10| + H_4|01\rangle\langle 01| = \begin{bmatrix} H_1 & & & \\ & H_2 & & \\ & & H_3 & \\ & & & H_4 \end{bmatrix}. \tag{37}$$

The H_i are acting only on the cavity and have the form

$$H_1 = (\omega_C + \chi_1 + \chi_2)a^\dagger a \tag{38}$$
$$H_2 = (\omega_C - \chi_1 - \chi_2)a^\dagger a \tag{39}$$
$$H_3 = (\omega_C + \chi_1 - \chi_2)a^\dagger a \tag{40}$$
$$H_4 = (\omega_C - \chi_1 + \chi_2)a^\dagger a. \tag{41}$$

To simplify we also rewrite the qubit states $|11\rangle = |1\rangle$, $|00\rangle = |2\rangle$, $|10\rangle = |3\rangle$, $|01\rangle = |4\rangle$. So they have the same indices as the corresponding Hamiltonians.
Therefore our density matrix has the form

$$\rho = \rho_{11}|1\rangle\langle 1| + \rho_{12}|1\rangle\langle 2| + \rho_{13}|1\rangle\langle 3| + \rho_{14}|1\rangle\langle 4| + \rho_{21}|2\rangle\langle 1| + \ldots = \begin{bmatrix} \rho_{11} & \rho_{12} & \rho_{13} & \rho_{14} \\ \rho_{21} & \rho_{22} & \cdots & \cdots \\ \vdots & \vdots & \vdots & \vdots \\ \rho_{41} & \rho_{42} & \rho_{43} & \rho_{44} \end{bmatrix}.$$

The Lindblad master equation can be solved component by component. The diagonal terms have the same form as the normal master equation.

$$\dot{\rho}_{11} = -i\big[H_1, \rho_{11}\big] + \kappa D\,[a]\,\rho_{11} \tag{42}$$
$$\vdots$$
$$\dot{\rho}_{44} = -i\big[H_4, \rho_{44}\big] + \kappa D\,[a]\,\rho_{44} \tag{43}$$

The off diagonal terms do not have a standard commutator, because if we commute the matrices H and ρ we get mixed terms.

$$\dot{\rho}_{12} = -i(H_1\rho_{12} - \rho_{12}H_2) + \kappa D\,[a]\,\rho_{12} \tag{44}$$
$$\dot{\rho}_{13} = -i(H_1\rho_{13} - \rho_{13}H_3) + \kappa D\,[a]\,\rho_{13} \tag{45}$$
$$\vdots$$
$$\dot{\rho}_{34} = -i(H_3\rho_{34} - \rho_{34}H_4) + \kappa D\,[a]\,\rho_{34} \tag{46}$$

Since the density matrix is hermitian, it is sufficient to calculate the terms above the diagonal. To solve this master equations we use the method of characteristic functions.
First we define the normal-ordered characteristic function

$$C_n^{[\rho]}(\lambda, \lambda^*, t) := tr\left[\rho(t)e^{\lambda a^\dagger}e^{-\lambda^* a}\right].$$

If we use the cyclic invariance of the trace e.g. $tr\,[AB] = tr\,[BA]$ and the commutators $\big[a, f(a, a^\dagger)\big] = \partial f/\partial a^\dagger$ and $\big[a^\dagger, f(a, a^\dagger)\big] = -\partial f/\partial a$ we get the following relations [3]:

$$C_n^{[\rho a^\dagger]} = tr\left[\rho a^\dagger e^{\lambda a^\dagger}e^{-\lambda^* a}\right] = \frac{\partial}{\partial \lambda}C^{[\rho]} \tag{47}$$
$$C_n^{[a\rho]} = tr\left[a\rho e^{\lambda a^\dagger}e^{-\lambda^* a}\right] = -\frac{\partial}{\partial \lambda^*}C^{[\rho]} \tag{48}$$
$$C_n^{[\rho a]} = tr\left[\rho a e^{\lambda a^\dagger}e^{-\lambda^* a}\right] = \big(\lambda - \frac{\partial}{\partial \lambda^*}\big)C^{[\rho]} \tag{49}$$
$$C_n^{[a^\dagger\rho]} = tr\left[a^\dagger\rho e^{\lambda a^\dagger}e^{-\lambda^* a}\right] = \big(-\lambda^* + \frac{\partial}{\partial \lambda}\big)C^{[\rho]} \tag{50}$$
$$C_n^{[a\rho a^\dagger]} = tr\left[a\rho a^\dagger e^{\lambda a^\dagger}e^{-\lambda^* a}\right] = \frac{\partial^2}{\partial \lambda \partial \lambda^*}C^{[\rho]} \tag{51}$$
$$C_n^{[\rho a^\dagger a]} = tr\left[\rho a^\dagger a e^{\lambda a^\dagger}e^{-\lambda^* a}\right] = \big(\lambda - \frac{\partial}{\partial \lambda^*}\big)\frac{\partial}{\partial \lambda}C^{[\rho]} \tag{52}$$
$$C_n^{[a^\dagger a\rho]} = tr\left[a^\dagger a\rho e^{\lambda a^\dagger}e^{-\lambda^* a}\right] = \big(\lambda^* - \frac{\partial}{\partial \lambda}\big)\frac{\partial}{\partial \lambda^*}C^{[\rho]} \tag{53}$$

Calculating the derivative of $C_n^{[\rho]}$ and using the relations from the equations (42) to (46) we get

$$\frac{d}{dt}C_n^{[\rho_{ij}]} = tr\left[\dot{\rho}_{ij}e^{\lambda a^\dagger}e^{-\lambda^* a}\right] = tr\left[(-i(H_i\rho_{ij} - \rho_{ij}H_j) + \kappa D\,[a]\,\rho_{ij})e^{\lambda a^\dagger}e^{-\lambda^* a}\right]. \tag{54}$$

To solve this equation we use the following ansatz for the matrix elements of the density matrix. For the diagonal elements we use the ansatz $\rho_{ii}(t) = |c_{ii}|^2 |\alpha_i(t)\rangle\langle\alpha_i(t)|$ where the phase factor is not time dependent and for the off-diagonal terms we have a time dependent phase factor $\rho_{ij}(t) = c_{ij}(t)|\alpha_i(t)\rangle\langle\alpha_j(t)|$. Here we used the same indices for the amplitudes of the coherent states as for the Hamiltonians. For example the index 1 corresponds again to the qubit state $|11\rangle$. With this ansatz the normal-ordered characteristic function takes the form

$$C_n^{[\rho]} = C_n^{[c(t)|\alpha\rangle\langle\alpha|]} = c(t)e^{(\lambda\alpha^* - \lambda^*\alpha)}. \tag{55}$$

If we use this Ansatz, the relations (47) to (53) and Eq. (55), we can calculate the matrix elements of $\rho(t)$ by comparing the coefficients λ and λ^*.

Since we are mainly interested in the dephasing we first calculate the off-diagonal terms of ρ. In the appendices 10.4 one can find the full calculation for ρ_{12}. If we calculate all the elements, we obtain the following differential equations:

$$\dot{\alpha}_1(t) = \alpha_1(t)\left[-i(\omega_C + \chi 1 + \chi 2) - \frac{\kappa}{2}\right] \tag{56}$$
$$\dot{\alpha}_2(t) = \alpha_2(t)\left[-i(\omega_C - \chi 1 - \chi 2) - \frac{\kappa}{2}\right] \tag{57}$$
$$\dot{\alpha}_3(t) = \alpha_3(t)\left[-i(\omega_C + \chi 1 - \chi 2) - \frac{\kappa}{2}\right] \tag{58}$$
$$\dot{\alpha}_4(t) = \alpha_4(t)\left[-i(\omega_C - \chi 1 + \chi 2) - \frac{\kappa}{2}\right] \tag{59}$$
$$\dot{c}_{12}(t) = -2ic_{12}(t)\alpha_1(t)\alpha_2^*(t)(\chi 1 + \chi 2) \tag{60}$$
$$\dot{c}_{13}(t) = -2ic_{13}(t)\alpha_1(t)\alpha_3^*(t)\chi 2 \tag{61}$$
$$\dot{c}_{14}(t) = -2ic_{14}(t)\alpha_1(t)\alpha_4^*(t)\chi 1 \tag{62}$$
$$\dot{c}_{23}(t) = +2ic_{23}(t)\alpha_2(t)\alpha_3^*(t)\chi 1 \tag{63}$$
$$\dot{c}_{24}(t) = +2ic_{24}(t)\alpha_2(t)\alpha_4^*(t)\chi 2 \tag{64}$$
$$\dot{c}_{34}(t) = +2ic_{34}(t)\alpha_3(t)\alpha_4^*(t)(\chi 1 - \chi 2) \tag{65}$$

In our case where we are interested in the dephasing of the even and odd parity subspaces we do not have to evaluate all the differential equations we just have to calculate $c_{12}(t)$ and $c_{34}(t)$ which stand for the dephasing between the states $|11\rangle$ and $|00\rangle$ respectively $|10\rangle$ and $|01\rangle$. The real part then of these phase factors is the intra subspace qubit dephasing induced by the photon decay of the cavity, which corresponds to the expectation value of $\sigma_1^x \otimes \sigma_2^x$. A way to see this is just by calculating $\langle\sigma_1^x \otimes \sigma_2^x\rangle = tr\left[\rho(\sigma_1^x \otimes \sigma_2^x)\right]$. But one has to be careful with the calculation of $\sigma_1^x \otimes \sigma_2^x$. Because in the basis we used in Eq. (37) $\sigma_1^x \otimes \sigma_2^x$ takes the form

$$\sigma_1^x \otimes \sigma_2^x = \begin{bmatrix} 0 & 1 & 0 & 0 \\ 1 & 0 & 0 & 0 \\ 0 & 0 & 0 & 1 \\ 0 & 0 & 1 & 0 \end{bmatrix} \tag{66}$$

and

$$\langle\sigma_1^x \otimes \sigma_2^x\rangle = tr\left[\rho(\sigma_1^x \otimes \sigma_2^x)\right] = c_{12}(t) + c_{21}(t) + c_{34}(t) + c_{43}(t). \tag{67}$$

Since $c_{ij}(t) = c_{ji}^*(t)$ we get the result

$$\langle\sigma_1^x \otimes \sigma_2^x\rangle = 2Re\left[c_{12}(t) + c_{34}(t)\right]. \tag{68}$$

The expectation value for the cavity occupation $\langle a^\dagger a\rangle$ does not have to be calculated properly because it is clear, that the cavity decays with $\exp(-\kappa t)$. Because we defined the cavity leakage to be κ. In the Appendix section 10.3 one can find the full calculation of the cavity occupation as a consistency check.

2.2.1 Calculating the expectation value of $\sigma_1^x \otimes \sigma_2^x$

For simplicity we assume $\chi_1 = \chi_2 = \chi$ and calculate the expectation value for $\sigma_1^x \otimes \sigma_2^x$ for the initial state $|\psi\rangle_E = 1/\sqrt{2}(|00\rangle + |11\rangle)$. Solving the differential equations for equations (56), (57) and (60) with the cavity in the initial state $|\alpha\rangle$ we get

$$\begin{aligned}\langle \sigma_1^x \otimes \sigma_2^x \rangle = 2Re\left[c_{12}(t) + c_{34}(t)\right] = \exp\left\{-\frac{16\alpha^2\chi^2}{\kappa^2 + 16\chi^2} + \chi\left[\frac{16\alpha^2\chi e^{-\kappa t}\cos(4\chi t) + 4\kappa\alpha^2 e^{-\kappa t}\sin(4\chi t)}{\kappa^2 + 16\chi^2}\right]\right\} \times \\ \cos\left\{\frac{4\alpha^2\chi\kappa}{\kappa^2 + 16\chi^2} - \chi\left[\frac{4\alpha^2\kappa e^{-\kappa t}\cos(4\chi t) - 16\alpha^2\chi e^{-\kappa t}\sin(4\chi t)}{\kappa^2 + 16\chi^2}\right]\right\}\end{aligned} . \tag{69}$$

The decay of the revivals is determined by the exponential in the function. Keeping in mind, that the time of the revival is $t = \frac{\pi}{2\chi}$ (see section 2.1.2) where $\sin(4\chi t)$ is vanishing and $\cos(4\chi t)$ is equal to 1. The decay function $\Gamma_{rev}(t)$ of the revivals simplifies to

$$\Gamma_{rev}(t) = \exp\left\{\frac{16\alpha^2\chi^2}{\kappa^2 + 16\chi^2}(e^{-\kappa t} - 1)\right\} . \tag{70}$$

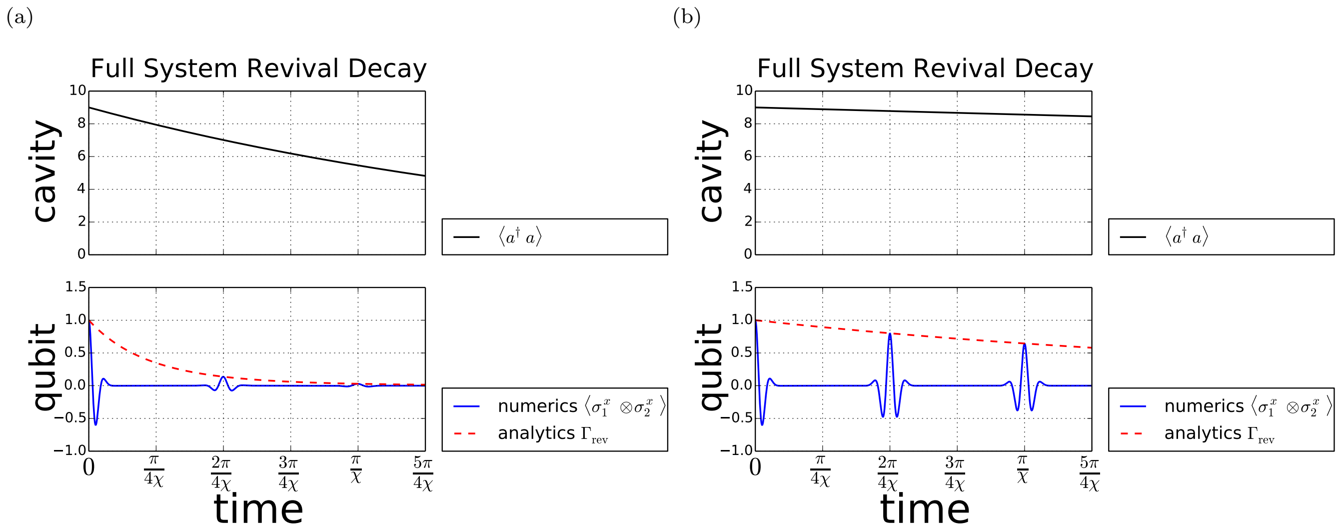

Figure 7: Cavity decay and dephasing of a leaky cavity with different ratios χ/κ of the dispersive shift to the cavity decay rate and the cavity amplitudes are initially set to $\alpha = 3$.
(a) The ratio of the dispersive shift to the decay rate is set to $\chi/\kappa = 1$
(b) The ratio of the dispersive shift to the decay rate is set to $\chi/\kappa = 10$

If we plot these results and compare it to the fully simulated system (figure 5), one can see two main differences of the shape of $\langle\sigma_1^x \otimes \sigma_2^x\rangle$ and the cavity decay $\langle a^\dagger a\rangle$.

- 1) Compared to the full system the leaky cavity continuously looses photons. In the full system one can see a saturation of the photon decay after losing one photon. This is a direct consequence of the detection of the photons with a JPM. After the detection of a photon the ground state of the JPM is not occupied anymore and therefore no more photons can exit the cavity via this channel. The consequence of this is that the height of the revival of the expectation value decreases continuously, whereas in the full system after detecting a photon the revival height stays at the same level.

- 2) The decay rate κ in the leaky-cavity-system is not the same as in the full system. In the full system the leakage out of the cavity is determined by the coupling g_J of the cavity to the JPM and the decay κ_J of the excited JPM level to the continuum.

Due to these two differences it will be necessary to determine an effective decay rate that contains approximatively the physics of the JPM. And then take somehow into account that the decay of the photons stops after a certain time when one photon has been emitted. In the next section we will first derive the effective decay rate of a cavity coupled to a JPM.

3 Analysis of the cavity-JPM interaction

3.1 Adiabatic elimination of the JPM

In this section we try to understand the second part of the system. In section 2.2 we discussed the behaviour of the qubits coupled to a lossy cavity. Now we try to understand the cavity coupled to the JPM. One of our main achievements in this thesis is that we have been able to eliminate the JPM and approximate the cavity-JPM interaction by a lossy cavity with an effective decay rate. Through this approximation it was possible to make analytic progress. This will all be described in this section. The JPM is here represented by a 3-level system.

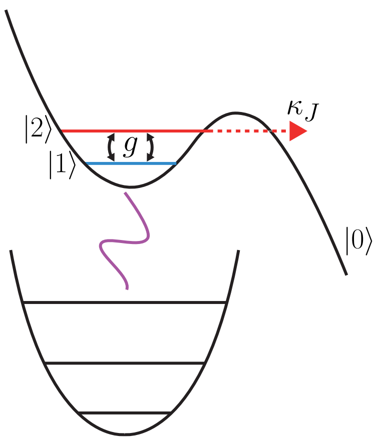

Figure 8: Cavity coupled to the JPM via Jaynes-Cummings-Interaction. The JPM is represented by a 3-level-system. $|1\rangle$ and $|2\rangle$ interact with the cavity. $|2\rangle$ can decay to the continuum which is here represented by the state $|0\rangle$.

The states $|1\rangle$ and $|2\rangle$ interact with the cavity and the state $|2\rangle$ can decay to the state $|0\rangle$. We describe this system with the Hamiltonian,

$$H = \omega_C a^\dagger a + \omega_{12}|2\rangle\langle 2| + g_J(a|2\rangle\langle 1| + a^\dagger|1\rangle\langle 2|) - \omega_0|0\rangle\langle 0| \tag{71}$$

The full system of qubits coupled to a cavity that decays through the JPM could only be calculated numerically. To gain more intuition and to make analytical progress we present an effective mapping to a simpler model which captures the physics in the relevant regime of the JPM. The cavity coupled to the JPM will be replaced by a cavity that decays through an effective decay rate.

3.1.1 Resonant case

The case where the JPM and the cavity are on resonance was already discussed in Ref. [18]. For completeness and to compare the result to the off-resonant case this thesis contains these derivations and results. In a first step we tune the cavity and the JPM on resonance by setting the excitation energy ω_{12} equal to the cavity frequency ω_C. The energy of the state $|1\rangle$ is here set to zero. The master equation has the form,

$$\dot{\rho} = -i\,[H,\rho] + \kappa D\,[|0\rangle\langle 2|]\,\rho \tag{72}$$

where $D\,[O]\,\rho = \frac{1}{2}(2O\rho O^\dagger - O^\dagger O\rho - \rho O^\dagger O)$ again is the Lindblad dissipator. We can rewrite the Hamiltonian into the reduced basis sates $|n+1,1\rangle, |n,2\rangle, |n,0\rangle$ and it gets the following form:

$$H_n = \begin{bmatrix} (n+1)\omega_C & \sqrt{n+1}g & 0 \\ \sqrt{n+1}g & (n+1)\omega_C & 0 \\ 0 & 0 & -\omega_0 \end{bmatrix} \tag{73}$$

If we define

$$\rho = \begin{bmatrix} \rho_{11} & \rho_{12} & \rho_{10} \\ \rho_{21} & \rho_{22} & \rho_{20} \\ \rho_{01} & \rho_{02} & \rho_{00} \end{bmatrix}, \tag{74}$$

we can obtain the differential equations

$$\dot{\rho}_{11} = -ig_J\sqrt{n+1}(\rho_{21} - \rho_{12}) \tag{75}$$
$$\dot{\rho_{22}} = -ig_J\sqrt{n+1}(\rho_{12} - \rho_{21}) - \kappa\rho_{22} \tag{76}$$
$$\dot{\rho_{00}} = \kappa\rho_{22} \tag{77}$$
$$\dot{\rho_{12}} = -ig_J\sqrt{n+1}(\rho_{22} - \rho_{11}) - \frac{\kappa}{2}\rho_{12} \tag{78}$$
$$\dot{\rho_{21}} = -ig_J\sqrt{n+1}(\rho_{11} - \rho_{22}) - \frac{\kappa}{2}\rho_{21}. \tag{79}$$

Under the initial conditions, that $\rho_{11}(0) = 1$ is occupied and $\rho_{22}(0) = Im\rho_{12}(0) = 0$ are unoccupied the differential equations can be solved either with a Laplace transformation or with matrix exponentials (see Appendix 10.6 or 10.5). When we define $\beta_n = g_J\sqrt{n+1}$, we get

$$\rho_{22}(t) = \frac{\beta_n^2}{\kappa^2 - 4\beta_n^2}\left(e^{\frac{\sqrt{\kappa^2-4\beta_n^2}}{2}t} + e^{\frac{-\sqrt{\kappa^2-4\beta_n^2}}{2}t} - 2\right)e^{-\frac{\kappa}{2}t}, \tag{80}$$

$$\rho_{11}(t) = 1 - \frac{8\beta_n^2}{\kappa_J^2 - 16\beta_n^2}\left(\frac{\kappa_J + \sqrt{\kappa_J^2 - 16\beta_n^2}}{2}e^{\frac{-\kappa_J+\sqrt{\kappa_J^2-16\beta_n^2}}{2}t} + \frac{\kappa_J - \sqrt{\kappa_J^2 - 16\beta_n^2}}{2}e^{\frac{-\kappa_J-\sqrt{\kappa_J^2-16\beta_n^2}}{2}t} - \kappa_J e^{-\frac{\kappa}{2}t}\right). \tag{81}$$

If we go back to the differential equations (75) to (79), we see $\dot{\rho}_{00} = \kappa\rho_{22}$. Since $\rho_{00}(0) = 0$ the solution for $\rho_{00}(t)$ can be found by integrating

$$\rho_{00}(t) = \kappa\int_0^t d\tau\rho_{22}(\tau) \tag{82}$$
$$= \frac{\kappa\beta_n^2}{\kappa^2 - 4\beta_n^2}\left[\frac{e^{(\sqrt{(\frac{\kappa}{2})^2-\beta_n^2}-\frac{\kappa}{2})t} - 1}{\sqrt{(\frac{\kappa}{2})^2 - \beta_n^2} - \frac{\kappa}{2}} - \frac{e^{(-\sqrt{(\frac{\kappa}{2})^2-\beta_n^2}-\frac{\kappa}{2})t} - 1}{\sqrt{(\frac{\kappa}{2})^2 - \beta_n^2} + \frac{\kappa}{2}} + \frac{4}{\kappa}(e^{\frac{-\kappa}{2}t} - 1)\right]. \tag{83}$$

3.1.2 Off-resonant case

With a Laplace transformation (Appendix 10.6) it was possible to solve the differential equation for a non zero detuning. For $\omega_C - \omega_{12} = \Delta \neq 0$

$$\dot{\rho}_{11} = -ig\sqrt{n+1}(\rho_{21} - \rho_{12}) \tag{84}$$
$$\dot{\rho}_{22} = -ig\sqrt{n+1}(\rho_{12} - \rho_{21}) - \kappa\rho_{22} \tag{85}$$
$$\dot{\rho}_{00} = \kappa\rho_{22} \tag{86}$$
$$\dot{\rho}_{12} = -ig\sqrt{n+1}(\rho_{22} - \rho_{11}) - \frac{\kappa}{2}\rho_{12} - i\Delta\rho_{12} \tag{87}$$
$$\dot{\rho}_{21} = -ig\sqrt{n+1}(\rho_{11} - \rho_{22}) - \frac{\kappa}{2}\rho_{21} + i\Delta\rho_{21} \tag{88}$$

To simplify the calculation we split ρ_{12} into its imaginary and real part.

$$\dot{\rho}_{12}^R = \frac{1}{2}(\dot{\rho}_{12} + \dot{\rho}_{21}) = -\frac{\kappa}{2}\rho_{12}^R + \Delta\rho_{12}^I \tag{89}$$

$$\dot{\rho}_{12}^{I} = \frac{1}{2i}(\dot{\rho}_{12} - \dot{\rho}_{21}) = -g\sqrt{n+1}(\rho_{22} - \rho_{11}) - \frac{\kappa}{2}\rho_{12}^{I} - \Delta\rho_{12}^{R} \tag{90}$$

When we apply a Laplace transformation from time to the s space with $\rho(0) = (1,0,0,0)^T$ we find the following equations.

$$\rho_{12}^{R} = \frac{\Delta}{s+\frac{\kappa}{2}}\rho_{12}^{I} \tag{91}$$

$$\rho_{22} = \frac{2\beta_n}{s+\kappa}\rho_{12}^{I} = \frac{2\beta_n}{s+\kappa}\rho_{12}^{I} \tag{92}$$

$$\rho_{11} = \frac{1}{s} - \frac{2\beta_n}{s}\rho_{12}^{I} \tag{93}$$

$$\rho_{12}^{I} = \frac{\beta_n}{s(\frac{\Delta^2}{s+\frac{\kappa}{2}} + 2\beta_n^2(\frac{1}{s} + \frac{1}{s+\kappa}))} = \frac{2\beta_n(s+\frac{\kappa}{2})(s+\kappa)}{s+\frac{\kappa}{2} + \Delta^2 s\,(s+\kappa) + \left(s+\frac{\kappa}{2}\right)^2 s\,(s+\kappa) + 2\beta_n^2\left((s+\kappa)\left(s+\frac{\kappa}{2}\right) + s\left(s+\frac{\kappa}{2}\right)\right)} \tag{94}$$

Here we used again the short-hand notation $\beta_n = g\sqrt{n+1}$. In the end we are interested in ρ_{00} which can be obtained by integrating ρ_{22}. To find ρ_{22} we just have to plug ρ_{12}^{I} into Eq. (92) and this will also cancel the factor $(s+\kappa)$.
To do the back transformation to the time space we have to calculate the integral

$$\rho_{kl}(t) = \frac{1}{2\pi i}\int_{\gamma-i\infty}^{\gamma+i\infty} ds\rho_{kl}(s)e^{st}, \tag{95}$$

which can be solved if we find the factorized form of the denominator of the function we want to integrate. If we find this form we only have to calculate the residua of the function and sum them up.
For $\Delta \neq 0$ the poles of ρ_{12}^{I} are

$$s_0 = \frac{1}{2}\left(+\frac{\sqrt{+\sqrt{\left(16\beta_n^2+\kappa^2+4\epsilon^2\right)^2 - 64\beta_n^2\kappa^2} - 16\beta_n^2 + \kappa^2 - 4\epsilon^2}}{\sqrt{2}} - \kappa\right) \tag{96}$$

$$s_1 = \frac{1}{2}\left(-\frac{\sqrt{-\sqrt{\left(16\beta_n^2+\kappa^2+4\epsilon^2\right)^2 - 64\beta_n^2\kappa^2} - 16\beta_n^2 + \kappa^2 - 4\epsilon^2}}{\sqrt{2}} - \kappa\right) \tag{97}$$

$$s_2 = \frac{1}{2}\left(+\frac{\sqrt{-\sqrt{\left(16\beta_n^2+\kappa^2+4\epsilon^2\right)^2 - 64\beta_n^2\kappa^2} - 16\beta_n^2 + \kappa^2 - 4\epsilon^2}}{\sqrt{2}} - \kappa\right) \tag{98}$$

$$s_3 = \frac{1}{2}\left(-\frac{\sqrt{+\sqrt{\left(16\beta_n^2+\kappa^2+4\epsilon^2\right)^2 - 64\beta_n^2\kappa^2} - 16\beta_n^2 + \kappa^2 - 4\epsilon^2}}{\sqrt{2}} - \kappa\right). \tag{99}$$

So the Laplace transfomed ρ_{22} takes the form

$$\rho_{22}(s) = \frac{2\beta_n(s+\frac{\kappa}{2})(s+\kappa)}{(s-s_0)(s-s_1)(s-s_2)(s-s_2)}. \tag{100}$$

To do the back transformation we again only have to calculate the residua of $\rho_{22}(s)e^{st}$ and after that we again integrate $\kappa\int_0^t \rho_{22}(\tau)d\tau$ to obtain $\rho_{00}(t)$
The whole derivation can be found in the Appendix 10.6. If we go to the limit where $\Delta^2 \ll g_J^2 \ll \kappa_J^2$ we find the simplified form of the occupation probability of the continuum state $|0\rangle$

$$\rho_{00}(t) = 1 - \exp\left(-\frac{4\beta_n^2}{\kappa} t \left(1 - 4\frac{\Delta^2}{\kappa_J^2}\right)\right). \tag{101}$$

Which leads to the effective decay rate in the detuned case

$$\kappa_{\text{eff}}^n = \frac{4\beta_n^2}{\kappa}\left(1 - 4\frac{\Delta^2}{\kappa_J^2}\right). \tag{102}$$

This result is still photon number dependent and is valid for the dressed states $|n+1,1\rangle$, $|n,2\rangle$ and $|n,0\rangle$ now we have to generalize it for a coherent state.

3.2 Approximation to make the transition from an initial Fock state to a coherent state

For simplicity we can sum this solution of ρ_{00} over all n weighted with the squared Poissonian probability mass function $P_{n+1} = \frac{e^{-|\alpha|^2}|\alpha|^{2(n+1)}}{(n+1)!}$ which we justify in section 3.6. The index $n+1$ comes from the initial Fock state $|n+1\rangle$. To keep that in mind we add the index n to ρ_{00} and change $\rho_{00} \to \rho_{00}^n$. As discussed in Section 3.6 with this calculation we can approximate an initial coherent state with the solutions for the dressed states. Therefore

$$\rho_{00} = \sum_{n=0}^{\infty} P_{n+1}\rho_{00}^n. \tag{103}$$

The mean value and the variance of the Poissonian distribution are equal. In the high photon number limit we can transform the Poissonian to a Gaussian distribution. Therefore we go to the limit $|\alpha|^2 \gg 1$ and rewrite $\sigma^2 = \mu = \bar{n} = |\alpha|^2$ and $\sum_n P_{n+1}$ becomes,

$$\sum_{n=0}^{\infty} \frac{e^{-|\alpha|^2}|\alpha|^{2(n+1)}}{(n+1)!} \approx \int_0^\infty \frac{1}{\sigma\sqrt{2\pi}} \exp\left(-\frac{(n-\mu)^2}{2\sigma^2}\right) dn = \int_0^\infty \frac{1}{\alpha\sqrt{2\pi}} \exp\left(-\frac{(n-|\alpha|^2)^2}{2|\alpha|^2}\right) dn. \tag{104}$$

By Taylor expanding ρ_{00}^n around $\bar{n} = |\alpha|^2$, we can evaluate the integral and check the relevance of higher order corrections. For short hand notation we set $\Delta = 0$ which is for the expansion nothing more than a constant change of κ_{eff}^n with the factor $(1 - 4\Delta^2/\kappa_J^2)$, which can be redone in the end again.

$$\begin{aligned}
\sum_{n=0}^{\infty} P_{n+1}\rho_{00}^n &\to \int_0^\infty \frac{1}{\alpha\sqrt{2\pi}} \exp\left(-\frac{(n-|\alpha|^2)^2}{2|\alpha|^2}\right) \rho_{00}^n dn && (105)\\
&= \int_0^\infty \frac{1}{\alpha\sqrt{2\pi}} \exp\left(-\frac{(n-|\alpha|^2)^2}{2|\alpha|^2}\right) \left[\sum_{i=0}^{\infty} \left(\left(\frac{d}{dn}\right)^i \rho_{00}^n\right)(|\alpha|^2)\frac{(n-|\alpha|^2)^i}{i!}\right] dn && (106)\\
&= \int_0^\infty \frac{1}{\alpha\sqrt{2\pi}} \exp\left(-\frac{(n-|\alpha|^2)^2}{2|\alpha|^2}\right) \left[\rho_{00}^n(|\alpha|^2) + \frac{d}{dn}\rho_{00}^n(\bar{n})(n-|\alpha|^2) + O^2(n)\right] dn && (107)
\end{aligned}$$

This integral can easily be solved. For zeroth order for the Taylor expansion we get,

$$\int_0^\infty \frac{1}{\alpha\sqrt{2\pi}} \exp\left(-\frac{(n-|\alpha|^2)^2}{2|\alpha|^2}\right) \rho_{00}^n(|\alpha|^2) dn = \frac{1}{2}\left(\sqrt{\frac{1}{|\alpha|^2}}\alpha + Erf\left[\frac{\alpha}{\sqrt{2}}\right]\right)\rho_{00}^n(|\alpha|^2), \tag{108}$$

where Erf is the error function which goes to 1 in the limit $\alpha \to \infty$. Since we are in this limit,

$$\int_0^\infty \frac{1}{\alpha\sqrt{2\pi}} \exp\left(-\frac{(n-|\alpha|^2)^2}{2|\alpha|^2}\right) \rho_{00}^n(|\alpha|^2) dn = \rho_{00}^n(|\alpha|^2). \tag{109}$$

The first order correction then is

$$\int_0^\infty \frac{1}{\alpha\sqrt{2\pi}} \exp\left(-\frac{(n-|\alpha|^2)^2}{2|\alpha|^2}\right)(n-|\alpha|^2)\frac{d}{dn}\rho_{00}^n(|\alpha|^2)dn = \frac{\alpha e^{-\frac{|\alpha|^2}{2}}}{\sqrt{2\pi}}\frac{d}{dn}\rho_{00}^n(|\alpha|^2). \tag{110}$$

The first order correction already is suppressed by the factor $\exp(-\frac{|\alpha|^2}{2})$ and can be neglected. In the second order correction we have to be careful, because the integral is not vanishing for $\alpha \gg 1$. The second order correction has the form

$$\int_0^\infty \frac{1}{\alpha\sqrt{2\pi}} \exp\left(-\frac{(n-|\alpha|^2)^2}{2|\alpha|^2}\right)(n-|\alpha|^2)^2\frac{d^2}{dn^2}\rho_{00}^n(|\alpha|^2)dn \approx \left(|\alpha|^2\frac{\alpha e^{-\frac{|\alpha|^2}{2}}}{\sqrt{2\pi}} + |\alpha|^2\right)\frac{d^2}{dn^2}\rho_{00}^n(|\alpha|^2). \tag{111}$$

The first term in the brackets of (111) is again vanishing exponentially but the second one with the term $|\alpha|^2$ is not negligible. However we also have to take into account the second derivative of ρ_{00}^n. In the limit $\kappa_J \gg \beta_n$ we have already seen that ρ_{00}^n simplifies to $1 - e^{-\frac{4\beta_n^2}{\kappa_J}t}$. Keeping in mind that $\beta_n = g\sqrt{n+1}$ the second derivative of ρ_{00}^n is

$$\frac{d^2}{dn^2} e^{-\frac{4\beta_n^2}{\kappa_J}} - 1 \approx e^{-4\frac{\beta_n^2}{\kappa_J}}\frac{16g^4}{\kappa_J^2}. \tag{112}$$

Multiplying equation (112) with the non-vanishing part in the brakets of equation (111) yields $e^{-\frac{\beta_{\bar{n}}^2}{\kappa_J}}\frac{g^4|\alpha|^2}{\kappa_J^2}$. And since we evaluate this term at $n = \bar{n}$ and $\bar{n} \gg 1$, β_n will simplify to $\beta_{\bar{n}} = g\sqrt{\bar{n}+1} \to g\sqrt{\bar{n}} = g|\alpha|$. So the second order correction can be rewritten as

$$O(n^2) = e^{-\frac{\beta_{\bar{n}}^2}{\kappa_J}}\frac{g^4|\alpha|^2}{\kappa_J^2} = e^{-\frac{\beta_{\bar{n}}^2}{\kappa_J}}\frac{\beta_{\bar{n}}^2}{\kappa_J^2}. \tag{113}$$

We are also in the limit $\kappa_J \gg \beta_{\bar{n}}$ and so this correction is also negligibly small compared to the zeroth order. This pattern repeats at higher orders. Odd order corrections are suppressed with the factor $\exp(-|\alpha|^2/2)$. Even order corrections vanish because of the factor β^n/κ^n at order n. From this it follows that the effective decay rate of the the initial JPM state $|1\rangle$ to the continuum $|0\rangle$ in the limit $\kappa_J \gg \beta_n$ with $\beta_n = g\sqrt{n+1}$ and with $\bar{n} = |\alpha|^2 \gg 1$ is

$$\kappa_{\text{eff}}^{\text{JPM}} \approx \frac{\beta_{\bar{n}}^2}{\kappa_J} = \frac{4g^2\bar{n}}{\kappa_J} = \frac{4g^2|\alpha|^2}{\kappa_J}. \tag{114}$$

3.3 Effective decay rate of the cavity

The decay rate $\kappa_{\text{eff}}^{\text{JPM}}$ of the initial state of the JPM $|1\rangle$ to the continuum state $|0\rangle$ does not describe the decay of the cavity accurately. But we know that a single photon has decayed from the cavity if the state $|0\rangle$ is occupied and therefore the cavity occupation converges to

$$\langle a^\dagger a\rangle = |\alpha|^2 - \rho_{00}(t) = |\alpha|^2 - 1 + \exp(-\kappa_{\text{eff}}^{\text{JPM}}t). \tag{115}$$

And the cavity decay stops after one photon has decayed because the phase of the JPM is trapped in the continuum state. The cavity starts at $|\alpha|^2$ and its occupation changes approximately the same way as the occupation of the continuum state and if the phase particle of the JPM decayed to the continuum state also the cavity occupation does not change any more. The cavity occupation of a leaking cavity is $\langle a^\dagger a\rangle = |\alpha|^2\exp(-\kappa t)$. For short times the leaking cavity and the effective model must decay with the same rate therefore we can expand both models for short times.

$$|\alpha|^2 - \rho_{00}(t) = |\alpha|^2 - 1 + \exp(-\kappa_{\text{eff}}^{\text{JPM}}t) \approx |\alpha|^2 - \kappa_{\text{eff}}^{\text{JPM}}t + \cdots \tag{116}$$

$$|\alpha|^2\exp(-\kappa t) \approx |\alpha|^2(1 - \kappa t + \cdots) \approx |\alpha|^2 - |\alpha|^2\kappa t \tag{117}$$

If we compare the two equations we find that the effective decay rate for the cavity is

$$\kappa_{\text{eff}}^{\text{cav}} = \frac{\kappa_{\text{eff}}^{\text{JPM}}}{|\alpha|^2} = \frac{4g_J^2}{\kappa_J}\left(1 - 4\frac{\Delta^2}{\kappa_J^2}\right). \tag{118}$$

Because we have two different effective decay rates for the JPM and the cavity we label them. Mostly it should be clear which decay rate we are using. If we examine a decaying cavity we use $\kappa_{\text{eff}}^{\text{cav}}$ and if we examine the decaying JPM we use $\kappa_{\text{eff}}^{\text{JPM}}$.

3.4 Physical interpretation of the results: Purcell picture

For the derivation of κ_{eff} in section 3.1 we used a model similarly to the Purcell effect [3]. The Purcell effect describes a Qubit coupled to a single mode cavity via Jaynes-Cummings interaction with an environment. But the environment only couples to the cavity and not the qubits. Nevertheless the relaxation of the cavity leads to a relaxation of the qubits. If we look at the model given by

$$\frac{d}{dt}\rho = -i\left[H,\rho\right] - \kappa D\left[a\right]\rho - \Gamma D\left[\sigma^-\right]\rho, \tag{119}$$

with the Jaynes-Cummings Hamiltonian $H = g(\sigma^- a^\dagger + \sigma^+ a) + \frac{\omega_{qb}}{2}\sigma^z + \omega_C a^\dagger a$ and the Lindblad superoperator $D\left[O\right]\rho = \frac{1}{2}(2O\rho O^\dagger - O^\dagger O\rho - \rho O^\dagger O)$. This equation describes a qubit with frequency ω_{qb} coupled to a cavity with frequency ω_C. The cavity decays with the rate κ and the qubit itself decays with the rate Γ. The coupling strength of the qubit to the cavity is denoted by g. To find the influence that the decay of a photon out of the cavity has on the decay rate of the qubit we follow the calculations of Keeling [10] to solve this system for the simplest states $|e,0\rangle$, $|g,1\rangle$ and $|g,0\rangle$. The last state cannot evolve into anything else and can therefore be neglected. Like in section 3.1 we can solve this differential equation by changing the basis to these dressed states and rewrite

$$H_0 = \begin{bmatrix} \omega_C - \frac{\omega_{qb}}{2} & g \\ g & \frac{\omega_{qb}}{2} \end{bmatrix}. \tag{120}$$

If we define

$$\rho = \begin{bmatrix} \rho_{gg} & \rho_{ge} \\ \rho_{eg} & \rho_{ee} \end{bmatrix}, \tag{121}$$

leads us to the closed set of differential equations

$$\dot{\rho}_{ee} = -ig(\rho_{ge} - \rho_{eg}) - \Gamma\rho_{ee} \tag{122}$$

$$\dot{\rho_{gg}} = -ig(\rho_{eg} - \rho_{ge}) - \kappa\rho_{gg} \tag{123}$$

$$\dot{\rho_{eg}} = -ig(\rho_{gg} - \rho_{ee}) - \frac{\kappa+\Gamma}{2}\rho_{eg} - i(\omega_C - \omega_{qb})\rho_{eg}. \tag{124}$$

Due to conservation $\rho_{ee}\rho_{gg} - |\rho_{eg}|^2 = 0$ and therefore we can rewrite $\rho_{ee} = |\alpha|^2$, $\rho_{gg} = |\beta|^2$ and $\rho_{eg} = \alpha\beta^*$. If we use the product rule i.e. $\dot{\rho}_{ee} = d/dt|\alpha|^2 = \dot{\alpha}\alpha^* + \alpha\dot{\alpha}^*$ we can find the simplified form

$$\frac{d}{dt}\begin{bmatrix}\alpha \\ \beta\end{bmatrix} = \begin{bmatrix} -\frac{\Gamma}{2} & -ig \\ -ig & i(\omega_C - \omega_{qb}) - \frac{\kappa}{2}\end{bmatrix}\begin{bmatrix}\alpha \\ \beta\end{bmatrix}. \tag{125}$$

The eigenvalues lead to the frequencies

$$\left(i\nu - \frac{\Gamma}{2}\right)\left(i\nu + i(\omega_C - \omega_{qb}) - \frac{\kappa}{2}\right)g^2 = 0. \tag{126}$$

In the bad cavity limit $\kappa \gg \Gamma$ the equation can be solved with

$$\nu = -\frac{i}{2}\left(\Gamma + \frac{\kappa g^2}{\frac{\kappa^2}{4} + (\omega_C - \omega_{qb})^2}\right) + \frac{(\omega_C - \omega_{qb})g^2}{\frac{\kappa^2}{4} + (\omega_C - \omega_{qb})^2}. \tag{127}$$

So the qubit decay rate which is the real part of the eigenvalue $i\nu$ is enhanced by the factor

$$\Gamma' = \frac{\kappa g^2}{\frac{\kappa^2}{4} + (\omega_C - \omega_{qb})^2}. \tag{128}$$

Which simplifies in the resonant case to our already known effective decay rate $4g^2/\kappa$. In the strongly off resonant case where $(\omega_C - \omega_{qb}) \gg \kappa$ it simplifies to the off resonant Purcell rate $\kappa g^2/\delta$ where δ is the detuning.
So if we compare our results from section 3.1 with these results, we see that our effective model is a manifestation of the Purcell effect. But in our model of a decaying 2-level system to the continuum we have the difference that we can decouple the differential equations for a given subsystem $|2, n\rangle$, $|1, n+1\rangle$ and $|0, n\rangle$. The decoupling is a consequence of the switching off behaviour of the JPM. The cavity-JPM interaction stops after the decay and therefore no more photons can leave the cavity. In figure 9 the coupling of the subsystems is illustrated.

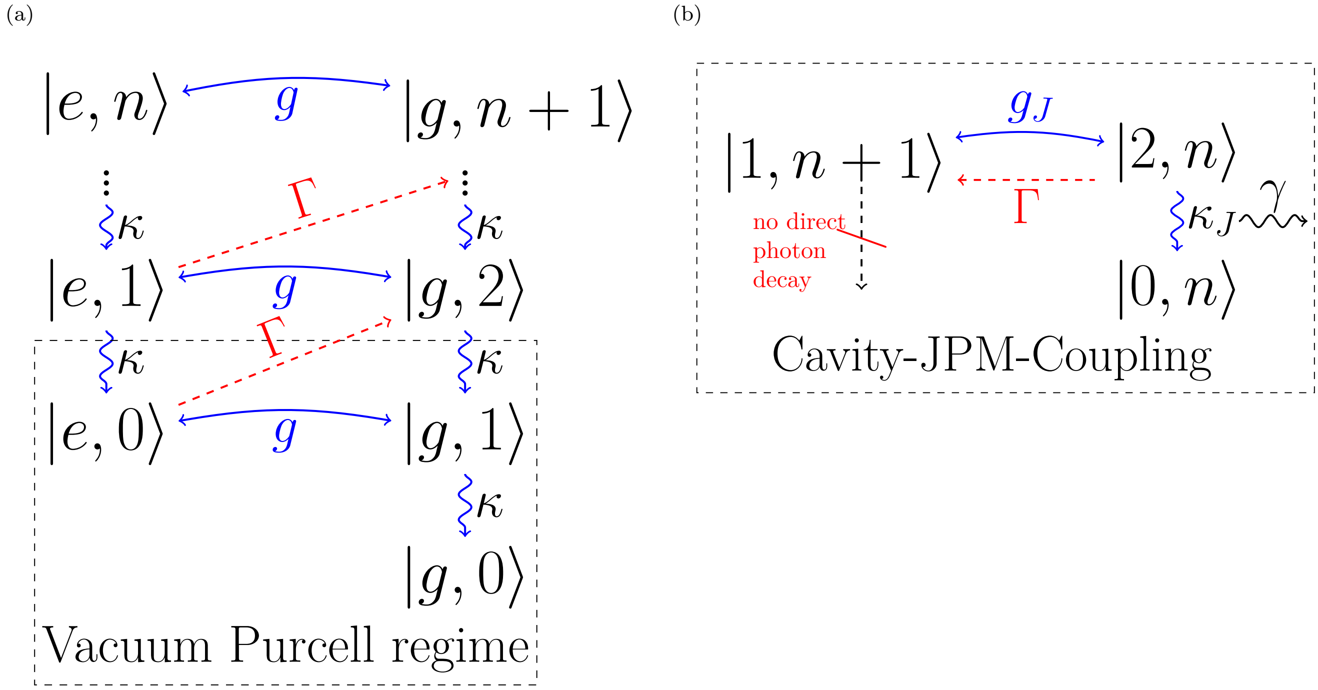

Figure 9: a): **Purcell picture** Dressed states of a two level system ($|g\rangle$, $|e\rangle$) coupled to a decaying cavity. The differential equations for a non-zero initial Fock state $|e, n \neq 0\rangle$ are all coupled until $n = 0$ through the decay channel κ. The cavity can decay from its initial state until its ground state and can therefore couple with every other possible state below the initial Fock state. The vacuum Purcell effect therefore only takes into account the states $|e, 0\rangle$, $|g, 1\rangle$, $|g, 0\rangle$.
b): **Cavity-JPM-Coupling** In our ideal model, where the cavity itself has no leakage, the dressed states of a set $|1, n + 1\rangle$, $|2, n\rangle$ and $|0, n\rangle$ can not couple to other states of different cavity states. So the ground state $|1\rangle$ of the JPM couples via Jaynes-Cummings interaction to the excited state $|2\rangle$ which can decay to the continuum state $|0\rangle$ via the decay channel κ. The emitted photon γ then will be detected. We also neglected the direct 2-level-decay rate Γ because we are in the regime $\kappa \gg g$

Mathematically the difference between these two problems is that the Cavity-JPM-Coupling leads to a block diagonal matrix for the differential equation of ρ with sets of differential equations of the same form as in the equations (75) - (79). If we want to calculate this system for a coherent state we only have to solve it for one block like we did in section 3.1. The Purcell problem on the other hand cannot be written as a block diagonal matrix and far more difficult to solve if the cavity is not in the vacuum state. The blocks for a certain subset of dressed states will be coupled via the decay rate κ.

3.5 Interpretations

For the resonant effect it is somehow surprising that the effective decay rate is getting smaller if we go to bigger κ. Intuitively one could think that the cavity decays faster if we go to higher decay rates of the JPM. If we imagine an empty cavity with a decay rate κ from the Purcell effect we know, that the 2-level-system in this cavity is protected against decay because in the cavity it can only couple to a discrete amount of modes instead of a infinite amount of modes in the continuum. If we add a decay channel κ to the cavity the discrete energy levels of the cavity broadens proportional to κ. And the density of states at the cavity frequency ω_C is proportional to $1/\kappa$ (See figure 10). This means if the 2-level system is on resonance with the cavity with $\kappa = 0$ the system is not protected against decay compared to the vacuum because it can directly couple to the cavity states. If we now add a decay channel there are less states available because the density of states shrinks with growing κ. Therefore the decay rate of the 2-level system shrinks. This is the resonant Purcell effect. In the off resonant case the decay rate of the 2-level system grows with κ. If we again imagine a cavity without decay there are only states available at the cavity frequency ω_C and the qubit can only decay with its intrinsic decay rate Γ. If we add a non-zero decay rate to the cavity the energy levels again smear out and now in the off-resonant case the probability of the 2-level system to couple to such a mode increases. Therefore the off-resonant Purcell effect scales proportionally with κ.

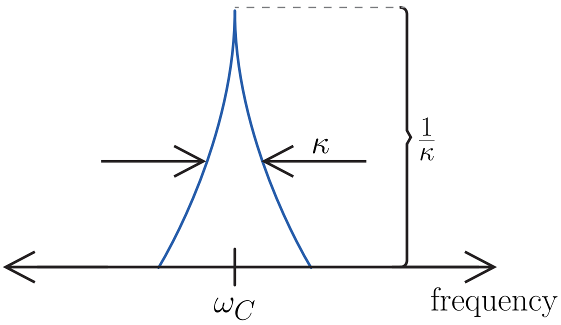

Figure 10: Density of states of a single mode cavity of frequency ω_C with a decay channel κ. With growing decay rate the density of states of the cavity smears out and even if the qubit that is coupled to the cavity is off-resonant it can coupled to the cavity states.

3.6 How good is the approximation of κ_{eff} on the example of ρ_{00}

To go from a cavity that is initially in a Fock state to a cavity in a coherent state we just summed the resulting continuum occupation ρ_{00}^n with the Poissonian probability mass function (section 3.2). In figure 9 one can see why this is reasonable. The dressed states of a given Fock state n give a closed set of states that do not interact with a set of dressed states of an other Fock state m. This implies that the master equation can be represented by a block-diagonal matrix. And the matrix exponential of such a matrix is again block-diagonal. And therefore an initial coherent state will lead to a sum of the results of the Fock states. To perform the sum to come from the dressed state picture to an initial coherent state we had to go to the limit $\alpha \gg 1$. In this section we will test this result by comparing the analytic solution of $\rho_{00}(t)$ with the numerics of a cavity that is coupled to the JPM. The analytic solution of $\rho_{00}(t)$ was

$$\rho_{00}(t) = 1 - \exp(-\kappa_{\text{eff}}^{\text{JPM}}). \tag{129}$$

For the cavity coupled to the JPM we solve numerically the master equation for the Hamiltonian

$$H = \omega_C a^\dagger a + \omega_{12}|2\rangle\langle 2| + g_J(a|2\rangle\langle 1| + a^\dagger|1\rangle\langle 2|) - \omega_0|0\rangle\langle 0|. \tag{130}$$

The JPM is modeled again by a 3-level system like in section 3.1 figure 8. The cavity is coupled to the states $|1\rangle$ and $|2\rangle$ via Jaynes-Cummings interaction and the excited state $|2\rangle$ can decay to the continuum via the decay chanel κ_J. In figure 11 we can see that the analytical and numerical solutions match better if we go to bigger cavity amplitudes α. For $\alpha = 1$ we obtain that the continuum state $|0\rangle$ is not occupied completely. This is because the probability of having lost a photon in a cavity that is initially set to $\alpha = 1$ is far from 1 after the time $t = 1/\kappa_{\text{eff}}$. So in this limit the effective decay picture completely fails. But for $\alpha \gg 1$ it holds and gets better for growing α.

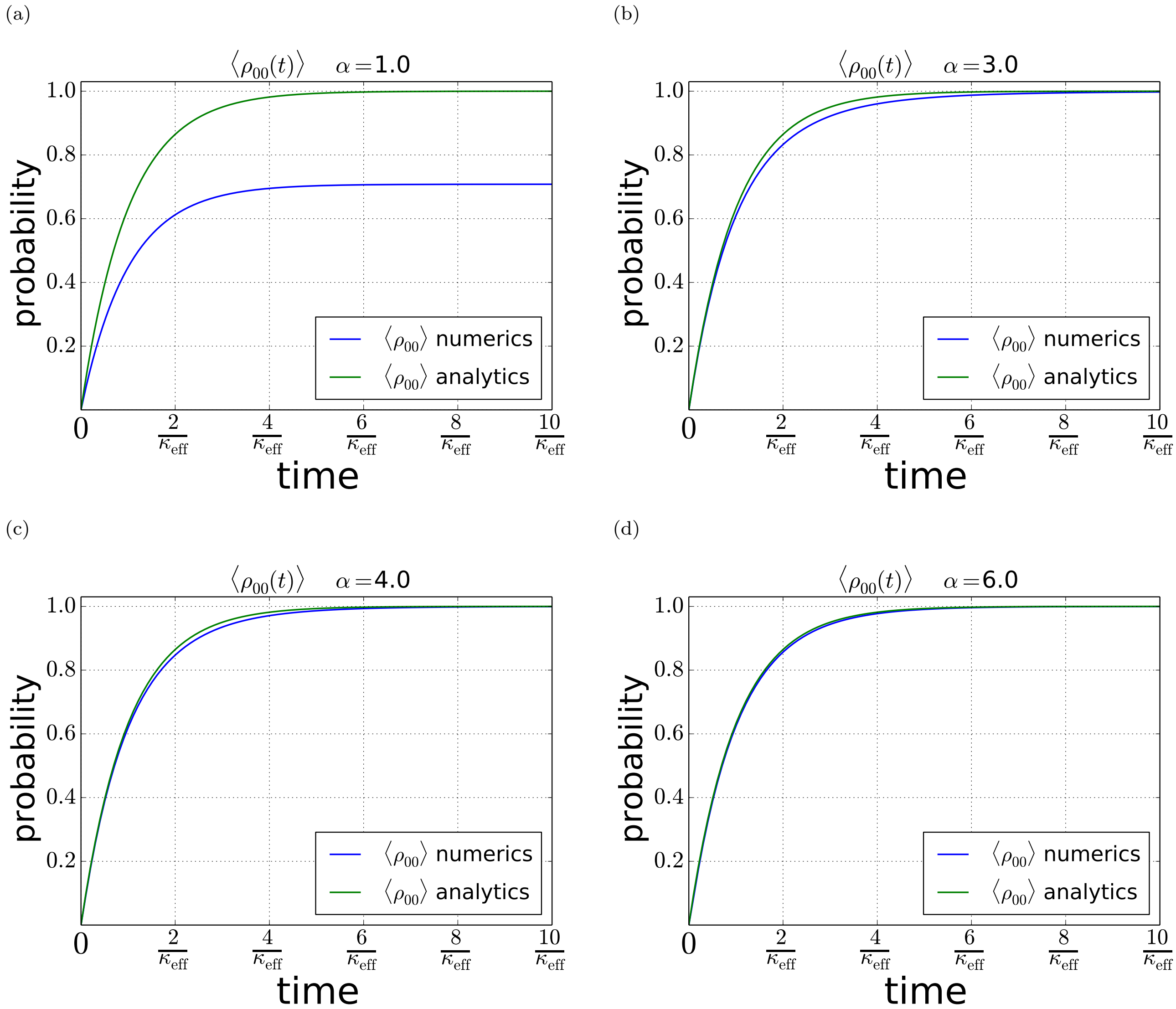

Figure 11: Occupation probability $\langle\rho_{00}(t)\rangle$ of the continuum state of a cavity coupled to the JPM with different alpha. We compare the analytic with the numerical solution. The time scale changes with different α because the effective decay rate κ_{eff} grows with bigger α.
(a) $\alpha = 1$ (b) $\alpha = 3$
(c) $\alpha = 4$ (d) $\alpha = 6$

3.7 κ_{eff} at short times with Non-Markovian behaviour

If we do a proper expansion of ρ_{00} (Eq. (83) for $\frac{\beta^2}{\kappa^2} \ll 1$ we get

$$\rho_{00}(t) = \frac{\beta_n^2}{\kappa^2 - 16\beta_n^2}\left(\left(e^{-\frac{4\beta_n^2}{\kappa}t} - e^{-\kappa t}e^{\frac{4\beta_n^2}{\kappa}t}\right) + \frac{\kappa^2}{2\beta_n^2}\left(1 - e^{-\frac{4\beta_n^2}{\kappa}t}\right) + 4\left(e^{-\frac{\kappa}{2}t} - 1\right)\right) \tag{131}$$

Since $\kappa \gg \beta_n$ the second term will be dominant. According to section 3.1 we get for $\beta_n \approx g_J|\alpha|$ the effective decay rate

$$\kappa_{\text{eff}}^{\text{JPM}} = \frac{4g_J^2|\alpha|^2}{\kappa_J}. \tag{132}$$

And $\rho_{00}(t)$ simplifies to

$$\rho_{00}(t) \approx 1 - \exp(-\kappa_{\text{eff}}^{\text{JPM}} t). \tag{133}$$

If we expand $\rho_{00}(t)$ from equation (131) in time we can see that this approximation does not hold. For short times the occupation probability of the continuum becomes

$$\rho_{00}(t \ll 1) \approx \frac{g_J^2 |\alpha|^2 \kappa_J}{3} t^3. \tag{134}$$

So for short times the effective decay rate does not hold any more. To find out at which times this is the case we compare the exponential decay with the effective decay rate in equation (133) and the expansion of $\rho_{00}(t)$ in t from equation (134).
This effect is crucial for the calculation of errors that occur during the measurement at short times. Because for very short times the exponential decay can be approximated linearly but in reality ρ_{00} behaves t^3.

$$\frac{d^2}{dt^2}\rho_{00} = \frac{4\beta^2\kappa_J\left(-\frac{\left(-\sqrt{\frac{\kappa_J^2}{4}-4\beta^2}-\frac{\kappa_J}{2}\right)^2 e^{t\left(-\sqrt{\frac{\kappa_J^2}{4}-4\beta^2}-\frac{\kappa_J}{2}\right)}}{\sqrt{\frac{\kappa_J^2}{4}-4\beta^2}+\frac{\kappa_J}{2}} + \left(\sqrt{\frac{\kappa_J^2}{4}-4\beta^2}-\frac{\kappa_J}{2}\right) e^{t\left(\sqrt{\frac{\kappa_J^2}{4}-4\beta^2}-\frac{\kappa_J}{2}\right)} + \kappa_J e^{-\frac{1}{2}(\kappa_J t)}\right)}{\kappa_J^2 - 16\beta^2} \tag{135}$$

Since t^3 has a positive curvature and $1 - \exp(-\kappa_{eff} t)$ a negative curvature we only have to find the point where the 2nd derivative is zero. This is then the time where the short time approximation t^3 crosses over to the exponential behaviour.
If we go to the limit $\kappa_J \gg \beta$ it simplifies to

$$\approx \frac{4\beta^2\kappa_J}{\kappa_J^2 - 16\beta^2}\left(\kappa_J e^{-\frac{\kappa_J}{2}t} - \frac{4\beta^2}{\kappa_J} e^{-\frac{4\beta^2}{\kappa_J}t} - e^{-\kappa_J t + \frac{4\beta^2}{\kappa_J}t}\right). \tag{136}$$

To find the time where this approximation is zero we can expand the exponentials and solve a polynomial equation. Since we are in the short time limit of this expression this is reasonable. If we neglect $\mathcal{O}(\beta^2/\kappa_J^2)$ terms we find that at the time scale of

$$t_{BM} = \frac{1}{\kappa_J} \tag{137}$$

we change from the t^3 to exponential behaviour. Since the only boundaries we have for the decay rate are $\kappa_J \ggg_J \gg \chi$ we theoretically can keep this time scale as small as we want by going to the limit $\kappa_J \to \infty$. If we would like to include this behaviour in our calculations we would have to go to the so called Non-Markovian limit where the Born-Markov approximation does not hold any more and the environment has a memory. In this limit one could model a decay function $\kappa(t)$ which full fills the properties $\rho_{00}(t \ll 1) \approx t^3$ and $\rho_{00}(t > 0) \approx 1 - \exp(-\kappa t)$. We do not have any restrictions on κ_J we can go to time scales t_{BM} where the Born-Markov approximation holds almost from the very beginning and the non-Markovian behaviour is negligible. Therefore we neglect it in this thesis. In [16] there is a discussion about the non-Markovian limit of Jaynes-Cummings which could lead to a better understanding of short time inaccuracy.

4 Quantum Trajectory

In the last sections we tried to understand the cavity-JPM interaction with master equations. We have been able to derive an effective decay rate for a lossy cavity which is a good approximation for this system. A master equation is the average over infinitely many measurements and ignores the outcome of the measurement. Since we want to model a quantum measurement and its back-action on the system being measured we need a formalism that goes beyond the master equation and keeps track of the measurement outcome. A trajectory on the other hand is a conditional

state which reproduces the physics of a system to given stochastic variables. The quantum trajectory formalism provides us with a description of the state of the measured system that accounts for the information gained during the measurement. Therefore we can model again a lossy cavity with the effective decay rate κ_{eff} and use the trajectories to investigate what happens to the system if we would detect a decaying photon.
An other thing we can keep track of in the quantum trajectory picture is that the full model only loses one photon because the JPM cuts off the decay. If we do the mapping from the full system to a leaky cavity with an effective decay rate κ_{eff} we lose this feature. A leaking cavity just keeps on decaying until its amplitude is zero. But now in the trajectory picture we can just investigate the system until it loses the first photon and take the cut-off behaviour into account.

4.1 Theory

The main idea of a quantum trajectory is to keep track of every measurement of the system. The master equation on the other side is an averaged solution over infinitely many measurements. If we know every measurement record (REC) we can write the density matrix as the sum over every possible measurement outcome. [9]

$$\rho = \sum_{REC} P_{REC} |\psi_{REC}\rangle\langle\psi_{REC}|, \tag{138}$$

where P_{REC} is the probability of a certain measurement outcome. A possible measurement of our system could have the form

$$REC = \left\{ \emptyset,\ \begin{matrix}\gamma_J \\ t_J\end{matrix},\ \emptyset \right\}, \tag{139}$$

which means that first nothing is recorded until a photon γ_J has been detected at time t_J and afterwards nothing is recorded any more. If we now measure only a single record REC, we know that we are in the state

$$\rho = |\psi_{REC}\rangle\langle\psi_{REC}|, \tag{140}$$

which is a pure state and can be unraveled and be represented as a state $|\psi_{REC}\rangle$ instead of a density matrix ρ. This state is called a quantum trajectory.
If we now want to unravel an arbitrary density matrix we have to go back to the master equation. A state $\rho(t)$ at zero temperature in Born-Markov regime evolves according to the Linblad master equation

$$\dot{\rho}(t) = -i\,[H, \rho] + \kappa\mathcal{D}\,[a]\,\rho(t) \tag{141}$$

We can rewrite the Lindblad super operator into a part between the photon decays $\mathcal{L}_B$ and in a part that causes the photon decay $\mathcal{S}_\kappa$. [9]

$$\dot{\rho} = (\mathcal{L}_B + \mathcal{S}_\kappa)\rho \tag{142}$$

Where

$$\mathcal{L}_B \cdot = -i\,[H, \cdot] - \frac{\kappa}{2}(a^\dagger a \cdot + \cdot\, a^\dagger a) \tag{143}$$

$$\mathcal{S}_\kappa \cdot = \kappa a \cdot a^\dagger. \tag{144}$$

If we have a pure initial state $\rho = |\psi\rangle\langle\psi|$ we can rewrite the term between the jumps with the non hermitian Hamiltonian $H_B = H - i\frac{\kappa}{2}a^\dagger a$

$$\mathcal{L}_B|\psi\rangle\langle\psi| = \frac{1}{i}(H_B|\psi\rangle\langle\psi| + |\psi\rangle\langle\psi|H_B{}^\dagger) \tag{145}$$

If H_B is plugged in, one can see that this is equivalent to the master equation without the jump term $\kappa a \cdot a^\dagger$.
We can solve Eq. (142) without the jump part formally as $\rho(t) = \exp(\mathcal{L}_B t)\rho(0)$. And in the derivation in Appendix 10.7 we can see that the following relation holds:

$$\rho(t) = \exp(\mathcal{L}_B t)\rho(0) = \exp(-iH_B t)\rho(0)\exp(iH_B t) \tag{146}$$

Important about this is that if we start in a pure state $\rho(0) = |\psi\rangle\langle\psi|$ the state remains pure and we can unravel the density matrix at any time in a state $|\psi\rangle = \exp(-iH_B t)|\psi(0)\rangle$. If we also want to include the jump part of the Lindblad operator into this pure state we can look at it the following way:

The time evolution of the state is given by the differential equation

$$\frac{d}{dt}|\psi\rangle = -iH_B|\psi\rangle. \tag{147}$$

Since H_B is non hermitian we have to renormalise the state $|\psi'\rangle = |\psi\rangle + d|\psi\rangle$ an infinitesimally short time after the state $|\psi\rangle$. Which is

$$|\psi'\rangle = \left(1 - iH\ dt - \frac{\kappa}{2}a^\dagger a\ dt\right)|\psi\rangle. \tag{148}$$

If we demand $\langle\psi'|\psi'\rangle \stackrel{!}{=} 1$ we get the following relation:

$$\langle\psi'|\psi'\rangle = \langle\psi'|\left(1 + iH\ dt - \frac{\kappa}{2}a^\dagger a\ dt\right)\left(1 - iH\ dt - \frac{\kappa}{2}a^\dagger a\ dt\right)|\psi'\rangle = 1 - \kappa\langle a^\dagger a\rangle dt. \tag{149}$$

Here we used the Ito rule [15] $dt^2 = 0$ and therefore we get the normalized state

$$|\psi'\rangle = \frac{1 - iH\ dt - \frac{\kappa}{2}a^\dagger a\ dt}{\sqrt{1 - \kappa\langle a^\dagger a\rangle\ dt}}|\psi\rangle = \left(1 - iH\ dt - \frac{\kappa}{2}\left(a^\dagger a - \langle a^\dagger a\rangle\right)dt\right)|\psi\rangle. \tag{150}$$

At some time during this evolution a photon can decay from the cavity which we can model by applying an annihilation operator on the state $\sqrt{\kappa}a|\psi\rangle$. Since the decay is instantaneous we do not have to include time evolution when a jump happens. If we normalize this jump part we get

$$|\psi'\rangle = \frac{a}{\sqrt{\langle a^\dagger a\rangle}}|\psi\rangle \tag{151}$$

An infinitesimal change of our state is given by $d|\psi\rangle = |\psi'\rangle - |\psi\rangle$. If we introduce the stochastic variable dN which is 1 if a jump happens and 0 if not we can put the time evolution and the jump part together and can write the change of our state as

$$d|\psi\rangle = -\left(iH\ dt + \frac{\kappa}{2}\left(a^\dagger a - \langle a^\dagger a\rangle\right)dt\right)|\psi\rangle + \left(\frac{a}{\sqrt{\langle a^\dagger a\rangle}} - 1\right)dN\ |\psi\rangle. \tag{152}$$

This is the stochastic Schrödinger equation.

4.2 Analytic solution of the stochastic Schrödinger equation

The stochastic Schrödinger equation is non-linear because of the appearance of $\langle a^\dagger a\rangle$ which makes the solution complicated. By choosing the normalization such that $\langle a^\dagger a\rangle = 1$ we can simplify the equation to the linear stochastic Schrödinger equation which we can solve. [3]

$$d|\psi\rangle = \left(\frac{\kappa}{2} - iH - \frac{\kappa}{2}a^\dagger a\right)\ dt\ |\psi\rangle + (a - 1)\,dN\ |\psi\rangle \tag{153}$$

Using the identity $1 + A\ dN = \exp(\ln(1 + A)dN) = (1 + A)^{dN}$, which follows from the fact that $dN^2 = dN$, and that $dt\ dN = 0$ we can write to first order in dt

$$|\psi(t + dt)\rangle = |\psi(t)\rangle + d|\psi\rangle = \exp\left(\left(\frac{\kappa}{2} - iH - \frac{\kappa}{2}a^\dagger a\right)dt\right)a^{dN}|\psi(t)\rangle \tag{154}$$

By applying the reordering identity $a\exp(\varepsilon a^\dagger a) = \exp(\varepsilon)\exp(\varepsilon a^\dagger a)a$ repeatedly we find the unnormalized solution of the stochastic Schrödinger equation which we will also refer to as a quantum trajectory

$$|\psi(t)\rangle = \exp\left\{\left[\frac{\kappa}{2} - \left(iH + \frac{\kappa}{2}\right)a^\dagger a\right]t\right\}\exp\left\{-\left(iH + \frac{\kappa}{2}\right)Y(t)\right\}a^{N(t)}|\psi(0)\rangle, \tag{155}$$

with $Y(t) = \int_0^t dt' N(t') = \sum_{n=1}^{N(t)} t_n$. This stochastic variable sums up all the jump times t_n and is zero until the first jump occurs, then it is constantly t_1 until the second jump occurs etc.

5 Master equation vs. Quantum trajectories picture

In this section we investigate a single qubit that is coupled to a cavity which is initially either in a Fock state or in a coherent state. First we will consider a perfect cavity with no leakage. Later we will also include leakage. We will use these few examples to understand the mechanisms of quantum trajectory when we compare them with the master equation. For the non leaking cases the solution of the master equation and the trajectory are identical. Which should be clear, since there are no photon jumps. The Hamiltonian of the system is

$$H = \omega_C a^\dagger a + \frac{\omega_{qb}}{2}\sigma^z + \chi a^\dagger a \sigma^z. \tag{156}$$

5.1 Cavity in a Fock state, without leakage

The first simple case we investigate is a single qubit dispersively coupled to a cavity in a Fock state $|4\rangle$. The cavity occupation constant at $\langle a^\dagger a\rangle = 4$.
If we go to a rotating frame with the bare qubit frequency ω_{qb} and the bare cavity frequency ω_C the time evolution is simply determined by the Hamiltonian $H = \chi a^\dagger a \sigma^z$. If we choose our initial state to be $|\psi_0\rangle = \frac{1}{\sqrt{2}}(|e\rangle + |g\rangle) \otimes |m\rangle$, the state at a certain time is given by

$$|\psi(t)\rangle = e^{-\chi a^\dagger a \sigma^z t}|\psi_0\rangle = \frac{1}{\sqrt{2}}(e^{-i\chi m t}|e\rangle + e^{+i\chi m t}|g\rangle) \otimes |m\rangle. \tag{157}$$

Between the qubit states there is now a phase. With this specific initial state the qubit points in x-direction on the Bloch sphere at the start and $\langle\sigma^x(t)\rangle = \cos(2m\chi t)$. With the time evolution it starts rotating in the x-y-plane and it will point again in x-direction if the phase becomes $e^{\pm i\chi m t} = e^{\pm i\pi}$. Therefore the frequency of the qubit rotation depends on the state of the cavity and the phase between the qubit states vanishes for $\chi m t = \pi$. In figure 12 the phase of the qubit is visible.

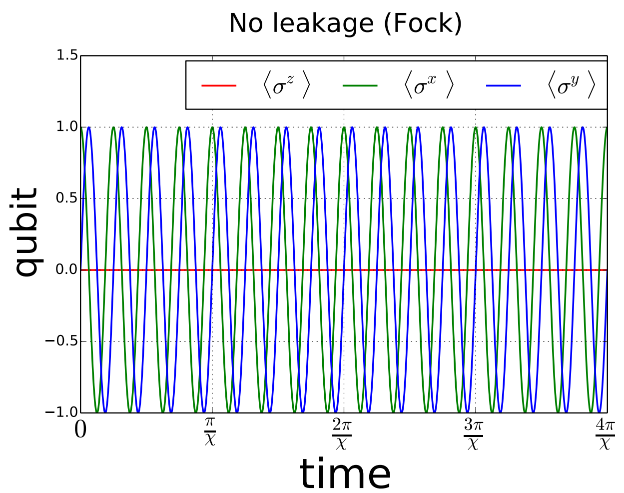

Figure 12: **Initial Fock, no leakage:** qubit coupled to cavity with no leakage. The cavity is in a Fock state of $|4\rangle$

5.2 Cavity in a coherent state, without leakage

If we are initially in a coherent state and start with $|\psi_0\rangle = \frac{1}{\sqrt{2}}(|e\rangle + |g\rangle) \otimes |\alpha\rangle$, we get

$$|\psi(t)\rangle = e^{-\chi a^\dagger a \sigma^z t}|\psi_0\rangle = c_e|e\rangle \otimes |e^{-i\chi t}\alpha\rangle + c_g|g\rangle \otimes |e^{+i\chi t}\alpha\rangle. \tag{158}$$

and,

$$\langle\sigma^x\rangle = \langle\psi(t)|\sigma^x|\psi(t)\rangle = c_e^* c_g \langle e^{-i\chi t}\alpha|e^{+i\chi t}\alpha\rangle + c_e c_g^* \langle e^{+i\chi t}\alpha|e^{-i\chi t}\alpha\rangle = c_e^* c_g e^{-|\alpha|^2(1-e^{-2i\chi t})} + c_e c_g^* e^{-|\alpha|^2(1-e^{+2i\chi t})}. \tag{159}$$

In the last step we used the relation $\langle\alpha|\beta\rangle = \exp(-(|\alpha|^2 + |\beta|^2)/2 + \alpha^*\beta)$.
$\langle\sigma^x\rangle$ is maximal for $(1 - e^{\pm 2i\chi t}) = 0$. This is the case if $t = \pi/\chi$. At this point we have the first revival which can be seen in figure 13 The difference to the initial Fock state is, that in the coherent case the revival is just dependent on χ and the number of qubits and not on the cavity amplitude.

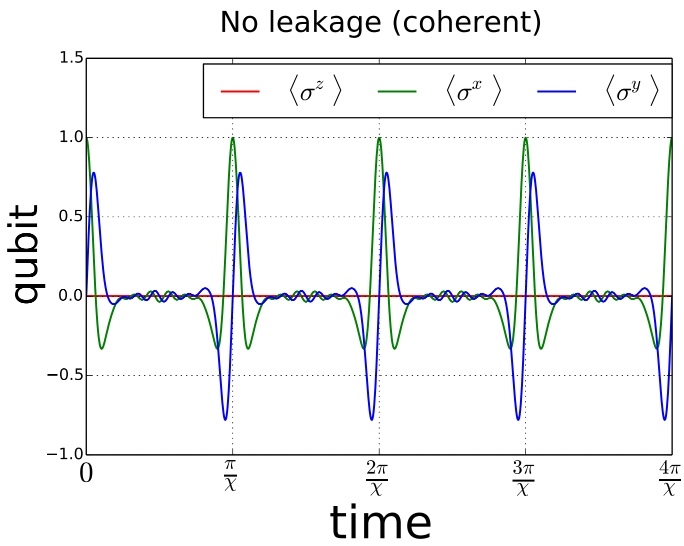

Figure 13: **Initial coherent, no leakage:** qubit coupled to cavity with no leakage. The cavity is in a coherent state with amplitude $\alpha = 3.0$.

5.2.1 Comparison of a coherent and a Fock state

The different behaviour of a qubit coupled to a Fock or a coherent state can be understood if we think of the coherent state as a superposition of Fock states.

$$|\alpha\rangle = e^{-|\alpha|^2/2} \sum_n^\infty \frac{\alpha^n}{\sqrt{n!}}|n\rangle \tag{160}$$

If the qubits are coupled to a Fock state $|m\rangle$ we know that the speed of the phase rotation between the qubits is dependent on m. So if we couple a qubit to a coherent state $\langle\sigma^x\rangle$, it is approximately a superposition of $\sum_m \cos(2m\chi t)$ and these cosine interfere always except at $t = \frac{\pi}{\chi}$.
But it is not obvious why $\langle\sigma^x\rangle$ almost vanishes between the revivals with this picture because there might be a point where the $\cos(2mt\chi)$ factors do not completely interfere. A simple explanation for that is, if we have a look at the time evolution in the coherent case. In contrast to the cavity in the Fock state we do not get a simple phase between the qubits by the time evolution. The time evolution is absorbed into the coherent state which can bee seen in equation (158)
To calculate the expectation value we have to calculate the matrix elements $\langle e^{-i\chi t}\alpha|e^{+i\chi t}\alpha\rangle$. But these are coherent states that are rotating in opposite direction and therefore have almost no overlap except for the times $t = \frac{n\pi}{\chi}$ with $n \in \mathbb{N}$. This behaviour has already been described in section 1.4 figure 6.

5.3 Cavity in a Fock state, with leakage

The quantum trajectory with the Hamiltonian $H = \omega a^\dagger a + \chi\sigma^z a^\dagger a$ of a cavity dispersively coupled to a single qubit but now with leakage is

$$|\psi(t)\rangle = \exp\left\{\left[\frac{\kappa}{2} - \left(i\omega + i\chi\sigma^z + \frac{\kappa}{2}\right)a^\dagger a\right]t\right\}\exp\left\{-\left(i\omega + i\chi\sigma^z + \frac{\kappa}{2}\right)Y(t)\right\}a^{N(t)}|\psi(0)\rangle \tag{161}$$

and for a cavity with leakage we get the following results:

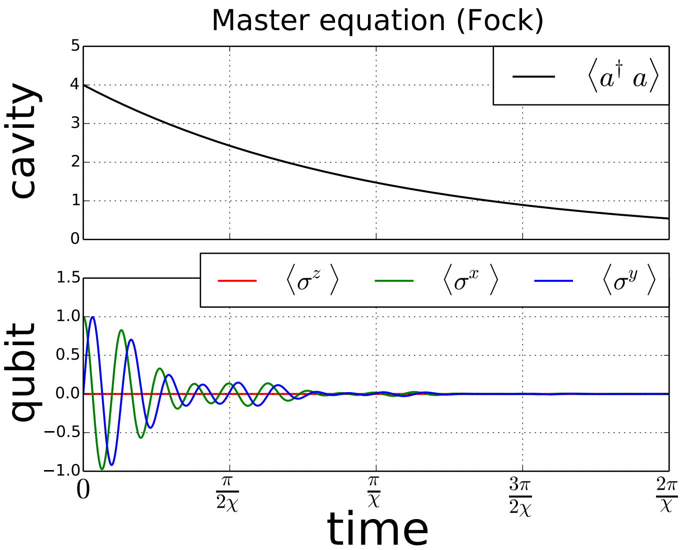

Figure 14: **Master Equation, Cavity initially in Fock with leakage:** qubit coupled to cavity with leakage. The cavity is initially prepared in a Fock state $|4\rangle$. The decay rate κ is set such that $1/\kappa = \pi/\chi$.

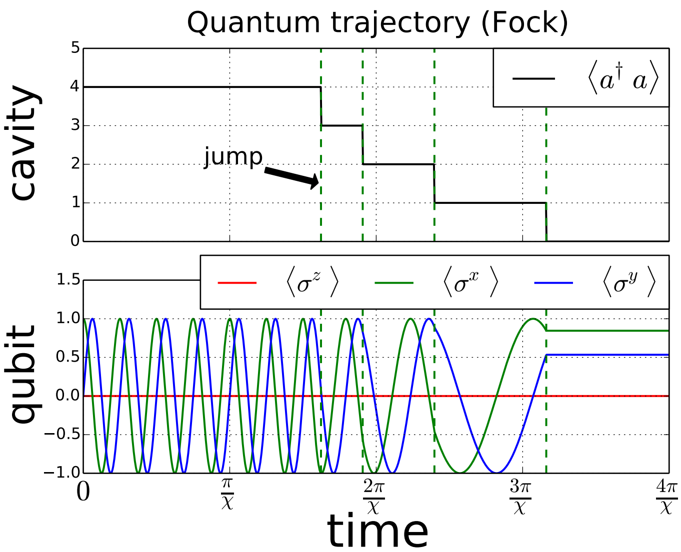

Figure 15: **Quantum Trajectory: Initial fock with leakage:** qubit coupled to cavity with leakage. The cavity is initially prepared in a Fock state $|4\rangle$. The decay rate κ is set such that $1/\kappa = \pi/\chi$.

In this case for the trajectory picture there is still no loss of coherence. The Bloch vector has always the length 1 and spins with a frequency that depends on the number of photons that are still left in the cavity. So there is always a revival except for the case where the last photon leaves the cavity and the Bloch vector freezes. With our initial state $|\psi_0\rangle = (c_e|e\rangle + c_g|g\rangle) \otimes |m\rangle$ the trajectory from Eq. (161) gets the form

$$\begin{aligned}
|\psi(t)\rangle = &\exp\left\{\frac{\kappa}{2}t\right\}\exp\left\{-\left(i\omega+\frac{\kappa}{2}\right)(m-N(t))t\right\}\exp\left\{-\left(i\omega+\frac{\kappa}{2}\right)Y(t)\right\}\sqrt{\frac{m!}{(m-N)!}} \\
&\times\Bigg[c_e\exp\left\{-i\chi(m-N(t))t\right\}\exp\left\{-i\chi Y(t)\right\}|e\rangle \\
&+c_g\exp\left\{+i\chi(m-N(t))t\right\}\exp\left\{+i\chi Y(t)\right\}|g\rangle\Bigg]\otimes|m-N(t)\rangle.
\end{aligned} \tag{162}$$

For this purpose we can simplify it to the form

$$\begin{aligned}
|\psi(t)\rangle = \mathcal{N}(N)\mathcal{N}(Y(t))\Bigg[&c_e\exp\left\{-i\chi(m-N(t))t\right\}\exp\left\{-i\chi Y(t)\right\}|e\rangle \\
&+c_g\exp\left\{+i\chi(m-N(t))t\right\}\exp\left\{+i\chi Y(t)\right\}|g\rangle\Bigg]\otimes|m-N(t)\rangle,
\end{aligned} \tag{163}$$

because the first line in equation (162) only affects the normalization and gives a global phase. This factor will vanish after the normalization of the state.
The operators $a^\dagger a$ only affect the state $|m-N(t)\rangle$ to calculate the expectation value $\langle a^\dagger a\rangle = \langle\psi(t)|a^\dagger a|\psi(t)\rangle$. Therefore

$$\langle a^\dagger a\rangle = \langle m-N(t)|a^\dagger a|m-N(t)\rangle \propto m-N(t), \tag{164}$$

which corresponds to the Figure 15. $N(t)$ is a stochastic variable that starts at 0 and is increased by 1 at every jump. So after $N(t)$ losses of photons the cvaity is obviously in the state $m-N(t)$.
The calculation of the expectation value of σ^x leads to

$$\langle\sigma^x\rangle = \Big[c_e c_g^*\exp\left\{-2i\chi(m-N(t))t\right\}\exp\left\{-2i\chi Y(t)\right\} + c_e^* c_g\exp\left\{+2i\chi(m-N(t))t\right\}\exp\left\{+2i\chi Y(t)\right\}\Big]. \tag{165}$$

In the figure 15 we see, that after every jump the frequency of the qubit rotation decreases. This comes from the factor $\exp\{-2i\chi(m-N(t))t\}$. The rotation starts with the frequency $2\chi m$ and is decreased with every jump by 2χ until it stops at $N(t)=m$. This corresponds to the simulation. The factor $\exp\{-2i\chi Y(t)\}$ is the phase that the qubit gained until the jump occurred. $Y(t)$ can be understood as the memory of our wave function. We can interpret the wave function as follows: The qubit rotates until the first jump occurred with the frequency $2i\chi m$ and after the jump it rotates with the reduced frequency $2i\chi(m-1)$. If we would not include the term $\exp(-2i\chi Y(t))$ in our wave function we would only know the rotation frequency at a certain time t but not the phase the qubit has gained until that time.

5.4 Cavity in a coherent state, with leakage

A similar examination of two qubits coupled to a cavity in a coherent state has already be done by Govenius et al. [17]. We would like to apply their results on the same case as we have discussed before, a single qubit coupled to a cavity to compare all possible cases. Since in the end we will have multi qubit states that are coupled to a cavity in a coherent state, we will need this case for our approximation of the full system with the effective model.

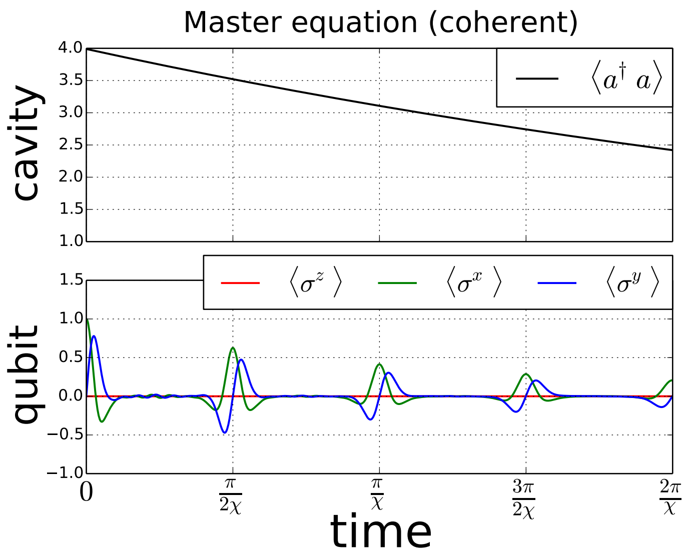

Figure 16: **Master equation: Initial coherent with leakage:** qubit coupled to cavity with leakage. The cavity is in a coherent state with $\alpha = 2.0$. The decay rate κ is set such that $1/\kappa = \pi/\chi$.

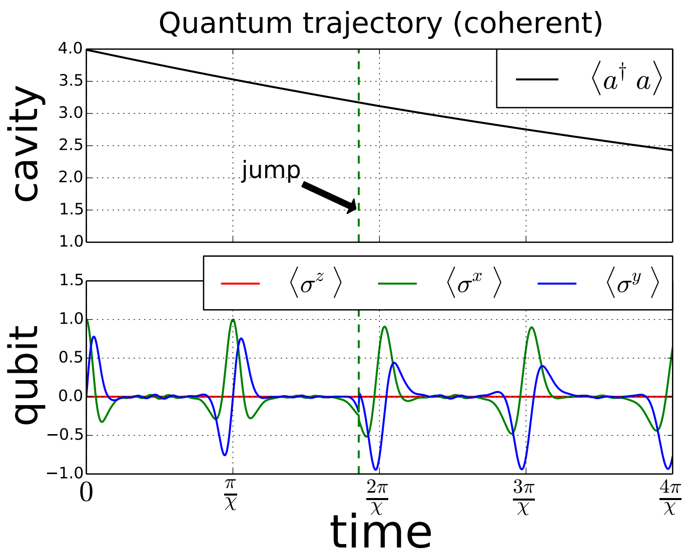

Figure 17: **Quantum trajectory, Cavity initially coherent with leakage:** qubit coupled to cavity with leakage. The cavity is in a coherent state with $\alpha = 2.0$. The decay rate κ is set such that $1/\kappa = \pi/\chi$.

At first we see, that the cavity occupation decays exponentially with $e^{-\kappa t}$. We again start with the analytic solution for the quantum trajectory for a leaking cavity dispersively coupled to a single qubit from Eq. (161).
With the initial state $|\psi(0)\rangle = (c_e|e\rangle + c_g|g\rangle) \otimes |\alpha\rangle$ we get

$$
\begin{aligned}
|\psi(t)\rangle &= \overbrace{\alpha^{N(t)}\exp\left\{\frac{\kappa}{2}t\right\}}^{\mathcal{N}(N)}\overbrace{\exp\left\{-(i\omega+\frac{\kappa}{2})Y(t)\right\}}^{\mathcal{N}(Y(t))} \\
&\times\left\{c_e e^{-i\chi Y(t)}|e\rangle\otimes e^{-\frac{|\alpha|^2}{2}}\sum_n\frac{\alpha^n}{\sqrt{n!}}e^{-(i\omega+\frac{\kappa}{2}+i\chi)nt}|n\rangle + c_g e^{+i\chi Y(t)}|g\rangle\otimes e^{-\frac{|\alpha|^2}{2}}\sum_n\frac{\alpha^n}{\sqrt{n!}}e^{-(i\omega+\frac{\kappa}{2}-i\chi)nt}|n\rangle\right\} \\
&= \mathcal{N}(N)\mathcal{N}(Y(t))\left\{c_e e^{-i\chi Y(t)}|e\rangle\otimes e^{-\frac{|\alpha|^2}{2}(1-e^{-\kappa t})}|e^{-(i\omega+\frac{\kappa}{2}+i\chi)t}\alpha\rangle\right. \\
&\left. +c_g e^{+i\chi Y(t)}|g\rangle\otimes e^{-\frac{|\alpha|^2}{2}(1-e^{-\kappa t})}|e^{-(i\omega+\frac{\kappa}{2}-i\chi)t}\alpha\rangle\right\}.
\end{aligned}
\tag{166}
$$

Here we had to keep in mind, that the state $|e^{-(i\omega+\frac{\kappa}{2}+i\chi)t}\alpha\rangle = e^{-\frac{|\alpha|^2}{2}e^{-\kappa t}}\sum_n e^{-(i\omega+\frac{\kappa}{2}+i\chi)nt}\frac{\alpha^n}{\sqrt{n!}}|n\rangle$ has a different normalization than the original $|\alpha\rangle$ because the damping factor $e^{-\frac{\kappa}{2}t}$ in the cavity state affects the norm. But since this factor appears as a factor in both qubit subspaces we can also absorb it in the norm and denote it as $\mathcal{N}(\alpha) = e^{-\frac{|\alpha|^2}{2}(1-e^{-\kappa t})}$

$$
|\psi(t)\rangle = \mathcal{N}(N)\mathcal{N}(\alpha)\mathcal{N}(Y(t))\left\{c_e e^{-i\chi Y(t)}|e\rangle\otimes|e^{-(i\omega+\frac{\kappa}{2}+i\chi)t}\alpha\rangle + c_g e^{+i\chi Y(t)}|g\rangle\otimes|e^{-(i\omega+\frac{\kappa}{2}-i\chi)t}\alpha\rangle\right\}
\tag{167}
$$

To normalize this state we only have to apply a prefactor of $\frac{1}{\mathcal{N}(N)\mathcal{N}(\alpha)\mathcal{N}(Y(t))}$ because from the initial state we already know that $(|c_e|^2+|c_g|^2)=1$. If we calculate now the cavity occupation $\langle a^\dagger a\rangle$ we get

$$
\langle\psi(t)|a^\dagger a|\psi(t)\rangle = \underbrace{(|c_e|^2+|c_g|^2)}_{=1}|\alpha|^2 e^{-\kappa t} = |\alpha|^2 e^{-\kappa t}.
\tag{168}
$$

For the decoherence we get

$$
\langle\sigma^x\rangle = \left\{c_e c_g^* e^{-2i\chi Y(t)}\langle\overbrace{e^{-(i\omega+\frac{\kappa}{2}+i\chi)t}\alpha}^{\beta}|\overbrace{e^{-(i\omega+\frac{\kappa}{2}-i\chi)t}\alpha}^{\gamma}\rangle + h.c.\right\}.
\tag{169}
$$

Here we can use that $\langle\beta|\gamma\rangle = e^{-\frac{|\beta|^2+|\gamma|^2}{2}+\beta^*\gamma}$ and we get

$$
\begin{aligned}
\langle\sigma^x\rangle &= \left\{c_e c_g^* e^{-2i\chi Y(t)}e^{-|\alpha|^2 e^{-\kappa t}(1-e^{2i\chi t})} + h.c.\right\} \\
&= \left\{c_e c_g^* e^{-2i\chi Y(t)}\underbrace{e^{-|\alpha|^2 e^{-\kappa t}(1-\cos(2\chi t))}}_{Amplitude}\underbrace{e^{i|\alpha|^2 e^{-\kappa t}\sin(2\chi t)}}_{Phase}+h.c.\right\}.
\end{aligned}
\tag{170}
$$

To interpret this we have to look at the factors separately. The factor $e^{-|\alpha|^2 e^{-\kappa t}(1-2i\chi t)}$ can be split in a real amplitude part and an imaginary phase part. The amplitude is maximal if $\cos(2\chi t)=1$ which is again the revival condition $t_{\text{rev}} = \pi n/\chi$. The phase is also time dependent and is zero for the revival condition because $\sin(2\chi t_{\text{rev}})=0$. If we picture the qubit again in the Bloch sphere it starts in x direction if we choose $c_e = c_g = 1/\sqrt{2}$ The amplitude decreases with the time and increases back to 1 at the revival. But the rotation in x-y-plane is not a whole rotation any more. If we start in x-direction it is a small oscillation around the x-axis in the x-y-plane. The factor $e^{-2i\chi Y(t)}$ is a phase factor that changes its value at every jump. So when a jump occurs the qubit can flip in every direction in the x-y plane. This can also be seen in the Figure 17. So the whole motion that comes from the first factor is still unchanged but not any more along the initial direction which was in our case the x-axis. Furthermore the jump is not visible in the cavity occupation because a coherent state $|\alpha\rangle$ is an eigenstate of the annihilation operator a.

5.5 Average trajectories, to get back to the density matrix picture

In this section we would like to show that the average of infinitely many trajectories leads to the same result as the solution of a master equation. Since we would like to investigate qubits dispersively coupled to a cavity in the end we show it with the simple case of one dispersively coupled qubit to a cavity. For simplicity we choose the cavity to be initially in a Fock state which will also simplify the averaging.

5.5.1 Cavity in Fock state

For $H = (\omega + \chi\sigma^z)a^\dagger a$ the trajectory has the form

$$|\psi(t)\rangle = \exp\left\{\left[\frac{\kappa}{2} - \left(i\omega + i\chi\sigma^z + \frac{\kappa}{2}\right)a^\dagger a\right]t\right\}\exp\left\{-\left(i\omega + i\chi\sigma^z + \frac{\kappa}{2}\right)Y(t)\right\}a^{N(t)}|\psi(0)\rangle. \tag{171}$$

If we have the initial state $|\psi(0)\rangle = (c_e|e\rangle + c_g|g\rangle) \otimes |m\rangle$ it gets the form

$$\begin{aligned}|\psi(t)\rangle = &\exp\left\{\frac{\kappa}{2}t\right\}\exp\left\{-\left(i\omega + \frac{\kappa}{2}\right)(m - N(t))t\right\}\exp\left\{-\left(i\omega + \frac{\kappa}{2}\right)Y(t)\right\}\sqrt{\frac{m!}{(m-N)!}}\\ &\times\Big[c_e\exp\{-i\chi(m - N(t))t\}\exp\{-i\chi Y(t)\}|e\rangle\\ &+ c_g\exp\{+i\chi(m - N(t))t\}\exp\{+i\chi Y(t)\}|g\rangle\Big] \otimes |m - N(t)\rangle.\end{aligned} \tag{172}$$

At first we have to realize that $|\psi\rangle$ is not normalized and we have to be careful with the normalization. Therefore we denote the unnormalized state $|\psi\rangle$ and the normalized state $|\hat{\psi}\rangle$. The probability density of the final state $|\psi\rangle$ is given by

$$P(|\psi\rangle, t) = \int_0^t \langle\psi|\psi\rangle\tilde{P}(N, \{t_i\}, t), \tag{173}$$

where $\tilde{P}(N, \{t_i\}, t)$ is the joint ostensible probability distribution for having had, after time t, N jumps at the times $t_1...t_N$. $\tilde{P}(N, \{t_i\}, t) = \tilde{P}(N, t)\tilde{P}(\{t_n\}|N, t)$. Ostensible, because it has to be reassessed with the factor $\langle\psi|\psi\rangle$ to lead to the actual probability $P(|\psi\rangle, t)$ of a certain trajectory $|\psi\rangle$. To find the density matrix we have to asses every normalized trajectory $|\hat{\psi}\rangle$ with its probability.

$$\rho(t) = \sum_{N=0}^{m} P(|\psi\rangle, t)|\hat{\psi}\rangle\langle\hat{\psi}| \tag{174}$$

The bare qubit density matrix is the partial trace of $\rho(t)$ over the cavity states,

$$\rho_{qb}(t) = \sum_n \langle n|\rho(t)|n\rangle \tag{175}$$

If we now plug together the equations (173) and (174) and use that $|\hat{\psi}\rangle = \frac{1}{\mathcal{N}}|\psi\rangle$ and $\mathcal{N} = \sqrt{\langle\psi|\psi\rangle}$ the calculation simplifies to.

$$\rho(t) = \sum_N^m \int_0^t P(N, \{t_i\}, t)|\psi\rangle\langle\psi|dt_1 \cdots dt_N \tag{176}$$

As an example for the matrix element $|e\rangle\langle g|$ we get

$$\rho^{\uparrow\downarrow}(t) = \sum_N^m \int_0^t \underbrace{e^{\kappa t}\frac{m!}{(m-N)!}e^{-\kappa t(m-N)}e^{-\kappa Y(t)}e^{-2i\chi(m-N)}e^{-2i\chi Y(t)}}_{|\psi\rangle\langle\psi|_{eg}}\underbrace{\frac{\kappa^N e^{-\kappa t}}{N!}}_{P(N,\{t_i\},t)}|e\rangle\langle g| \otimes |m - N\rangle\langle m - N|dt_i, \tag{177}$$

where we denote the element $|e\rangle\langle g|$ with $\uparrow\downarrow$ as a short hand notation. Now we can use that $\frac{m!}{(m-N)!}\frac{1}{N!} = \binom{m}{N}$ and trace out the degree of the cavity by applying $\sum_n \langle n| \cdots |n\rangle$.

$$\rho_{qb}^{\uparrow\downarrow} = c_e c_g^* \sum_n^m \left(\frac{\kappa}{\kappa + 2i\chi}\right)^{m-n} \binom{m}{n} e^{-nt(\kappa+2i\chi)} \left(1 - e^{-t(\kappa+2i\chi)}\right)^{m-n} \tag{178}$$

Which can be shown is the same result as we have already found for the master equation in the Appendix 10.8 Eq. (386). By using the binomial formula $(x+y)^m = \sum_n^m \binom{m}{n} x^n y^{m-n}$ we get

$$\rho_{qb}^{\uparrow\downarrow} = c_e c_g^* \left(\frac{\kappa}{\kappa + 2i\chi}\left(1 - e^{-t(\kappa+2i\chi)}\right) + e^{-t(\kappa+2i\chi)}\right)^m \tag{179}$$

$$= \frac{c_e c_g^*}{(\kappa + 2i\chi)^m}\left(\kappa\left(1 - e^{-t(\kappa+2i\chi)}\right) + (\kappa + 2i\chi)e^{-t(\kappa+2i\chi)}\right)^m \tag{180}$$

$$= \frac{c_e c_g^*}{(\kappa + 2i\chi)^m} e^{-mt(\kappa+2i\chi)} \left(\kappa e^{t(\kappa+2i\chi)} + 2i\chi\right)^m . \tag{181}$$

This can be done analogous for every other element of the density matrix of the qubits and verifies that the average over infinitely many quantum trajectories correspond to the solution of the master equation.

5.5.2 Calculation of $\langle\sigma^x\rangle$

If we look at expectation value $\langle\sigma^x\rangle = 2Re[\rho_{qb}^{\uparrow\downarrow}]$ we can examine another phenomena which links the quantum trajectory to the density matrix. We can see that $\langle\sigma^x\rangle$ does not go to zero for $t \to \infty$. The qubit rotation in figure 15 slows down for every photon that leaves the cavity and if the cavity is empty the rotation stops. At which point the rotation stops is completely random and can not be predicted. But we can show that this expectation value averaged over the trajectories converges to zero if we go to higher initial Fock states m or if we increase the qubit rotation frequency χ.

$\langle\sigma^x\rangle$ is proportional to the real part of $\rho_{qb}^{\uparrow\downarrow}$. In the limit $t \to \infty$ Eq. (181) simplifies to

$$\rho_{qb}^{\uparrow\downarrow}(t \to \infty) = \frac{c_e c_g^*}{(\kappa + 2i\chi)^m}\kappa^m = \frac{c_e c_g^*}{(\kappa^2 + 4\chi^2)^m}\kappa^m(\kappa - 2i\chi)^m. \tag{182}$$

To find the real part of this term we have to separate imaginary part and the real part of $(\kappa - 2i\chi)^m$. For a complex number the relation $z^m = r^m e^{im\phi}$ holds. For this let us call

$$z = Re(z) + iIm(z) = \kappa - i\ 2\chi. \tag{183}$$

Therefore

$$r = \sqrt{Re(z)^2 + Im(z)^2} = \sqrt{\kappa^2 + 4\chi^2}. \tag{184}$$

Since we are interested in the minimum of the coherence that is left after starting the evolution in a Fock state $|n\rangle$ we can look at the absolute value of the whole expression for $\rho_{qb}^{\uparrow\downarrow}$ and therefore neglect the phase $e^{im\phi}$

$$|\rho_{qb}^{\uparrow\downarrow}(t \to \infty)| = \frac{c_e c_g^*\ \kappa^m r^m}{(\kappa^2 + 4\chi^2)^m} = \frac{c_e c_g^*\ \kappa^m(\kappa^2 + 4\chi^2)^{m/2}}{(\kappa^2 + 4\chi^2)^m} = \frac{c_e c_g^* \kappa^m}{(\kappa^2 + 4\chi^2)^{m/2}} = \frac{c_e c_g^*}{1 + \frac{4\chi^2}{\kappa^2}} \tag{185}$$

We can physically interpret this result as follows: If we start at Fock states with high occupation numbers, $m \to \infty$, the final values of a single trajectory of $\langle\sigma^x\rangle$ average to zero. So the qubit stop randomly pointing in any direction of the x-y-plane of the Bloch sphere and that averages to zero. If we go with $\kappa \to \infty$ the decay is instantaneous and the qubits stay in the initial direction because they have no time to rotate. And if we go to qubit rotation frequencies $\chi \to \infty$ we end up in a similar case as in $m \to \infty$ because if the qubits initially rotate at high frequencies their direction in the x-y-plane is also distributed equally and averages to zero.

6 Full system numerics in the quantum trajectory picture

Now we go to the 3-qubit case. Since the effective decay rate for the JPM is to first order correction quadratic in the detuning we could not obtain any difference in the decay rate between the parity subspaces for the 2-qubit case because the dispersive shifts of the cavity are equal for the odd states $|01\rangle$ and $|10\rangle$. With 3 qubits we can construct an initial state where the cavity is shifted differently for the same parity states. If we define an odd parity as a state with odd number of qubits in the excited state $|1\rangle$ we construct the initial state

$$|\psi\rangle = \frac{1}{\sqrt{2}}(|\underbrace{111}_{u}\rangle + |\underbrace{100}_{d}\rangle) \otimes |\alpha\rangle \otimes |1\rangle_{\text{JPM}}. \tag{186}$$

To visualize phase factors that we gain in the odd parity subspace it is helpful to map a multi qubit state on a logical qubit state $|u\rangle$ or $|d\rangle$. This is possible because the time evolution caused by the Hamiltonian cannot flip the qubits. Therefore we stay in theses parity subspace. We restrict ourself to the 3-qubit case because the simulation time grows exponentially with the number of qubits.

For a better understanding what happens to the qubits we perform a mapping of the qubits to a 3-qubit Bloch sphere. This can be achieved by defining Pauli operators for 3 qubits similar to the 1 qubit case. This is only possible for two parity subspaces at the same time. This is also a reason why we restrict ourself to the qubit states $|111\rangle$ and $|100\rangle$. We could also include any permutation of the former state but this would us not allow to use the more intuitive picture of a Bloch sphere. We define the Pauli matrices analogous to the 1-qubit case where $|u\rangle$ is the eigenstate of σ^z to the eigenvalue 1, σ^x changes from one qubit state to the other, etc. If we do so we get the following multi qubit Pauli matrices:

$$\sigma_{\tilde{z}} = |\mathrm{u}\rangle\langle\mathrm{u}| - |\mathrm{d}\rangle\langle\mathrm{d}| \tag{187}$$
$$\sigma_{\tilde{x}} = |\mathrm{u}\rangle\langle\mathrm{d}| + |\mathrm{d}\rangle\langle\mathrm{u}| \tag{188}$$
$$\sigma_{\tilde{y}} = -i|\mathrm{u}\rangle\langle\mathrm{d}| + \mathrm{i}|\mathrm{d}\rangle\langle\mathrm{u}| \tag{189}$$

With these operators we can like for a single qubit describe the qubits with the direction on the Bloch sphere. E.g. $\langle\sigma^{\tilde{x}}\rangle = 1$, $\langle\sigma^{\tilde{y}}\rangle = 0$ and $\langle\sigma^{\tilde{z}}\rangle = 0$ for the initial state $|\psi\rangle$. That means the Bloch vector is pointing in x-direction at $t = 0$.

6.1 Probability preserving intra-parity subspace phase-kicks

The dispersive term of the Hamiltonian leads to the qubit state dependent cavity phases

$$|u\rangle \to e^{-3i\chi t} \tag{190}$$
$$|d\rangle \to e^{+i\chi t}. \tag{191}$$

So a revival will occur if the two cavity states overlap again and the revival condition is

$$e^{-3i\chi t} = e^{+i\chi t} \to 2\pi - 3\chi t = \chi t \to t_{\text{rev}} = \frac{\pi}{2\chi}. \tag{192}$$

The Hamiltonian of the full system is the same as in section 1.4 with one more dispersive term for the 3rd qubit. If we assume that the dispersive shifts of the qubits are equal $\chi_{Q_1} = \chi_{Q_2} = \chi_{Q_3} = \chi$ it follows that

$$H = \chi(\sigma_1^z + \sigma_2^z + \sigma_3^z)a^\dagger a + g(a|1\rangle\langle 2| + a^\dagger|2\rangle\langle 1|) + \omega_1|1\rangle\langle 1| + \omega_2|2\rangle\langle 2| + \omega_C a^\dagger a. \tag{193}$$

From equation (167) we know how the stochastic wave function looks like. The only difference now is that we have other cavity phases and two different decay rates corresponding to the qubit state (κ_u, κ_d).

$$|\psi(t)\rangle = \mathcal{N}\left\{\mathcal{N}_{\kappa_\mathrm{u}}\; e^{-3i\chi Y(t)}|u\rangle \otimes |e^{-(i\omega + \frac{\kappa_\mathrm{u}}{2} + 3i\chi)t}\alpha\rangle + \mathcal{N}_{\kappa d}\; e^{+i\chi Y(t)}|d\rangle \otimes |e^{-(i\omega + \frac{\kappa_\mathrm{d}}{2} - i\chi)t}\alpha\rangle\right\} \tag{194}$$

Like we mentioned in section 5.4 we have to take care of the renormalization of the decaying coherent states because $\exp(-\kappa/2\, t\, a^\dagger a)|\alpha\rangle$ is not equal to $|\alpha \exp(-\kappa/2\, t)$ and now we cannot absorb the renormalization into a global prefactor because the decay rates are different for the qubit subspaces. Nevertheless the normalization condition is not important to find out more about the complex phase we gain through a photon decay. In the next section it will be discussed further because there will be two different effects. On one side we will have qubit rotations in the logical x-y-plane on our new logical Bloch sphere which will be part of this section. And on the other hand we will obtain decoherence in z-direction that is caused by the normalization that is part of the next section.
If we map this state similar as in equation (170) on the multi qubit Bloch sphere we get

$$\begin{aligned} \langle \sigma^{\tilde{x}} \rangle = \mathcal{N}^2 \Bigg\{ & \mathcal{N}_{\kappa_\mathrm{u}} \mathcal{N}_{\kappa_\mathrm{d}}\ e^{-4i\chi Y(t)}\ \underbrace{e^{-|\alpha|^2 e^{-\kappa_u t}(1-\cos(4\chi t))}}_{Amplitude} \underbrace{e^{i|\alpha|^2 e^{-\kappa_u t}\sin(4\chi t)}}_{Phase} \\ & + \mathcal{N}_{\kappa_\mathrm{d}} \mathcal{N}_{\kappa_\mathrm{u}}\ e^{+4i\chi Y(t)}\ \underbrace{e^{-|\alpha|^2 e^{-\kappa_d t}(1-\cos(4\chi t))}}_{Amplitude} \underbrace{e^{-i|\alpha|^2 e^{-\kappa_d t}\sin(4\chi t)}}_{Phase} \Bigg\}. \end{aligned} \tag{195}$$

For the revival condition $t_\mathrm{rev} = \pi/2\chi$ the factors that are denoted as amplitude and phase are both equal to 1 and the expectation value simplifies to

$$\langle \sigma^{\tilde{x}}(t = t_\mathrm{rev}) \rangle = \mathcal{N}^2_{\kappa_\mathrm{u,d}} \cos(4\chi Y(t)). \tag{196}$$

$\mathcal{N}^2_{\kappa_\mathrm{u,d}}$ is the new normalization which will be investigated further in the next section. $Y(t)$ is the stochastic variable $Y(t) = \sum_i t_i$ which summed up all the jump times. Since we only have one jump in our model it will only have the values $Y(t) = 0$ if no jump occurred and $Y(t) = t_J$ after the jump where t_J is the jump time. The same procedure leads to the expectation value in y-direction

$$\langle \sigma^{\tilde{y}}(t = t_\mathrm{rev}) \rangle = \mathcal{N}^2_{\kappa_\mathrm{u,d}} \sin(4\chi Y(t)). \tag{197}$$

These are exact results and therefore we know the direction that the Bloch vector points to in the x-y-plane at the revival when we measure a decaying photon and record the jump time t_J.

Figure 18 shows the numerics of the full system time evolution in the quantum trajectory picture. It summaries the main results of this section.
At first we can see that the cavity decays until the jump occurs and after that there is no more decay. This is due to the cut-off behaviour of the JPM. The expectation values of the Pauli matrices show that there is no decoherence before the jump and at the jump the Bloch vector gets a kick in a random direction in the x-y-plane. The expectation values after the jump at the revival time $t = t_\mathrm{rev}$ are plotted as a dashed line and called "X-Kick" respectively "Y-Kick". According to equations (196) and (197) they are simply the sine and cosine of $4\chi t_J$. The marked intersection (red circle) shows the amplitude of $\sigma^{\tilde{x}}$ and $\sigma^{\tilde{y}}$ at the revival time. The only thing we did not take into account is the renormalization factor $\mathcal{N}^2_{\kappa_\mathrm{u,d}}$ which can be understood as a squeezing of the projection of the Bloch vector in the x-y-plane. Which is nothing else than a shift of the vector to the z-axis. This will be the subject of the next section.

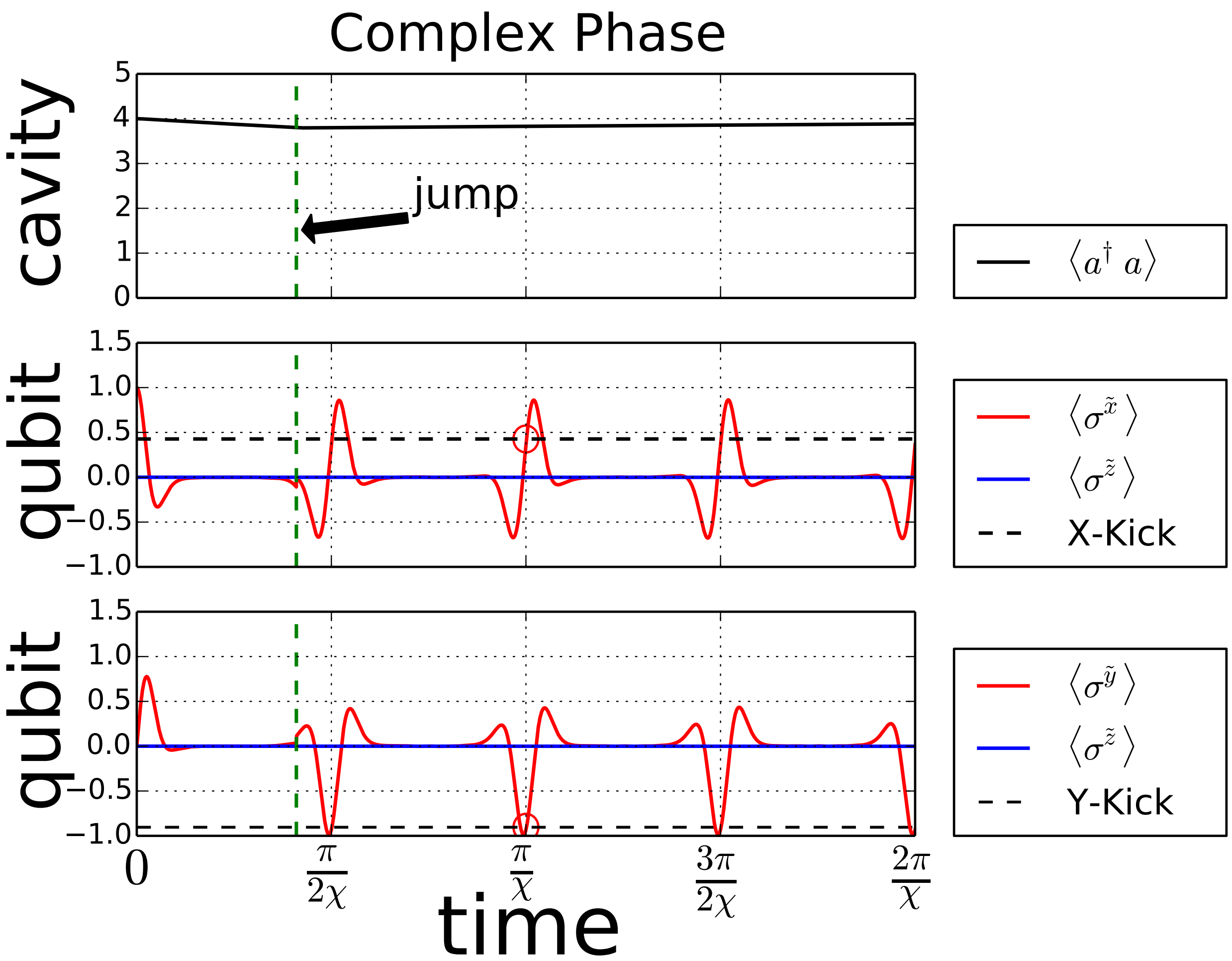

Figure 18: **Full system numerical calculation of the quantum trajectory:** The first subplot shows the cavity occupation and how the decay stops after the jump. The second and third subplots show the direction of the Bloch vector in x-y-plane $\langle \sigma^i \rangle$. The black dashed lines "X-" / "Y-Kick" show the analytic result of the Bloch vectors phase at the revival time t_{rev}. The red circle marks the intersection of the revival time $t = n\pi/2\chi$ with the expectation value and shows that there is a good agreement with the analytics (X / Y-Kick).

6.2 Probability altering intra-parity subspace rotation

Because of the parity state dependent effective decay rate besides the complex phase between the odd parity states we also gain a real prefactor. This prefactor can be interpreted analogously to the 1 qubit case as a shift of the qubit in the z-direction. If we again start in the state $|\psi(0)\rangle = \frac{1}{\sqrt{2}}(|\underbrace{111}_{\mathrm{u}}\rangle + |\underbrace{100}_{\mathrm{d}}\rangle) \otimes |\alpha\rangle$ the state at any time t before the jump is

$$|\psi(t)\rangle = \frac{\left(e^{-\frac{|\alpha|^2}{2}(1-e^{-\kappa_{\mathrm{u}} t})}|\mathrm{u}\rangle \otimes |\alpha e^{-\frac{\kappa_{\mathrm{u}}}{2}t} e^{-it\phi_{\mathrm{u}}}\rangle + e^{-\frac{|\alpha|^2}{2}(1-e^{-\kappa_{\mathrm{d}} t})}|\mathrm{d}\rangle \otimes |\alpha e^{-\frac{\kappa_{\mathrm{d}}}{2}t} e^{-it\phi_{\mathrm{d}}}\rangle\right)}{\sqrt{e^{|\alpha|^2(1-e^{-\kappa_{\mathrm{u}} t})} + e^{|\alpha|^2(1-e^{-\kappa_{\mathrm{d}} t})}}}. \tag{198}$$

We will focus on the real factors that we gain from time evolution and furthermore the complex phases $\phi_{\mathrm{u,d}}$ have been already discussed in Section 6.1. Therefore we neglect them for this section.

The denominator comes from the normalization of $|\psi\rangle$ and the prefactors $e^{\frac{|\alpha|^2}{2}(1-e^{-\kappa_{\mathrm{u,d}}t})}$ come from the renormalization of $e^{-\frac{\kappa}{2}a^\dagger a t}|\alpha\rangle$ because this is not exactly equal $|\alpha e^{-\frac{\kappa}{2}t}\rangle$,

$$e^{-\frac{\kappa}{2}a^\dagger a t}|\alpha\rangle = e^{-\frac{\kappa}{2}a^\dagger a t}e^{-\frac{|\alpha|^2}{2}}\sum_n \frac{\alpha^n}{\sqrt{n!}}|n\rangle = e^{-\frac{|\alpha|^2}{2}}\sum_n \frac{(\alpha e^{-\frac{\kappa}{2}t})^n}{\sqrt{n!}}|n\rangle, \tag{199}$$

and if we want this to be equal

$$\mathcal{N}|\alpha e^{-\frac{\kappa}{2}t}\rangle = \mathcal{N}e^{|\alpha|^2 e^{-\kappa t}}\sum_n \frac{(\alpha e^{-\frac{\kappa}{2}t})^n}{\sqrt{n!}}|n\rangle, \tag{200}$$

we have to compare coefficients and find that

$$\mathcal{N} = e^{-\frac{|\alpha|^2}{2}(1-e^{-\kappa t})}. \tag{201}$$

If we have different decay rates for the states $|\mathrm{u},\mathrm{d}\rangle$ these prefactors from the normalization do not vanish in the expectation value of $\sigma_{\tilde{z}}$ as a global prefactor.

$$\langle\sigma_{\tilde{z}}(t<t_J)\rangle = \frac{e^{-|\alpha|^2(1-e^{-\kappa_{\mathrm{u}}t})} - e^{-|\alpha|^2(1-e^{-\kappa_{\mathrm{d}}t})}}{e^{-|\alpha|^2(1-e^{-\kappa_{\mathrm{u}}t})} + e^{-|\alpha|^2(1-e^{-\kappa_{\mathrm{d}}t})}} \tag{202}$$

For $\kappa_{\mathrm{u}} = \kappa_{\mathrm{d}}$ $\langle\sigma_{\tilde{z}}\rangle$ is constantly zero. If they are not equal it becomes non-zero for $t>0$ and it vanishes again for $t\to\infty$. If a jump occurs we apply the collapse operator $\sqrt{\kappa}a$ on our state. And since we have two different decay rates for the two qubit states we apply $\sqrt{\kappa_{\mathrm{u}}a}$ on the cavity state corresponding to the qubit state $|\mathrm{u}\rangle$ and $\sqrt{\kappa_{\mathrm{d}}a}$ on $|\mathrm{d}\rangle$ The state than becomes

$$\begin{aligned}|\psi(t>t_J)\rangle = \mathcal{N}_\psi\Bigg(&\alpha\sqrt{\kappa_{\mathrm{u}}}e^{-(\frac{\kappa_{\mathrm{u}}}{2}+i\phi_{\mathrm{u}})t_J}e^{-\frac{|\alpha|^2}{2}(1-e^{-\kappa_{\mathrm{u}}t_J})}|\mathrm{u}\rangle\otimes|\alpha e^{-\frac{\kappa_{\mathrm{u}}}{2}t_J}e^{-it\phi_{\mathrm{u}}}\rangle \\ &+\alpha\sqrt{\kappa_{\mathrm{d}}}e^{-(\frac{\kappa_{\mathrm{d}}}{2}+i\phi_{\mathrm{d}})t_J}e^{-\frac{|\alpha|^2}{2}(1-e^{-\kappa_{\mathrm{d}}t_J})}|\mathrm{d}\rangle\otimes|\alpha e^{-\frac{\kappa_{\mathrm{d}}}{2}t_J}e^{-it\phi_{\mathrm{d}}}\rangle\Bigg).\end{aligned} \tag{203}$$

Again we neglected the complex phases of the coherent state and the prefactor. The former would not stop spinning even after the jump and the later has been discussed in the last section. The normalization is

$$\mathcal{N}_\psi = \frac{1}{\sqrt{|\alpha|^2\kappa_{\mathrm{u}}e^{-\kappa_{\mathrm{u}}t_J}e^{|\alpha|^2(1-e^{-\kappa_{\mathrm{u}}t_J})} + |\alpha|^2\kappa_{\mathrm{u}}e^{-\kappa_{\mathrm{d}}t_J}e^{|\alpha|^2(1-e^{-\kappa_{\mathrm{d}}t_J})}}}. \tag{204}$$

And the expectation value after the jump is constantly

$$\langle\sigma_{\tilde{z}}(t>t_J)\rangle = \frac{\kappa_{\mathrm{u}}e^{-\kappa_{\mathrm{u}}t_J}e^{-|\alpha|^2(1-e^{-\kappa_{\mathrm{u}}t_J})} - \kappa_{\mathrm{d}}e^{-\kappa_{\mathrm{d}}t_J}e^{-|\alpha|^2(1-e^{-\kappa_{\mathrm{d}}t_J})}}{\kappa_{\mathrm{u}}e^{-\kappa_{\mathrm{u}}t_J}e^{-|\alpha|^2(1-e^{-\kappa_{\mathrm{u}}t_J})} + \kappa_{\mathrm{d}}e^{-\kappa_{\mathrm{d}}t_J}e^{-|\alpha|^2(1-e^{-\kappa_{\mathrm{d}}t_J})}}. \tag{205}$$

In figure 19 we plot the numerics of the full system against the analytic results of the behaviour of the Bloch vector in z-direction. The analytical expectation values $\langle\sigma_{\tilde{z}}(t<t_J)\rangle$ and $\langle\sigma_{\tilde{z}}(t>t_J)\rangle$ agree very well with the numerics of the full system. There is a small difference coming from the non Markovian behaviour of the cavity decay at short times which we discussed in section 3.7.

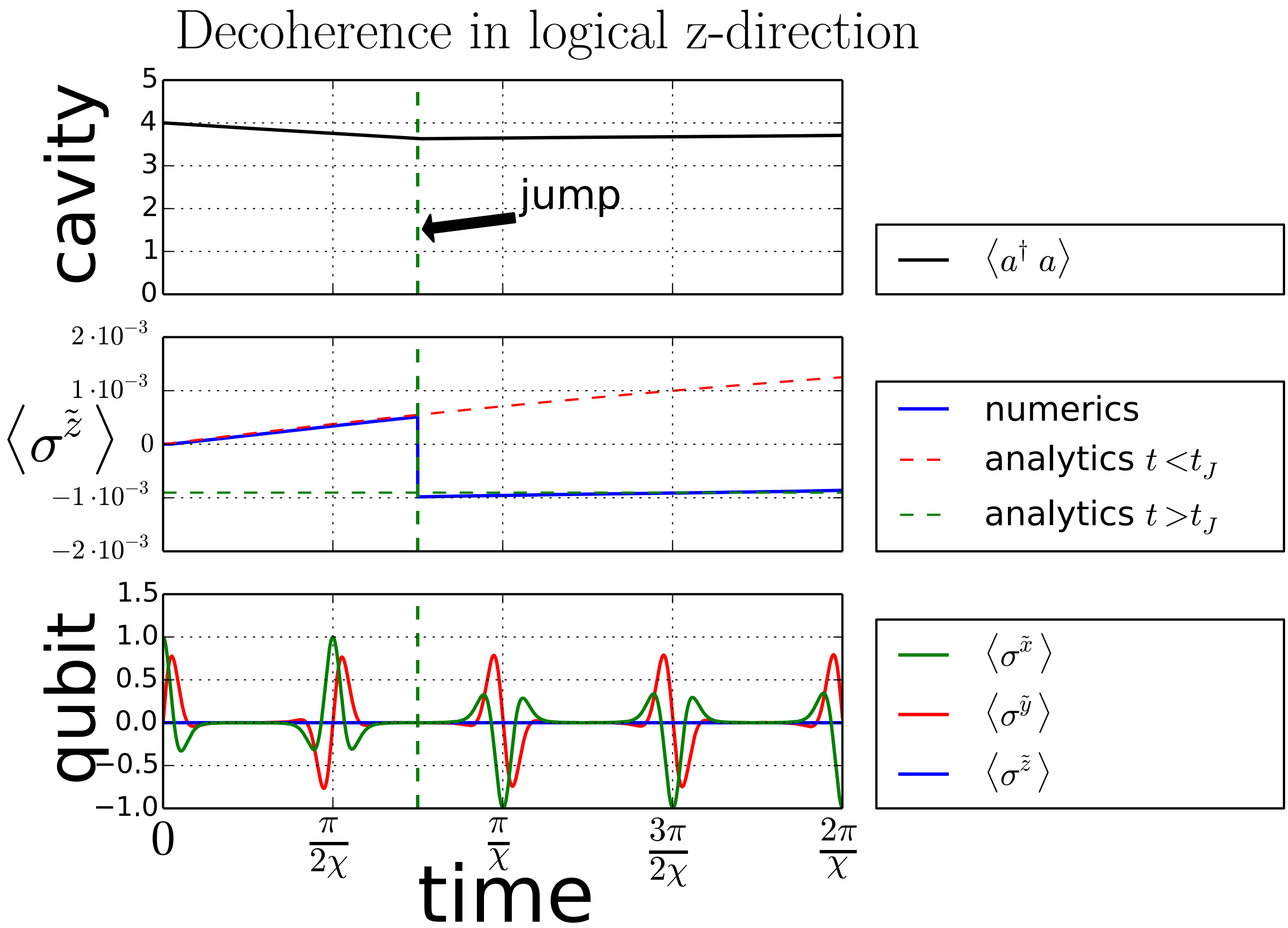

Figure 19: **Full system numerical calculation of the quantum trajectory:** The first subplot shows the cavity occupation and how the decay stops after the jump. The second subplot shows the direction of the Bloch vector in z-direction. Here we compare the full system numerics (solid blue line) with the numerical values before (dashed red) and after (dashed green) the jump. The third subplot shows the direction of the Bloch vector in x-y-z-direction ($\langle \sigma^i \rangle$). The change in z-direction is very small and therefore not visible in the third subplot.

In conclusion we showed that we can, analogously to the one dimensional case, predict X, Y and Z shifts of the odd parity state for three qubits accurately before and after the jump and we can describe the wave function of the system with high accuracy (equations (198), (203)). Furthermore we can also see that the transversal decoherence in z direction is a small effect compared to the "kicks" in the x-y-plane.
There is no restriction for qubit states with qubit number $N > 3$. The calculations can be made in a similar way. Only the mapping on a Bloch sphere will not work for more than two qubit states per parity subspace. Nevertheless the state can be predicted in the same exact manner for more than three qubits. Also if we assume that we have an unknown initial 3-qubit state of the form,

$$|\psi\rangle = c_1|q_1\rangle + c_2|q_2\rangle + \cdots \tag{206}$$

where $|c_i|$ can have any value between 0 and 1. The prediction of the phase and transversal decoherence of a single ket $|q_i\rangle$ does not depend on the other states that are part of the superposition. Therefore we can predict the prefactor we gain for every substate that is part of the superposition separately and we do not have to know what the initial state of the qubits was. We only have to know the initial state of the cavity that is entangled to the qubits, which we will do after the measurement. This is necessary because the decoherence is dependent on whether the cavity was bright or empty. This information and an exact tracking of the measurement time will be sufficient for a prediction.

7 The reset stage

At the end of our qubit parity measurement we want to disentangle the cavity state from the qubit parity subspaces. This will be necessary that we are able to write the state of the full system again as a product state of a multi qubit state $|\psi\rangle$ and a cavity state $|\alpha\rangle$. If we are able to do so, the qubit state can be separated from the cavity. In this section we would like to achieve this by driving the cavity back to vacuum. If the parity subspaces are both entangled with the vacuum the separation of qubit and cavity states is fulfilled. To see if the reset to vacuum was successful we investigate the overlapp of the cavity state with the vacuum $\langle\alpha_{\text{end}}|0\rangle$ for different dispersive shifts χ and different ratios for $\frac{g_J}{\kappa_J}$. If this overlapp is close to 1 we know that the cavity was reset exactly.

A cavity displacement can be achieved by driving it with a Gaussian pulse. In our case where we will have multi cavity states whose frequency depend on the corresponding qubit parity state we have to drive every cavity state with its own frequency. Furthermore we have to take care that the drive for one cavity state does not affect an other cavity state. In frequency space the Gaussian pulse has the form

$$\frac{\xi}{\sigma\sqrt{2\pi}}\exp\left(-\frac{1}{2}\left(\frac{\omega-\omega_D}{\sigma}\right)^2\right), \tag{207}$$

where ω_D is the frequency of the cavity drive, σ is the variance of the Gaussian in frequency space and ξ is the amplitude of the drive. The first case where we have different effective decay rates for the same parity states is in the 3 qubit case. The states $|111\rangle$ and $|100\rangle$ both have odd parity but the former has a dispersive shift of $+3\chi$ and the latter has $-\chi$ and therefore the effective decay rate κ_{eff} varies. The cavity frequencies for odd qubit states are separated by 4χ. Due to this separation we have to choose the variance σ such that the pulses do not overlap and this can be achieved by setting $\sigma \leq \chi/2$. The variance should not be chosen to small because in time space the Gaussian peak is getting broader with smaller σ and the resetting would take too long. In time space the drive has the form

$$\frac{\xi}{\sqrt{2\pi}}\exp\left(-\frac{1}{2}t^2\sigma^2\right)\cos(\omega_D t). \tag{208}$$

To modulate the time where the Gaussian has its maximum one can just substitute $t \to t - t_0$ where t_0 is the time where the Gaussian pulse has its maximum.
The Hamiltonian of a cavity driven with a Gaussian pulse has the form

$$H = \omega_C a^\dagger a + \frac{\xi}{\sqrt{2\pi}}\exp\left(-\frac{1}{2}t^2\sigma^2\right)\cos(\omega_D t+\phi_0)(a^\dagger + a) = \omega_C a^\dagger a + \frac{\xi}{2\sqrt{2\pi}}\exp\left(-\frac{1}{2}t^2\sigma^2\right)\left(e^{i(\omega_D t+\phi_0)} + e^{-i(\omega_D t+\phi_0)}\right)(a^\dagger + a). \tag{209}$$

At this point we can use the rotating wave approximation (see also Appendix 10.9 and neglect the counter rotating terms.

$$H = \omega_C a^\dagger a + \frac{\xi}{2\sqrt{2\pi}}\exp\left(-\frac{1}{2}t^2\sigma^2\right)\left(e^{-i(\omega_D t+\phi_0)}a^\dagger + e^{i(\omega_D t+\phi_0)}a\right) \tag{210}$$

with the unitary operator $U = \exp\left(i\omega_C a^\dagger a t\right)$ we go to the frame rotating with the bare cavity frequency ω_C. If we use $\tilde{H} = UHU^\dagger - U\dot{U}^\dagger$ and the relations

$$e^{-\lambda a^\dagger a} a e^{\lambda a^\dagger a} = e^{\lambda} a \tag{211}$$
$$e^{-\lambda a^\dagger a} a^\dagger e^{\lambda a^\dagger a} = e^{-\lambda} a^\dagger \tag{212}$$
$$\tag{213}$$

we get the Hamiltonian

$$H = \frac{\xi}{2\sqrt{2\pi}} \exp\left(-\frac{1}{2}t^2\sigma^2\right)\left(e^{-i((\omega_D-\omega_C)t+\phi_0)}a^\dagger + e^{i((\omega_D-\omega_C)t+\phi_0)}a\right) = \frac{\xi}{2\sqrt{2\pi}} \exp\left(-\frac{1}{2}t^2\sigma^2\right)\left(e^{-i\phi_0}a^\dagger + e^{i\phi_0}a\right). \tag{214}$$

The second equality holds in our case since we want to drive the cavity modes on resonance. The evolution of a state by this Hamiltonian has the form

$$|\psi(t)\rangle = \exp\left(-i\int_{\tau_0}^{\tau} \frac{\xi}{2\sqrt{2\pi}} \exp\left(-\frac{1}{2}t^2\sigma^2\right)\left(e^{-i\phi_0}a^\dagger + e^{i\phi_0}a\right) dt\right)|\psi(0)\rangle. \tag{215}$$

This integral can not be solved exactly for finite integration boundaries. But since the Gaussian peak is only non zero for some time range around its mean value we can expand the integral boundaries to infinity. Because in the experiment we want the whole Gaussian pulse to be inbetween our starting and end point of the reset.

$$\int_{-\infty}^{\infty} \exp\left(-\frac{1}{2}t^2\sigma^2\right) dt = \sqrt{\frac{2\pi}{\sigma^2}} \tag{216}$$

Therefore

$$|\psi(t)\rangle = \exp\left(-i\frac{\xi}{2\sigma}\left(e^{-i\phi_0}a^\dagger + e^{i\phi_0}a\right) dt\right)|\psi(0)\rangle \tag{217}$$

If we now compare this exponential with the displacement operator $D(\alpha) = \exp(\alpha a^\dagger - \alpha^* a)$ we can see that

$$\alpha = -i\frac{\xi}{2\sigma}e^{-i\phi_0} \Longleftrightarrow \xi = 2i\alpha\sigma e^{i\phi_0}. \tag{218}$$

Here we have to keep in mind that α in this formula is the amount of displacement we want to achieve. Since we want to reset the cavity from α back to zero we also gain a minus sign.

$$\xi = -2i\alpha\sigma e^{i\phi_0} \tag{219}$$

7.1 The state after the measurement

If we again start in an initial state $|\psi\rangle = \frac{1}{\sqrt{2}}(|111\rangle + |100\rangle) \otimes |\alpha\rangle$. With our analytic solution for the effective decay rate of the cavity we can predict the cavity state after the detection of a photon which is highly entangled with the qubits. To disentangle the qubits from the cavity we reset the cavity state to zero after the measurement. According to section 6 the state before the jump is

$$|\psi(t)\rangle = e^{-\frac{|\alpha|^2}{2}(1-e^{-\kappa_u t})}|u\rangle \otimes |\alpha e^{-\frac{\kappa_u}{2}t}e^{-it(\omega_C+3\chi)}\rangle + e^{-\frac{|\alpha|^2}{2}(1-e^{-\kappa_d t})}|d\rangle \otimes |\alpha e^{-\frac{\kappa_d}{2}t}e^{-it(\omega_C-\chi)}\rangle, \tag{220}$$

again with the one dimensional analogy $|u\rangle = |111\rangle$ and $|d\rangle = |100\rangle$ to map the multi qubit states on the Bloch sphere for better intuition. If a jump occurs at the time t_J the decay of the cavity stops but it will still rotate with the same frequency dependent on the qubit state and χ. The phase factors that occur because of the application of the annihilation operator a during the jump are not of interest for the reset stage. To reset a cavity state we only have to know its amplitude α, its frequency ω and its phase ϕ and not how likely it is to be in that state. So after tracing out the qubit degrees of freedom we are left with a cavity state of the form

$$|\psi_{\text{cav}}\rangle = c_u|\alpha e^{-\frac{\kappa_u}{2}t_J}e^{-it(\omega_C+3\chi)}\rangle + c_d|\alpha e^{-\frac{\kappa_d}{2}t_J}e^{-it(\omega_C-\chi)}\rangle. \tag{221}$$

To reset such a superposition of cavity states we have to drive both states with their frequency. The drive then has the form

$$H_D = \left(\frac{\xi_1}{\sqrt{2\pi}} \exp\left(-\frac{1}{2}(t-t_1)^2\sigma^2\right) \cos(\underbrace{(\omega_C + 3\chi)}_{\omega_{D_1}} t + \phi_1) + \frac{\xi_2}{\sqrt{2\pi}} \exp\left(-\frac{1}{2}(t-t_2)^2\sigma^2\right) \cos(\underbrace{(\omega_C - \chi)}_{\omega_{D_2}} t + \phi_2) \right) \left(a + a^\dagger\right) . \tag{222}$$

t_1 and t_2 are the times where the Gaussian pulses have their maxima. The reset also works if it is for both cavity states at the same time $t_1 = t_2 = t_0$ which we will do for simplicity. If we perform the rotating wave approximation we are left with

$$\frac{1}{2\sqrt{2\pi}} \exp\left(-\frac{1}{2}(t-t_0)^2\sigma^2\right) \left(\xi_1 \left(e^{-i(\omega_{D_1}t+\phi_1)}a^\dagger + e^{i(\omega_{D_1}t+\phi_1)}a\right) + \xi_2 \left(e^{-i(\omega_{D_2}t+\phi_2)}a^\dagger + e^{i(\omega_{D_2}t+\phi_2)}a\right)\right) . \tag{223}$$

The complex phases are only dependent on the time when we start the reset stage. If we assume the reset stage starts directly after the detection of a photon at time t_J the phases are $\phi_1 = \omega_{D_1} t_J$ and $\phi_2 = \omega_{D_2} t_J$. If we would wait a time t' after the detection to start the Gaussian pulse the phases were $\phi_1 = \omega_{D_1}(t_J + t')$ and $\phi_2 = \omega_{D_2}(t_J + t')$.
The amplitude of the drives $\xi_{1,2} = 2i|\alpha|e^{-\kappa_{\mathrm{u,d}} t_J}$ are dependent on the effective decay rates κ_u and κ_d that correspond to the qubit states $|\mathrm{u}\rangle$ amd $|\mathrm{d}\rangle$. From section 3.1 we know that

$$\kappa_{\mathrm{eff}} = \frac{4g_J^2}{\kappa_J}\left(1 - 4\frac{\Delta^2}{\kappa_J^2}\right) \tag{224}$$

,
with $\Delta_{\mathrm{u}} = -3\chi$ and $\Delta_{\mathrm{d}} = \chi$. A very important fact here is that the cavity amplitude decays only until the time t_J and after that it stops. So we do not have to care about any further decay after the detection of a photon.

7.2 Simulation of the reset stage

In this section we simulate the whole measurement stage and the reset stage to find out if the cavity has been reset properly, which is equivalently to a proper disentanglement of the qubit and the cavity state. To do so we start in the state $|\psi\rangle = \frac{1}{\sqrt{2}}(|111\rangle + |100\rangle) \otimes |\alpha\rangle$ and let it evolve as described in Section 6. As a experimentalist we would measure a click on our photon detector at the jump time t_J. After that time we change to the reset stage and reset our cavity with a Gaussian pulse described in the last section. The accuracy of the reset to vacuum state is quantified by the overlap of the cavity state at the end of the reset stage and the vacuum $|\langle\alpha_{\mathrm{end}}|0\rangle|^2$. In figure 20 we ploted the reset accuracy against a broad range of values for g_J/κ_J and χ/κ.
In the plots we can see that the predictions of the cavity amplitude are exact and therfore the reset works well in the regime where the approxiamtion for κ_{eff} holds, which is $g_J \ll \kappa_J$ and also $\chi \ll \kappa_J$. The reset starts to fail if we leave this regime. We obtain that for $\kappa_J = 1000 g_J$ and $\chi \to 0$ we reach reset accuracies of almost 100%. Furthermore, we can see that for growing χ the reset accuracy decreases much faster, than for growing g_J. This is because of the expansion we did in Section 3.1, which is valid for $\Delta^2 \ll g_J^2 \ll \kappa_J^2$, where in this case here χ is proportional to the detuning Δ.

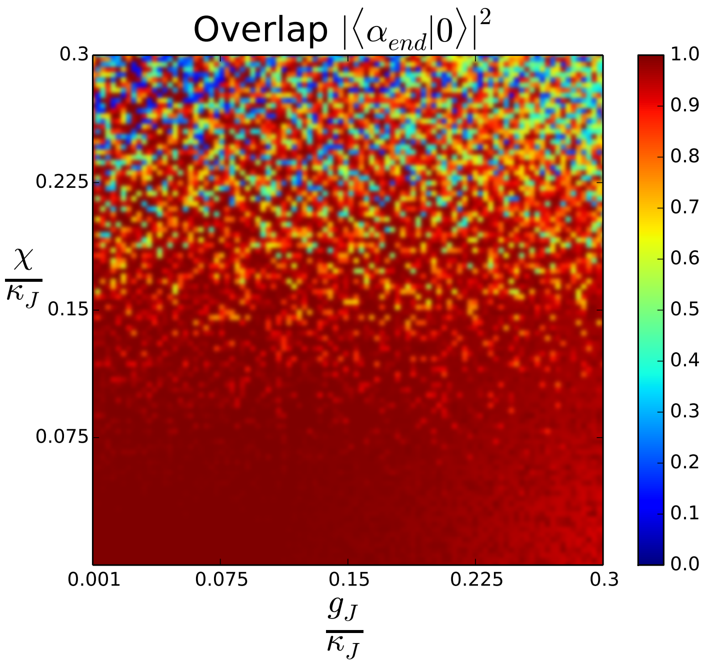

Figure 20: Overlap of reset state with the vacuum state.

Besides the decay of the reset fidelity for $\chi, g_J \to \kappa_J$ we can observe something different in figure 20. We can see that there is a lot of noise in the regime where the reset becomes worse. This noise has to do with the random distribution of the time when a jump occurs.

If we go to higher values for g_J where the κ_{eff} approximation does not hold any more the overlap of $|\alpha_{\text{end}}\rangle$ and the vacuum $|0\rangle$ is getting smaller. But there are still some points where the reset was successful and we reach overlap fidelities of more than 98 %. This can be the case if the jump happens immediately after the start of the measurement stage because the effective decay $\sim |\alpha|^2 \exp(-\kappa_{\text{eff}} t)$ can not diverge much from the full system numerical simulation and the reset amplitude is still a good approximation. In figure 21 one can see that the reset fidelity still goes to 1 if $t_J \to 0$.

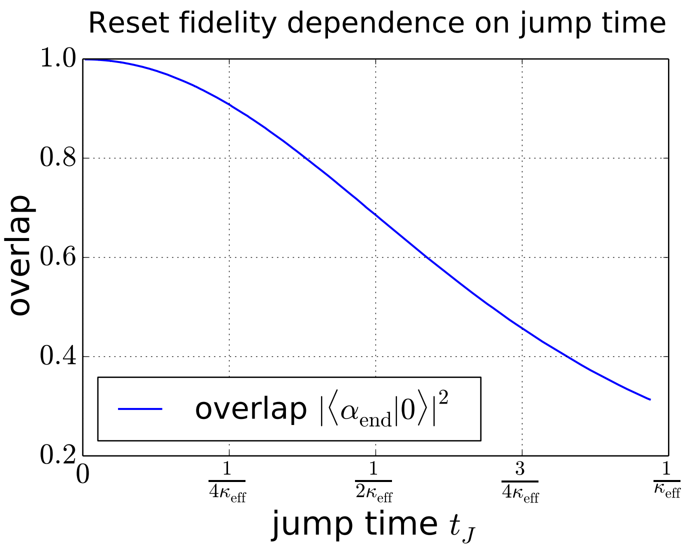

Figure 21: Overlap of reset state with the vacuum state for fixed parameters. $g_J/\kappa_J = 0.005$, $\chi/\kappa_J = 0.1$. Here we can see why the reset still can be successful even if we are not in the limits, where κ_{eff} holds. If the decay of the photon happens very fast and $t_J \to 0$, the overlap $|\langle\alpha_{\text{end}}|0\rangle|^2 \to 1$

7.3 Results of the reset stage and what happens with the qubits during the reset?

The last section was about the reset of the cavity after the jump. To do this properly we have to know the amplitude and the phase of the cavity. Furthermore we have to keep in mind that the initial cavity state entangles with the intra parity qubit states because the cavity phase and also decay rate is qubit state dependent. In the regime $g_J \ll \kappa_J$ and $\chi \ll \kappa_J$ where the effective decay rate κ_{eff} holds the reset fidelity is high which shows that the cavity part of equation (220) is a good approximation.
The question now arises what happens to the qubits during the cavity reset. Unfortunately it cannot be answered that easily. Since the drive part $\sim (a + a^\dagger)$ of the Hamiltonian, Eq. (210), does not commute with the dispersive part of the Hamiltonian of the system $\sim \chi a^\dagger a(\sigma_1^z + \cdots)$ the qubits will be affected through the reset stage and the changing amplitude of the cavity. We could avoid the dephasing of the qubits during the reset if we can get rid of the dispersive part of the Hamiltonian during this stage. In the next section we present a way how this can be done.

8 Evading back-action via Dynamical Decoupling

8.1 Dynamical Decoupling

A possible technique to suppress decoherence in our quantum system is the dynamical decoupling. We can take advantage of a time dependent modulation of our Hamiltonian to decouple the dispersive term from the rest of the Hamiltonian. [8]
If we have a piecewise constant Hamiltonian $H(t)$ that can be split into $H(t) = H_1 + H_2 + \cdots + H_n$ for time intervals $\tau_k = t_k - t_{k-1}$ and $t_k > t_{k-1} > \cdots > t_1$, we can write the unitary time evolution operator that evolves the system to the time t_{e} as

$$U(t_{\text{e}}, t_0) = \exp(-iH_n\tau_n)\cdots\exp(-iH_1\tau_1), \tag{225}$$

with

$$t_{\text{e}} = \sum_{k=1}^{n} \tau_k. \tag{226}$$

A product of unitary operations is again unitary. Therefore we can express the sequence of transformation by a single transformation with the average Hamiltonian $\bar{H}$.

$$U(t_{\text{e}}, t_0) = \exp(-i\bar{H}(t_{\text{e}} - t_0)) \tag{227}$$

This average Hamiltonian is then only applicable for a fixed time interval $[t_0, t_{\text{e}}]$. If the time dependent modulation of the Hamiltonian is periodic and t_{e} corresponds to the period of the modulation, $\bar{H}$ can also describe the time evolution over an extended period by the relation

$$U(nt_{\text{e}}) = U(t_{\text{e}})^n = \exp(-i\bar{H}nt_{\text{e}}), \tag{228}$$

where we set $t_0 = 0$ for simplicity. Now we would like to find such an average Hamiltonian for our system of dispersively coupled qubits to a cavity. For simplicity we investigate the single qubit case. The dispersive Hamiltonian in the rotating frame of the bare qubit frequency reads then

$$H = \omega_C a^\dagger a + \chi\sigma^z a^\dagger a. \tag{229}$$

Since we know that the dispersive part of this Hamiltonian leads to the entanglement of the parity states with the cavity and to a parity state dependent decay rate, we would like to decouple this term of the Hamiltonian. In section 5.4 we have seen that the dispersive term in the Hamiltonian $\chi\sigma^z a^\dagger a$ leads to a qubit state dependent rotation of the cavity. If we flip all the qubits, the cavity rotates in the opposite direction. If we imgaine the system also in the rotating frame of the bare cavity ferquency ω_C an intuitive picture is the following. If we let the system evolve for a time t and than flip the qubits and let it evolve again the same amount of time t we get back to the initial state of the cavity because the cavity rotation changes with the qubit flip.
If we assume the qubit flip to be instantaneous the unitary evolution operators of half a period are

$$U_1 = \exp(-i(\omega_C a^\dagger a + \chi\sigma^z a^\dagger a)t_1) \tag{230}$$
$$U_2 = \sigma^x \tag{231}$$
$$U_3 = \exp(-i(\omega_C a^\dagger a + \chi\sigma^z a^\dagger a)t_3). \tag{232}$$

If we rewrite $\exp(-i\sigma^z\omega t) = \cos(\omega t)\mathbb{I} - i\sin(\omega t)\sigma^x$, use the anti-commutation relation $\{\sigma^z, \sigma^x\} = 0$, $\sigma^z\sigma^x\sigma^z = -\sigma^x$ and set $t_1 = t_3 = t$ we find that

$$U_3U_2U_1 = \sigma^x \exp(2t\omega_C a^\dagger a). \tag{233}$$

So we see that the cavity only rotates with its bare frequency. This is only half a period because the qubit is still flipped which is something we do not want in an experiment. So if we apply such an evolution twice we get

$$U_6 \cdots U_1 = \exp(4t\omega_C a^\dagger a) \tag{234}$$

and our average Hamiltonian is $\bar{H} = \omega_C a^\dagger a$ which is the bare cavity Hamiltonian which rotates with the bare cavity frequency ω_C. So if we now use this average Hamiltonian in the dissipative dynamics where we will have photon decay we would theoretically not have to control the phase we get at such a jump. Furthermore we would also not have intra parity subspace decoherence because that also comes from the different dispersive shifts of the parity states and their influence on the decay rate (see section 6). There are some things we have to be careful with. In the model from above we did not include the cavity decay and therefore we have no limitation on the duration of one period. But if a photon can decay at any time we have to choose the period small enough so that the probability increases that we have a jump as close as possible to the end of a single time step. This requirement is a consequence of the splitting of the Hamiltonian in constant pieces at the beginning of this section. The approximation only holds for this piecewise evolution and breaks down if we interrupt during a time interval of a single unitary evolution $U_n = \exp(-iH_n\tau_n)$. The time scale of a period is therefore of the order $t \ll 1/\kappa$.

This was for instantanous qubit flips. If we now would like to perform a qubit rotation in a finite time we could do that with the unitary transformation

$$\exp(-i\omega t\sigma^x) = \begin{bmatrix} \cos(\omega t) & -i\sin(\omega t) \\ -i\sin(\omega t) & \cos(\omega t) \end{bmatrix}. \tag{235}$$

For $\omega t = \pi/2$ this corresponds to the σ^x operator with a global phase. If we now perform the flip in finite time we also have to include the time evolution during the flip an U_2 changes to

$$U_2 = \exp(-i(\omega_C a^\dagger a + \chi\sigma^z a^\dagger a + \omega\sigma^x)t_2). \tag{236}$$

For our purpose we restrict ourself to instantaneous qubit flips.

8.2 Imperfect detection

Until now we assumed that our detector was perfect. So every photon that decayed also was detected. If we now introduce the detection efficiency η the master equation from section 1.4 equation (22) changes [7] to

$$\dot{\rho} = -i\left[H, \rho\right] + \eta\kappa_J\mathcal{D}\left[|2\rangle\langle 0|\right] + (1-\eta)\kappa_J\mathcal{D}\left[|2\rangle\langle 0|\right]. \tag{237}$$

For $\eta = 1$ the density matrix again has the form,

$$\rho = \sum_{\mathrm{REC}} P_{\mathrm{REC}}|\psi_{\mathrm{REC}}\rangle\langle\psi_{\mathrm{REC}}| \tag{238}$$

and can be unraveled into its trajectories, because the measurement records are known. If the detection efficiency is smaller than 1 we can only unravel the part of the master equation according to η. For the $(1-\eta)$ term we do not have a record and therefore the solution ρ according to jumps that have not been detected is simply the solution of the master equation itself or the average over infinitely many trajectories. For this purpose we denote the solution of

the master equation with missed detection ρ_{av}. Av stands for the average over all outcomes. And the solution for a detection event is called ρ_{c} for a conditional outcome dependent on the measurement.
The crucial point of our system is that after the decay of a photon the JPM stops any further decay and therefore we only have to know if we detected a photon or not and according to that solve either the quantum trajectory or the master equation. And the resulting density matrix is

$$\rho = \eta\rho_{\mathrm{c}} + (1-\eta)\rho_{\mathrm{av}}. \tag{239}$$

To know how good the approximation of our calculated state is, we measure the fidelity of the numerically evaluated ρ with the analytically derived conditional state $\rho_{\mathrm{c}}^{\mathrm{an}}$. The definition of the fidelity for general density matrices ρ and σ by Nielsen and Chuang [5] is

$$F(\rho,\sigma) = Tr\left[\sqrt{\sqrt{\rho}\sigma\sqrt{\rho}}\right]. \tag{240}$$

If one state is pure e.g. $\rho = |\phi\rangle\langle\phi|$ the fidelity simplifies to

$$F(\rho,\sigma) = \sqrt{\langle\phi|\sigma|\phi\rangle}, \tag{241}$$

which is the case in our example. The conditional analytic state is $\rho_{\mathrm{c}}^{\mathrm{an}} = |\psi_{\mathrm{c}}^{\mathrm{an}}\rangle\langle\psi_{\mathrm{c}}^{\mathrm{an}}|$. So the fidelity of the full system numerical state with imperfect detection with the analytical solution is

$$F(\rho_{\mathrm{c}}^{\mathrm{an}},\rho) = \sqrt{\langle\psi_{\mathrm{c}}^{\mathrm{an}}|(\eta\rho_{\mathrm{c}} + (1-\eta)\rho_{\mathrm{av}})|\psi_{\mathrm{c}}^{\mathrm{an}}\rangle}. \tag{242}$$

If we square the fidelity we can split it into a conditional part and an average part

$$F^2(\rho_{\mathrm{c}}^{\mathrm{an}},\rho) = \langle\psi_{\mathrm{c}}^{\mathrm{an}}|\eta\rho_{\mathrm{c}}|\psi_{\mathrm{c}}^{\mathrm{an}}\rangle + \langle\psi_{\mathrm{c}}^{\mathrm{an}}|(1-\eta)\rho_{\mathrm{av}})|\psi_{\mathrm{c}}^{\mathrm{an}}\rangle = \eta\ F^2(\rho_{\mathrm{c}}^{\mathrm{an}},\rho_{\mathrm{c}}) + (1-\eta)F^2(\rho_{\mathrm{c}}^{\mathrm{an}},\rho_{\mathrm{av}}). \tag{243}$$

The question now arises at what time do we measure the fidelity? We do not have to measure it at all times because in an experiment we will wait a certain time until we measure a click on our detector or in the imperfect detection scenario we wait long enough so it is very probable that we have missed a click. So we decided to go to a time scale that is of the order $t_M = 1/\kappa_{\mathrm{eff}}$ and multiples of it. From equation (133) in section 3.7 we know that the probability $p(t)$ that the JPM relaxed to the continuum state at the time $t_M = 1/\kappa_{\mathrm{eff}}$ is $p(1/\kappa_{\mathrm{eff}}) = 1 - \exp(|\alpha|^2)$. Therefore already after t_M the photon must have decayed with 99.9% for $\alpha = 3$.
The conditional part of the fidelity will be measured directly after the detection of the photon and $F^2(\rho_{\mathrm{c}}^{\mathrm{an}},\rho_{\mathrm{c}})$ reaches fidelity values of more than 99.5% because if a jump has been detected the state is well known and has the form of equation (203) which we discussed in section 6.2.
On the contrary, if we do not detect a photon, we do not know anything about the state and the qubit phase. In this case we measure the fidelity of the analytic solution of the conditional state before the jump $\rho_{\mathrm{c}}^{\mathrm{an}}$, equation (198), with the numerical master equation solution which corresponds to a failed detection. In figure 22 we plot the complete fidelity $F^2(\rho_{\mathrm{c}}^{\mathrm{an}},\rho)$ dependent on the detection efficiency η. Here we can see that the fidelity goes to almost 100 % if the efficiency $\eta \to 1$. In this regime we are back in the quantum trajectory picture which we can predict exactly. For $\eta \to 0$ the fidelity decreases and for longer measurement time t_M the fidelity gets even smaller. Since the conditional part $F^2(\rho_{\mathrm{c}}^{\mathrm{an}},\rho_{\mathrm{c}}) \approx 1$ the function (243) simplifies to $\eta + (1-\eta)F^2(\rho_{\mathrm{c}}^{\mathrm{an}},\rho_{\mathrm{av}})$. The average part of the fidelity $F^2(\rho_{\mathrm{c}}^{\mathrm{an}},\rho_{\mathrm{av}})$ has been simulated for different measurement times $t_M = \frac{1}{\kappa_{\mathrm{eff}}}, \frac{2}{\kappa_{\mathrm{eff}}}, \frac{5}{\kappa_{\mathrm{eff}}}$. We can see that for decreasing detector efficiency the overlap of our analytic solution with the numerical state is getting very small so we will not be able to predict our qubit state any more.

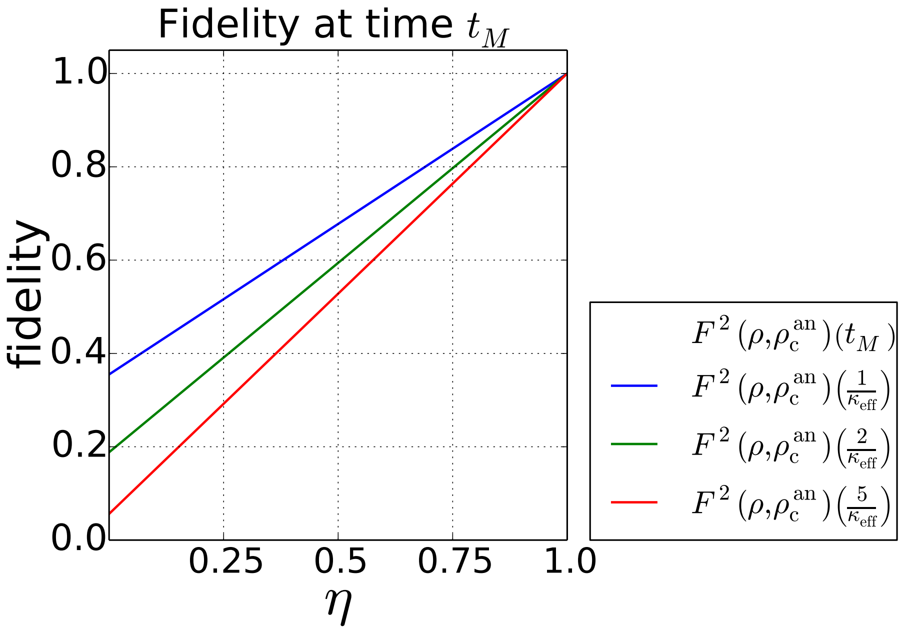

Figure 22: **Fidelity without dynamical decoupling** of the numerically calculated state $\rho = \eta\rho_c + (1-\eta)\rho_{av}$ with the analytical state ρ_c^{an} at the measurement time t_M for varying detector efficiency η. The measurement times varies from $1/\kappa_{eff}$ to $5/\kappa_{eff}$.

In a next step we use the technique of dynamical decoupling to test if the fidelity can be increased even if the detection fails. We have shown that the decoupling leads to an averaged Hamiltonian $\bar{H} = \omega_C a^\dagger a$ and therefore we measure the fidelity of the numerical state ρ with the conditional analytic state

$$|\psi_c^{an}\rangle = \frac{1}{\sqrt{2}}(|u\rangle + |d\rangle) \otimes |\alpha e^{-\frac{\kappa_{eff}}{2}} e^{-i\omega_C t}\rangle, \tag{244}$$

with the effective decay rate without detuning $\kappa_{eff} = 4g_J^2/\kappa_J$. This state holds in both cases. If we do not detect a click and even if we do. The phase kick and also the real decoherence were both caused by the dispersive Hamiltonian part $\sum_i \chi\sigma_i^z a^\dagger a$ and are therefore not any longer present.
In figure 23 we see that the fidelity can be increased for imperfect detection with the dynamical decoupling but it is still limited and not satisfying. The fidelity for the failed detection numerics ρ_{av} with the analytical state is still not good where on contrary the fidelity of the numerical and the analytical conditional state is still $F^2(\rho_c^{an}, \rho_c) \approx 1$.

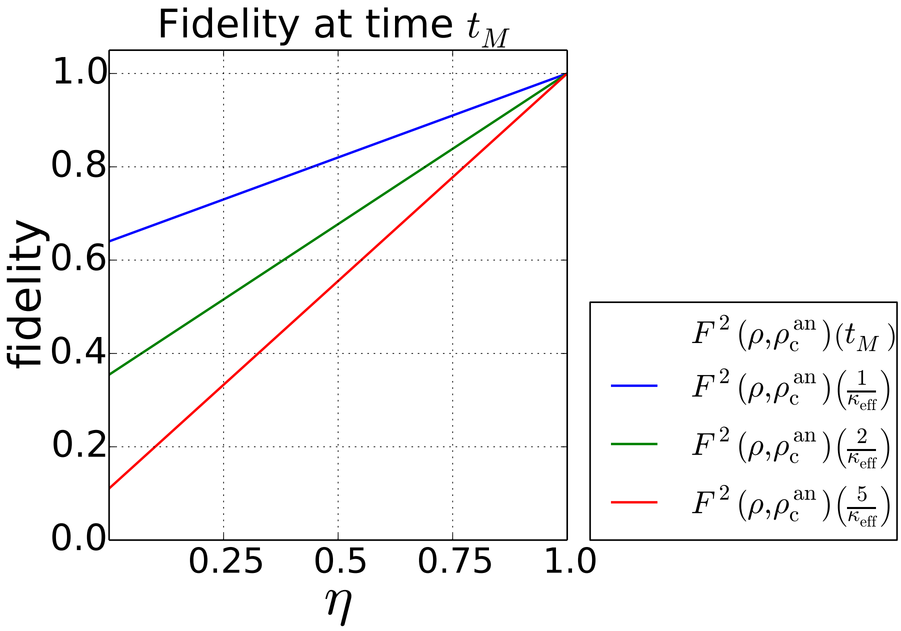

Figure 23: **Fidelity with dynamical decoupling** of the numerically calculated state $\rho = \eta\rho_c + (1-\eta)\rho_{av}$ with the analytical state ρ_c^{an} at the measurement time t_M for varying detector efficiency η. The measurement times varies from $1/\kappa_{eff}$ to $5/\kappa_{eff}$. The qubit flip frequency is set to 100 flips per $1/\kappa_{eff}$.

By increasing the qubit flip frequency one could also improve the fidelity for detector efficiencies $\eta \to 0$. But at this point we also have to evaluate what does a null measurement mean for a potential experiment. And is it even reasonable to increase the fidelity for such measurements where we miss a decaying photon. This question will be subject of the next section.

8.3 What does imperfect detection mean for the experiment

Until now we reduced our system to an odd parity state that is coupled to a cavity with an amplitude α. If we detect a click we know the qubit parity state and we showed that we also know the back-action of the measurement on the parity subspaces. The measurement then has been successful and with dynamical decoupling we did not change the parity subspace itself. For perfect detectors we only have to wait long enough so that the probability to detect a photon is high enough, if we are in odd parity space. If we now include imperfect detection we can misinterpret the outcome in different ways. Not detecting a photon can mean the following:

- The qubit system is in an odd parity state but we did not wait long enough that a photon can decay. (This can also happen in perfect detection).
- We missed the decaying photon and will not detect any other because of the cut-off behaviour of the JPM.
- The system is in even parity and it is indeed not possible to detect photons because the cavity is in the vacuum state.

As an experimenter one would define a measurement time t_M which is long enough that it is most likely that a photon would have decayed if the cavity is not in the vacuum state. Therefore after this measurement time t_M one would interpret the former outcomes all equally, namely that the system is in even parity. The problem hereby is that one is not able to distinguish a failed measurement from a measurement of even parity. We will refer to this behaviour as the asymmetry of the detector which means that the detection procedure we used until now is perfectly successful if the qubit system is in an odd parity state and the click has been detected and it leaves us with different options if we do not detect a click which can lead to wrong interpretations of the measurement outcome.
In this section we propose a technique to avoid this asymmetry of the detection and to distinguish between a successful parity measurement and a failed measurement that can be ignored and repeated. Assume we have an initial state

$$P_e|\psi\rangle \otimes |0\rangle + P_o|\psi\rangle \otimes |\alpha\rangle, \tag{245}$$

with the even and odd parity projection operators P_e and P_o. The state describes an arbitrary qubit state $|\psi\rangle$ whose even parity subspace is entangled with a cavity in the vacuum state and whose odd parity state is entangled with a cavity with amplitude α. If we apply the measurement procedure from above and wait a time t_M we can only be sure to be in the odd parity state if we detect a click and if not we can misinterpret the result. If we divide the measurement time t_M in smaller intervals t_{M_i} and apply after every interval the displacement operator $D(\mp\alpha)$ on the cavity we change between the states

$$P_e|\psi\rangle \otimes |0\rangle + P_o|\psi\rangle \otimes |\alpha(t)\rangle \tag{246}$$

and

$$P_e|\psi\rangle \otimes |-\alpha(t)\rangle + P_o|\psi\rangle \otimes |0\rangle. \tag{247}$$

.
We changed $\alpha \to \alpha(t)$ to remember that the cavity still decays and to keep track of this. If we now measure the cavity and detect a click we know that the qubits are either in an odd parity state for every even time step $t_{M_{2k}}$ or in an even parity state for every odd time step $t_{M_{2k+1}}$. And if we do not detect a click we have to ignore the measurement and repeat it. If we simultaneously use the technique of dynamical decoupling we can get rid of the complex phase and the real decoherence from section 6 during the measurement. Furthermore we do not have to take care of the different cavity frequencies that occur because of the dispersive shifts. We only have to displace the cavity at its frequency ω_C. The displacement $D(\mp\alpha(t))$ therefore can be done very fast in time space because we can choose the Gaussian pulse to be as broad as we want in frequency space.

8.4 Results

In this section we show the results of a complete measurement of a qubit parity state. If we start in a state $|\text{parity}\rangle \otimes |\text{cavity}\rangle$, where we do not know the parity state nor the cavity state we can apply the procedure from the last section where we periodically displace the cavity to evaluate in which parity state we have been. After the drive stage we know that odd parity states are entangled with a bright cavity with amplitude α, $|\text{odd}\rangle \otimes |\alpha\rangle$, and even parity states are entangled with the vacuum state of the cavity $|\text{even}\rangle \otimes |0\rangle$.
In the simulation we flip the qubits at fixed time steps $t_{\text{flip}} = t_M/1000$, where the measurement time is set to $t_M = 1/\kappa_{\text{eff}}$. In the simulation we choose $\kappa_J/g_J = 1000$. In this regime the effective decay rate is accurate and as we have shown in section 7 the estimated cavity amplitude $\alpha(t)$ is precise. In figure 24 we illustrate the cavity behaviour during the measurement. When we entangle the cavity state $|\alpha\rangle$ with the qubit state $|111\rangle$ the cavity rotates in positive direction with a frequency 3χ. If the initial cavity amplitude is set to a positive real value α_{init} it starts at position A and rotates in positive direction until the qubits are flipped in position B at time t_{flip}. At this point the cavity rotates back to position A which it reaches at time $2t_{\text{flip}}$. After $3t_{\text{flip}}$ it reaches position C where the qubits are flipped again and the cavity will rotate back to A and the whole procedure repeats. The phase that the cavity gains between two flips will be $\approx \chi t_{\text{flip}}$ and for slow cavity rotations ($\chi \ll 1$) the cavity states at position B and C will not be far separated from the initial position A. Therefore χ and our choice of t_{flip} will be the only parameters that influence the success of the dynamical decoupling. If $\chi \gg 1$ the cavity will rotate fast and therefore the state can gain more phase between two flips than a slow rotating cavity at the same flip rate. If now a jump happens if the state gained much phase the average Hamiltonian will not hold anymore. For this reason the fidelity of the actual state will diverge from the initial state. In the regime $g_J \ll \kappa_J$ we know that the cavity amplitude at position A is $\alpha_{\text{init}} \exp(-\kappa_{\text{eff}} t)$. Whereat the cavity comes back to position A at even multiples of the flip time $2nt_{\text{flip}}$ with $n \in \mathbb{N}$. Because of that it will be necessary to displace the cavity only if the cavity is in position A otherwise we would have to keep track of the cavity phase.

Compared to the qubit flip rate $1/t_{\text{flip}}$ the frequency of the cavity displacement does not have to be high. A reasonable value is to displace the cavity 4 to 20 times per measurement time t_M. Which is built on the fact that the photon most likely decays during $t \in [0,\ 1/\kappa_{\text{eff}}]$ and therefore we have to check for both parity states during this period several times.

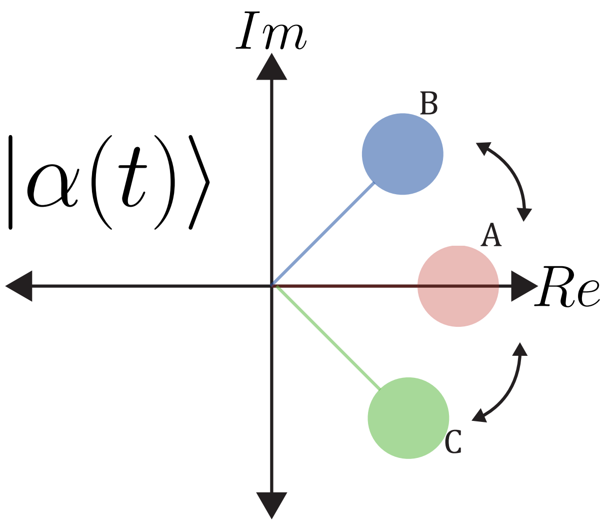

Figure 24: **Cavity phase evolution when qubits are flipped.** This figure illustrates the cavity behaviour in the rotating frame of the bare cavity frequency ω_C. If the initial cavity amplitude is real, the cavity amplitude starts at position A. Due to the dispersive term in the Hamiltonian the cavity state associated e.g. to the qubit state $|111\rangle$ will rotate in positive direction until the qubits are flipped in position B. After the qubit flip the cavity will rotate in negative direction. If it is back at position A the qubits are not flipped again and it will still rotate in negative direction until the qubits are flipped at position C. The cavity will rotate back to A and the whole procedure will be repeated. For an initial qubit state e.g. $|100\rangle$ the sequence will be reverse because this state is associated with a negative cavity frequency. It starts at A, goes to C, back to A, to B and then to A again.

If we repeat the measurement after a null-measurement (no click detected) our simulation shows that we can distinguish between odd and even parity state with very high accuracy. If we detect a click while the cavity is not displaced we know the qubit is in odd parity. If the cavity is displaced we know the qubit is in even parity. The success of this measurement depends on the accuracy of the displacement and this depends on our knowledge of the cavity amplitude $\alpha(t)$. On the other side we can see in Figure 25 that the fidelity of the state after the measurement with the initial state $\mathcal{F}(|\psi_{\text{meas}}\rangle, |\psi_{\text{init}}\rangle)$ decreases if we go to higher χ respectively if the cavity gains more phase per flip time t_{flip}. For the simulation we are following the steps:

- 1) initialize state $1/\sqrt{2}(|111\rangle + |100\rangle) \otimes |\alpha\rangle$
- 2) Split the measurement time in 1000 sub time steps $t_{\text{flip}} = 1/(1000\kappa_{\text{eff}})$.
- 3) Flip the qubits after every odd of these sub time steps which corresponds to a qubit flip at the positions B and C. Therefore the flip will be applied at times $k \cdot t_{\text{flip}}$ with $k \in \{1, 3, \cdots\}$
- 4) Displace the cavity every 120th sub time step $t_D = 120 \cdot t_{\text{flip}}$ with $D(\mp\alpha(t))$. With $\alpha(t) = \alpha \exp(-\kappa_{\text{eff}} t/2)$. The sign of the displacement will alternate from minus to plus, starting with minus. This corresponds to a cavity displacement of 8 times during the measurement time t_M. t_D has to be chosen such that the displacement will happen at position A, therefore it has to be chosen to be an even multiple of t_{flip}
- 5) If a jump is detected at time t_J we let the system evolve until the cavity amplitude reaches position A and reset the cavity with $D(-\alpha(t_J))$. If the jump happens at even multiples $k \in \{0, 2, \cdots\}$ of t_{flip} we know the cavity is rotating from B or C to A and we only have to wait until the last time interval of the time sub step $[kt_{\text{flip}}, (k+1)t_{\text{flip}}]$ is finished. If it happens at odd multiples of t_{flip} we know the cavity is moving from A to B or C and we have to wait one more sub time step t_{flip} that it can come back to position A until we reset.
- 6) If we do not detect a photon after $t_M = 1/\kappa_{\text{eff}}$ we reset the system and repeat the whole measurement.
- 7.a) If there would be a photon decay while the cavity is displaced we would know that the simulation procedure failed. Because we know in the simulation that we have an initial odd state. This error did not happen during the simulations because we chose $\kappa_J/g_J = 1000$ and therefore the cavity displacement is very accurate. (Even numbers of displacements $\rightarrow$ odd parity, odd numbers of displacements $\rightarrow$ even parity)
- 7.b) If we would have an arbitrary initial state and detect a photon while the cavity is displaced we know that the parity state was even. If we detect a photon while the cavity is not displaced we know the parity state was odd. To keep track of this one only has to know how many times the cavity has been displaced.

- 8) After the detection of a photon we reset the cavity at position A with the amplitude $\alpha_{\text{end}} = \alpha \exp(-\kappa_{\text{eff}} t_J)$ to fully disentangle the qubits from the cavity.

In a real measurement we would not know the initial state from the first point and we would therefore leave out 1). Furthermore we do have to choose g_J/κ_J such that an error like in 7a) is highly unlikely to happen. Which means it should not happen that the displacement of the cavity leads to an even parity state that is entangled with a non zero cavity while the cavity state that corresponds to an even qubit parity state should be zero. So if we start in an even parity state

$$|\psi\rangle = |\text{even}\rangle \otimes |0\rangle \tag{248}$$

and displace it after t_D with $D(-\alpha(t_D) + \delta\alpha_1)$ with some inaccuracy $\delta\alpha_1$ and do the 2nd displacement after $2 \cdot t_D$ with $D(+\alpha(2t_D) + \delta\alpha_2)$ we will end up in the state

$$|\psi\rangle = |\text{even}\rangle \otimes |\delta\alpha_2 - \delta\alpha_1\rangle. \tag{249}$$

Therefore we entangled the even parity state with a cavity with a non-zero amplitude while it should actually be zero. If now a photon decays from this cavity state we would assume that the parity state is odd because we displaced the cavity an even number of times (7b). To avoid this we have to go to the regime $g_J \ll \kappa_J$ where the cavity displacement is accurate. In section 7 we showed that we can reach very high cavity displacement accuracy in this regime.

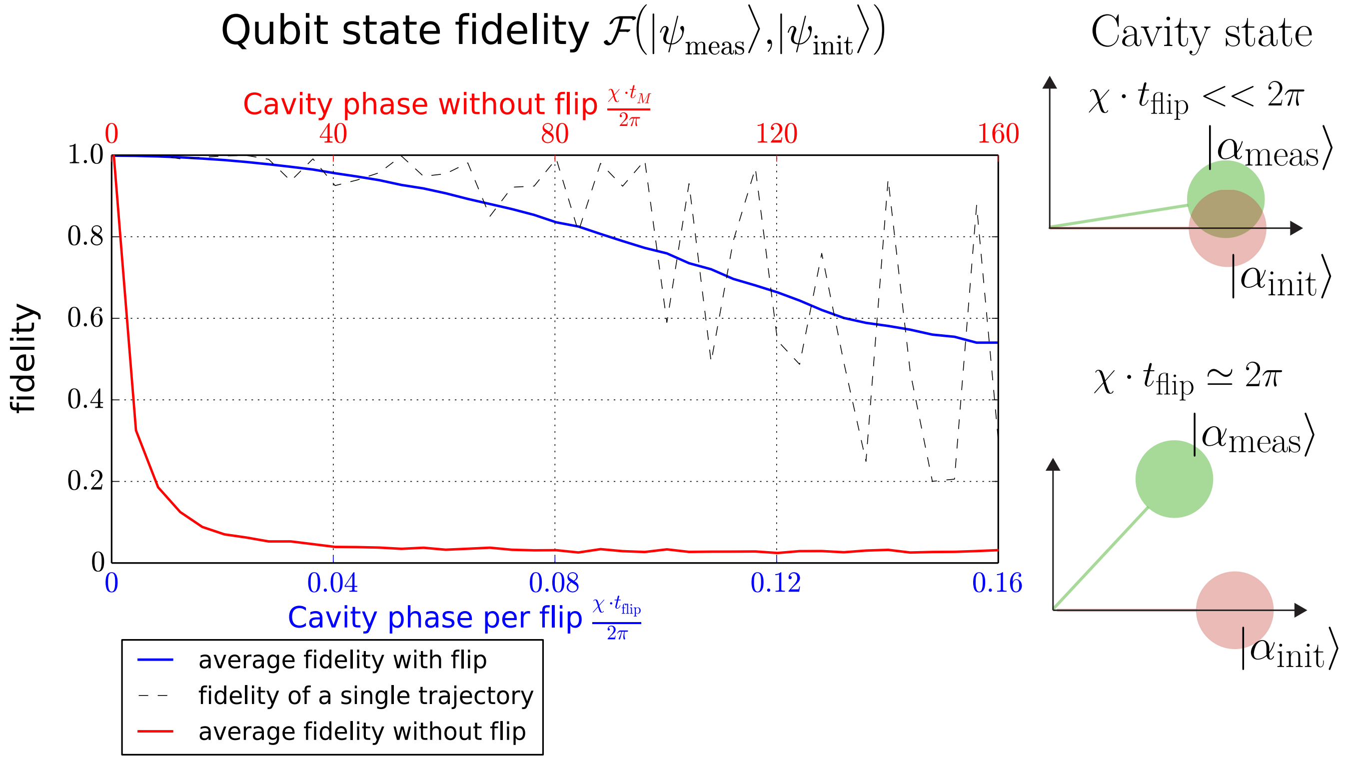

Figure 25: **Fidelity of the qubit state before and after the measurement.** The ratio $\kappa_J/g_J = 1000$ was fixed, $\alpha = 3.0$ and t_{flip} is set to $t_M = \frac{1}{1000\kappa_{\text{eff}}}$. Therefore for increasing χ the cavity gains more phase between the qubit flips and the fidelity decreases because the probability that a jump happens if the cavity is far rotated from the initial direction A increases. The black dashed line is the outcome of a single measurement at different χ. Here we can see the influence of the random photon jumps. If the photon decays if the cavity is exactly at its initial position A we still reach fidelity values $\mathcal{F} \to 1$. The blue line represents the average over 8000 single measurements. The red line is the fidelity if we do not flip the qubits and therefore the phase that the cavity can gain until the photon decays is simply χt_M. On the right one can see the cavity states that correspond to a high respectively to a low fidelity value.

Figure 25 shows the numerical values of the fidelity of the bare qubit state after the simulation. In this figure we only took data from successful measurements where a photon decayed during the measurement time $t_M = 1/\kappa_{\text{eff}}$. Because in an experiment we would have to repeat after a null-measurement. The detector furthermore is perfect which means that if a photon was released we detected it. In the simulation we focused on an initial odd parity state that is entangled with a bright cavity and displace the cavity 8 times during t_M. Therefore if the cavity is displaced we do not measure a photon. The only thing one has to be careful with in this matter is that the displacement has to happen if the cavity amplitude is at position A because in a realistic simulation we do not keep track of the cavity phase during the measurement. The cavity will gain some phase φ which is at the positions B and C of the order $\pm\chi t_{\text{flip}}$ and at position A it will be zero. The state before the jump therefore has the form

$$|\psi\rangle = |\mathrm{q}_1\rangle \otimes |\alpha \exp(-\frac{\kappa_{\text{eff}}}{2}\mathrm{t})\mathrm{e}^{\varphi_1(\mathrm{t})}\rangle + |\mathrm{q}_2\rangle \otimes |\alpha \exp(-\frac{\kappa_{\text{eff}}}{2}\mathrm{t})\mathrm{e}^{\varphi_2(\mathrm{t})}\rangle + \cdots , \tag{250}$$

with a qubit state dependent phase $\varphi_i(t) \in [-\varphi_{i,C}, \varphi_{i,B}]$ and arbitrary odd parity qubit substates $|\mathrm{q_i}\rangle$. If now a photon decays at a random time t_J. The cavity phases will appear as prefactors of the qubit subspaces

$$|\psi\rangle = e^{\varphi_1(t_J)}|\mathrm{q}_1\rangle \otimes |\alpha \exp(-\frac{\kappa_{\text{eff}}}{2}\mathrm{t})\mathrm{e}^{\varphi_1(\mathrm{t})}\rangle + \mathrm{e}^{\varphi_2(\mathrm{t_J})}|\mathrm{q}_2\rangle \otimes |\alpha \exp(-\frac{\kappa_{\text{eff}}}{2}\mathrm{t})\mathrm{e}^{\varphi_2(\mathrm{t})}\rangle + \cdots . \tag{251}$$

After the photon decay the cavity still rotates at the frequency $\varphi_i(t)$ but the prefactor is fixed at $\varphi_i(t_J)$. Therefore we wait until the cavity is back in position A and then reset the cavity to zero. In figure 25 one can see that we reach fidelity values of almost 100 % if $\chi t_{\text{flip}} \ll 1$. Because in this regime the cavity cannot gain much phase between the qubit flips and therefore the prefactor $e^{\varphi_i(t_J)} \approx 1$ and there is no dephasing. The dashed line in figure 25 represents the fidelity values of single measurements at different dispersive shifts χ and one can see its random character. If a jump happens if the cavity is almost at position A we can reach high fidelity values even for fast cavity rotations. Therefore we averaged this fidelity values over 8000 single measurements and see that on average we will have better fidelity values if we are in the regime $\chi t_{\text{flip}} \ll 1$, where the cavity does not gain much phase between the jumps. Imperfect detection with $\eta < 1$ does not change our measurement protocol. In step 5 from above we include both cases of how we cannot detect a photon. The measurement time t_M could be too short and there is a non-zero probability, that no photon can release the cavity after t_M even if it is bright. Or a photon actually leaked out of the cavity but the detector missed it. In an experiment we cannot distinguish this two cases. But as a consequence we would have to repeat the measurement. So the only effect an imperfect detector will have on our measurement will be that we have to repeat it more often due to a null-measurement. The probability of such a failed detection is simply $1 - \eta$. And the success of the measurement will be decreased by the factor η.
The red line is the fidelity of a simulation where we do not flip the qubits averaged over 4000 trajectories. In this case the cavity can gain a maximum phase of χt_M during the measurement and we can see that the fidelity is decreasing much faster compared to the flipped case. Already for small values for χ the cavity can gain phases of more than 2π during the measurement and therefore the photon jump can happen at almost any phase between 0 and 2π.

8.5 Interpretation of the numerical results with realistic parameters

Finally we would like to discuss our results for realistic physical values for our parameter. As already proposed by Govia et al. [1] it is desired to have dispersive shifts χ of the order $\approx$ 10MHz because at this regime we will have drive times of the order 100ns. If the dispersive shift is smaller the drive time will become longer.
If the cavity-JPM coupling strength g_J is of the order 10MHz a desirable decay rate κ_J would be of the order 10GHz. Which means that the JPM has to be driven in a way that the excited state almost directly tunnels through the potential well to the continuum. The condition $\kappa_J/g_J = 1000$ is not directly necessary for high fidelity values, but it will be necessary to displace the cavity with high accuracy. And this on the other hand is necessary to avoid the asymmetry of the detection which favoured measurement outcomes with a click (odd qubit parity states), compared to measurement outcomes without a click (even qubit parity states).
Therefore for a fixed measurement time $t_M = 1/\kappa_{\text{eff}}$ and 1000 flips per t_M we get the following fidelities:

	g_J [MHz]	χ [MHz]	κ_J [GHz]	t_{flip} [ns]	phase per flip	Fidelity [%]
a	10	10	10	25	0.04	95.5
b	20	10	20	12.5	0.02	98.8
c	10	20	10	25	0.08	83.5
d	20	20	10	12.5	0.04	95.5
e	10	5	10	25	0.02	98.8
f	20	5	10	12.5	0.01	99.1
g	10	10	1	2.5	0.004	99.8
h	20	10	2	1.25	0.002	99.9

The values for κ_J in line g and h (red colour) lead to a κ_J/g_J ratio of 100 and therefore the displacement accuracy is smaller which will be disadvantageous if we want to avoid the detection asymmetry, where we periodically displace the cavity. And since the flip rate is fixed at $1/(1000\kappa_{\text{eff}})$ the flip times reach values that are too small to be experimentally realized. But in these examples we can see that if $\chi \cdot t_{\text{flip}} \ll 2\pi$ we can reach fidelity values of more than 99%. Concerning this matter and if we compare e.g. line b, d and f we can see that it will be preferable to keep χ as small as possible because we want to gain as little phase as possible between two qubit flips. But this on the other hand prolongs the drive stage as mentioned before. In conclusion we can say that it is possible to reach fidelity values of more than 98% with realistic parameters if it is possible to engineer qubit flip times of around 10ns and without a dispersive shift χ that is too small. If it will somehow be possible to reach qubit flip times of the order 1ns fidelity values of more than 99.5% are within reach.

9 Discussion and Conclusion

In this section the main results of this project will be summarized and discussed.

9.1 Summary of the results

In this thesis we investigated an ancilla free qubit parity measurement proposed by Govia et al. [2], which is supposed to be a quantum non-demolition measurement (QND). To do so it was proposed to entangle odd qubit parity states with a displaced cavity of the amplitude α and the even parity states with a cavity in the vacuum state. Therefore the parity information can be read out by measuring a single photon that leaves the cavity. The measurement of such a photon is realized by coupling a current biased Josephson junction (CBJJ), which we also refer to as the Josephosn photon multiplier (JPM), to the cavity. In our model we describe the CBJJ as a 3-level system with the ground state $|1\rangle$, the excited state $|2\rangle$ and the continuum state $|0\rangle$. If the cavity contains photons they can excite the CBJJ from its ground state to the excited state, where it can tunnel to the continuum, which will result in a measurable voltage pulse across the CBJJ. The initial observation in this thesis was a decay of the qubit coherence during the parity measurement that was proposed by Govia et al. [2], which is a consequence of the insufficiency of a QND measurement in quantum error correction. Therefore we demand the parity measurement to be stronger than just quantum-non-demolition, for a successful QEC. It has to be eigenstate preserving QND. [6] As a first step we could show how the parity measurement corrupts the initial state. For this we found an effective decay rate that describes the cavity-JPM dynamics in a similar way as the vacuum Purcell effect. For a fast detector, where the tunnelling rate κ_J of the excited state to the continuum state of the CBJJ is much bigger than the Jaynes-Cummings coupling g_J of the cavity to the ground state and the excited state of the CBJJ, the occupation of the continuum state $|0\rangle$ of the CBJJ can approximated with

$$\rho_{00}(t) = 1 - \exp\left(-\kappa_{\text{eff}}^{\text{JPM}} t\right), \tag{252}$$

with the effective decay rate of the CBJJ

$$\kappa_{\text{eff}}^{\text{JPM}} = \frac{4g_J^2\alpha^2}{\kappa_J}\left(1 - 4\frac{\Delta^2}{\kappa_J^2}\right). \tag{253}$$

Where Δ is the detuning of the cavity and the CBJJ caused by the dispersive shift χ of the qubit. We also have been able to show that this approximation holds very well for $\alpha \gg 1$. In this regime we have a good agreement of the full system numerics with the analytical solution of ρ_{00}.

As a consequence of this we also have been able to approximate the effective decay rate of the cavity

$$\kappa_{\text{eff}}^{\text{cav}} = \frac{1}{\alpha^2}\kappa_{\text{eff}}^{\text{JPM}} \tag{254}$$

Due to the fact that we will measure single photons to determine the parity of the qubit state we changed to the quantum trajectory picture to get a better understanding of the back-action of a single measurement on the states. Furthermore we could take the behaviour of the CBJJ into account which cuts off the decay after the loss of one photon, when we approximate the cavity-CBJJ interaction with a leaking cavity with the effective decay rate $\kappa_{\text{eff}}^{\text{cav}}$. This can be achieved by calculating or simulating a lossy cavity in the quantum trajectory picture only until it loses one photon. In the regime $\kappa_J \gg g_J$ we could show that the cavity amplitude can be approximated very well by $\alpha \exp(-\frac{\kappa_{\text{eff}}^{\text{cav}}}{2}t)$.
Furthermore we could show that the cavity gains a qubit state dependent phase which comes from the dispersive term of the Hamiltonian $H_{\text{disp}} = (\chi_1\sigma_1^z + \chi_2\sigma_2^z + \cdots)a^\dagger a$. And this phase appears as a qubit prefactor when a photon decays which is the reason for the qubit decoherence. Additionally this prefactor is completely random since it contains the photon jump time t_J. The photon decay therefore leads to a random phase factor between the intra parity qubit states.
The dispersive term of the Hamiltonian also leads to a qubit state dependent detuning Δ between the cavity and the JPM. And since the effective decay rate $\kappa_{\text{eff}}^{\text{cav}}$ is dependent on the detuning we also obtain decoherence between the qubit states of the same parity state that is caused by the renormalization of the cavity. In the picture of the new logical Bloch sphere we called it decoherence in the logical z-direction. This effect is caused by the evolution before the photon jump, because through the detuning dependent effective decay rate, the cavity states are damped differently and therefore differently renormalized. The qubit states before and after the photon jump for the initial state $|\psi(0)\rangle = \frac{1}{\sqrt{2}}(|\underbrace{111}_{\text{u}}\rangle + |\underbrace{100}_{\text{d}}\rangle) \otimes |\alpha\rangle$ are

$$|\psi(t < t_J)\rangle = \frac{\left(e^{-\frac{|\alpha|^2}{2}(1-e^{-\kappa_{\text{u}}t})}|\text{u}\rangle \otimes |\alpha e^{-\frac{\kappa_{\text{u}}}{2}t}e^{-it\phi_{\text{u}}}\rangle + e^{-\frac{|\alpha|^2}{2}(1-e^{-\kappa_{\text{d}}t})}|\text{d}\rangle \otimes |\alpha e^{-\frac{\kappa_{\text{d}}}{2}t}e^{-it\phi_{\text{d}}}\rangle\right)}{\sqrt{e^{|\alpha|^2(1-e^{-\kappa_{\text{u}}t})} + e^{|\alpha|^2(1-e^{-\kappa_{\text{d}}t})}}} \tag{255}$$

and

$$\begin{aligned}|\psi(t > t_J)\rangle = \mathcal{N}_\psi \Big(&\alpha\sqrt{\kappa_{\text{u}}}e^{-(\frac{\kappa_{\text{u}}}{2}+i\phi_{\text{u}})t_J}e^{-\frac{|\alpha|^2}{2}(1-e^{-\kappa_{\text{u}}t_J})}|\text{u}\rangle \otimes |\alpha e^{-\frac{\kappa_{\text{u}}}{2}t_J}e^{-it\phi_{\text{u}}}\rangle \\ &+\alpha\sqrt{\kappa_{\text{d}}}e^{-(\frac{\kappa_{\text{d}}}{2}+i\phi_{\text{d}})t_J}e^{-\frac{|\alpha|^2}{2}(1-e^{-\kappa_{\text{d}}t_J})}|\text{d}\rangle \otimes |\alpha e^{-\frac{\kappa_{\text{d}}}{2}t_J}e^{-it\phi_{\text{d}}}\rangle\Big)\end{aligned}. \tag{256}$$

With the jump time t_J, the phases $\phi_u = +3i\chi$, $\phi_d = -i\chi$ and the normalization

$$\mathcal{N}_\psi = \frac{1}{\sqrt{|\alpha|^2\kappa_{\text{u}}e^{-\kappa_{\text{u}}t_J}e^{|\alpha|^2(1-e^{-\kappa_{\text{u}}t_J})} + |\alpha|^2\kappa_{\text{u}}e^{-\kappa_{\text{d}}t_J}e^{|\alpha|^2(1-e^{-\kappa_{\text{d}}t_J})}}}. \tag{257}$$

These calculation also can be applied for arbitrary other initial states and we also could show that they predict the time evolution of our state very accurate. Importantly we do not have to have any knowledge about the initial state to calculate the phases that the substates gain. We only have to know the jump time t_J, when a photon decays from the cavity and the parity measurement outcome. In a last step we proposed a way to avoid these corruptions of our initial state by applying the technique of dynamical decoupling, where we periodically flip the qubits. This leads to a new averaged Hamiltonian which does not contain the dispersive part any more. Simulations showed that this technique is very promising if we choose the qubit flipping fast enough compared to the inverse of the dispersive shift $t_{\text{flip}} \ll 1/\chi$ so the cavity cannot gain much phase between the flips. With this technique we reach qubit fidelity values of more than 98%. If we also take into account the imperfections of our detector we have to be aware of the asymmetry of the detection scheme of Govia et al. [2] If we detect a click everything is fine and we know that we measured odd parity. If we do not detect a click there are several options how the outcome can be interpreted. Therefore we propose to displace the cavity several times during the whole measurement time t_M and alternately entangle the bright cavity with the odd and the even qubit parity states. If we do this in the regime $g_J \ll \kappa_J$ the displacement is highly accurate and we can avoid the asymmetry of the detection since we know that initially the odd parity states are entangled with a bright cavity (where a photon can decay) and the even parity states are entangled with an empty cavity, where no detection is possible.

9.2 Conclusion

In conclusion we have found an extension of the measurement that was proposed by Govia et al. [2] with which we can avoid several problems that can occur during a measurement. If we dynamically decouple the dispersive term of the Hamiltonian during the measurement we can avoid qubit decoherence and reach qubit state fidelities of more than 98%. And even if we have imperfect detection and miss photons during the measurement we can distinguish between a failed and a successful measurement. The former has to be repeated and since the probability of a failed measurement is directly dependent on the detector efficiency η it will be necessary to have high detector efficiencies for a fast measurement. Furthermore we showed that we can reach high fidelity values if we are able to design the setup such that we can flip the qubits at a rate of the order 10ns.

10 Appendix

10.1 Derivation of the drive stage

For the derivation of the cavity occupation we start with the reduced cavity Hamiltonian coupled to two qubits:

$$H = \tilde{\omega}_C a^\dagger a + A(t)(a + a^\dagger) \tag{258}$$

with $\tilde{\omega}_C = \omega_C + \tilde{\chi}_Q$, where $\tilde{\chi}_Q$ is the qubit parity dependent dispersive shift. $\tilde{\chi}_Q = 0$ for odd parity, $\tilde{\chi}_Q = \pm 2\chi_Q$ for even parity. The drive has the form $A(t) = a_0 \cos(\omega_D t + \phi)$. Therefore we get the Hamiltonian:

$$H = (\omega_C + \tilde{\chi}_Q)\, a^\dagger a + \frac{a_0}{2}\left(e^{-i(\omega_D t+\phi)} + e^{+i(\omega_D t+\phi)}\right)\left(a^\dagger + a\right) \tag{259}$$

$$= (\omega_C + \tilde{\chi}_Q)\, a^\dagger a + \underbrace{\frac{a_0}{2}e^{-i\phi}}_{=\xi} e^{-i\omega_D t}\left(a^\dagger + a\right) + \underbrace{\frac{a_0}{2}e^{+i\phi}}_{=\xi^*} e^{+i\omega_D t}\left(a^\dagger + a\right) \tag{260}$$

Here we use the rotating wave approximation (RWA) [3]. For this we set our system to a rotating frame with the unitary transformation $U(t) = \exp(i\omega_C a^\dagger a t)$. Assuming now, that $|\omega_C + \omega_D| \gg |\omega_C - \omega_D|$. This assumption is reasonable, because the drive is just slightly detuned from the cavity frequency by the amount of χ_Q. Doing this transformation with the relations:

$$e^{-\lambda\hat{n}} a e^{\lambda\hat{n}} = e^{\lambda} a \tag{261}$$

$$e^{-\lambda\hat{n}} a^\dagger e^{\lambda\hat{n}} = e^{-\lambda} a^\dagger \tag{262}$$

$$\tilde{H} = U^\dagger H U - iU\dot{U}^\dagger \tag{263}$$

and $\hat{n} = a^\dagger a$, we get:

$$\tilde{H} = \tilde{\chi}_Q a^\dagger a + \xi^* a e^{it(\omega_D+\omega_C)} + \xi a^\dagger e^{-it(\omega_D+\omega_C)} + \xi^* a^\dagger e^{-it(\omega_D-\omega_C)} + \xi a e^{-it(\omega_D-\omega_C)} \tag{264}$$

To justify the dropping of the counter-rotating terms we consider the corresponding evolution operator [3]:

$$U_{evol}(t) = \exp\left(-i\int_0^t d\tau \tilde{H}(\tau)\right) \tag{265}$$

Performing the time integral one sees that the counter rotating terms are proportional to $1/|\omega_C + \omega_D|$ and the non-counter rotating terms are proportional to $1/|\omega_C - \omega_D|$. Due to the approximation $|\omega_C + \omega_D| \gg |\omega_C - \omega_D|$ we can neglect the counter rotating terms in the Hamiltonian. Therefore:

$$H = (\omega_C + \tilde{\chi}_Q)a^\dagger a + \xi a e^{it\omega_D} + \xi^* a^\dagger e^{-it\omega_D} \tag{266}$$

If we now look at the time evolution of the operator a with the Heisenberg equation of motion,

$$\frac{da}{dt} = -i\big[a, H\big] = -i\Big\{(\omega_C + \tilde{\chi}_Q)\big[a, a^\dagger a\big] + \xi^* e^{-i\omega_D t}\big[a, a^\dagger\big] + \xi e^{+i\omega_D t}\big[a, a\big]\Big\} \tag{267}$$

use commutator relations and we get:

$$= -i\big((\omega_C + \tilde{\chi}_Q)a + \xi^* e^{-i\omega_D t}\big) \tag{268}$$

Now we can integrate the differential equation:

$$a(t) = a(0) - i\int_0^t d\tau \xi(\tau) e^{-i(\omega_D - \omega_C - \tilde{\chi}_Q)\tau} e^{-i(\omega_C + \tilde{\chi}_Q)t} \tag{269}$$

Since the coherent state $|\alpha(t)\rangle$ is an eigenstate of $a(t)$ with eigenvalue $\alpha(t)$ we can look at the evolution of $\alpha(t)$ instead of the operator $a(t)$. By assuming that the resonator was initially in vacuum state $\alpha(0) = 0$. The state at the time t is given by $|\alpha(t)\rangle$ with the amplitude.

$$\alpha(t) = -i\bigg(\int_0^t d\tau \xi^*(\tau) e^{-i(\omega_D - \omega_C - \tilde{\chi}_Q)\tau}\bigg) e^{-i(\omega_C + \tilde{\chi}_Q)t} \tag{270}$$

Now assume $\xi(t)$ varies slowly compared to the detuning. $|\omega_d - \omega_C| \gg \dot{\xi(t)}/\xi(t)$ so we can take $\xi(t)$ out of the integral and evaluate it.

$$\alpha(t) \simeq \frac{\xi e^{-i(\omega_C + \tilde{\chi}_Q)t}}{\omega_D - \omega_C - \tilde{\chi}_Q}\big(e^{-i(\omega_D - \omega_C - \tilde{\chi}_Q)t} - 1\big) \tag{271}$$

if we calculate the absolute value squared, we get:

$$|\alpha(t)|^2 \simeq \frac{|\xi^*|^2}{|\omega_D - \omega_C - \tilde{\chi}_Q|^2}\big|e^{-i(\omega_D - \omega_C - \tilde{\chi}_Q)t} - 1\big|^2 \tag{272}$$

If we drive the cavity on resonance $\omega_D = \omega_C$ we can look at the even and the odd case separately in the following way. Odd case ($\tilde{\chi}_Q = 0$): The exponent is very small and we can expand it and leave higher order away.

$$|\alpha_O(t)|^2 = \frac{|\xi|^2}{|\omega_D - \omega_C - \tilde{\chi}_Q|^2}\big|1 - i(\omega_D - \omega_C - \tilde{\chi}_Q)t + \cdots - 1\big|^2 \tag{273}$$

$$= \frac{|\xi|^2}{\cancel{|\omega_D - \omega_C - \tilde{\chi}_Q|^2}}\cancel{\big|\omega_D - \omega_C - \tilde{\chi}_Q\big|^2}\big|t\big|^2 = |\xi|^2|t|^2 \overbrace{=}^{|\xi|^2=(a_0/2)^2} = \Big(\frac{a_0}{2}t\Big)^2 \tag{274}$$

In the even case ($\tilde{\chi}_Q = \pm 2\chi_Q$):

$$\big|e^{-i(\omega_D - \omega_C - \tilde{\chi}_Q)t} - 1\big|^2 = 4\sin^2\big(\frac{2\chi_Q t}{2}\big) = 4\frac{1}{2}(1 - \cos(2\chi_Q t)) \tag{275}$$

This holds weather $\tilde{\chi}_Q = +2\chi_Q$ or $\tilde{\chi}_Q = -2\chi_Q$.
Plug this into $\alpha(t)$, set again $\omega_D = \omega_C$ and $|\xi|^2 = (a_0/2)^2$.

$$|\alpha_E(t)|^2 = \frac{|\xi|^2}{|2\chi|^2}4\frac{1}{2}(1 - \cos(2\chi_Q t)) = \bigg(\frac{a_0}{2\chi_Q}\bigg)^2\frac{1}{2}(1 - \cos(2\chi_Q t)) \tag{276}$$

10.2 Rotating Frame

Putting a system to a rotating frame is sometimes useful to simplify the Hamiltonian and investigate for example the time evolution just caused by some specific terms of the Hamiltonian. In the specific case of section 2.1 we are interested in the time evolution caused by the dispersive shift of the cavity $\chi_n \sigma_n^z a^\dagger a$. The full Hamiltonian reads,

$$H = \omega_C a^\dagger a + \sum_{n=1}^{N} (\chi_{Q_n} a^\dagger a + \frac{\omega_{Q_n} + \chi_{Q_n}}{2}) \sigma_n^z \tag{277}$$

Defining a unitairy transformation $U(t) = \exp(i \sum_{n=1}^{N} \frac{\omega_{Q_n} + \chi_{Q_n}}{2} \sigma_n^z t) = \exp(i \sum_{n=1}^{N} \frac{\omega_n'}{2} \sigma_n^z t)$ the Hamiltonian transforms,

$$\tilde{H} = UHU^\dagger - iU\dot{U}^\dagger \tag{278}$$

evaluating first the second right hand term,

$$-iU\dot{U}^\dagger = -i \exp\left(i \sum_{n=1}^{N} \frac{\omega_n'}{2} \sigma_n^z t \right) \left(-i \sum_{n=1}^{N} \frac{\omega_n'}{2} \sigma_n^z \right) \exp\left(-i \sum_{n=1}^{N} \frac{\omega_n'}{2} \sigma_n^z t \right) \tag{279}$$

because $\left[\sigma_i^z, \sigma_j^z\right] = 0 \forall i, j$ the exponentials chancel and,

$$-iU\dot{U}^\dagger = -i \left(-i \sum_{n=1}^{N} \frac{\omega_n'}{2} \sigma_n^z \right) = - \left(\sum_{n=1}^{N} \frac{\omega_n'}{2} \sigma_n^z \right) \tag{280}$$

Evaluating the first second hand term of $\tilde{H}$ we can use the same arguments. $\left[a^\dagger a, \sigma_j^z\right] = 0$ and $\left[\sigma_i^z, \sigma_j^z\right] = 0 \forall i, j$ leads to,

$$UHU^\dagger = H \tag{281}$$

Plugging this together leads to,

$$\tilde{H} = UHU^\dagger - iU\dot{U}^\dagger = H - \left(\sum_{n=1}^{N} \frac{\omega_n'}{2} \sigma_n^z \right) \tag{282}$$

Therefore this transformation chancels simply the bare qubit term of the Hamiltonian. To get rid of the bare cavity term $\omega_C a^\dagger a$ one can repeat the same calculation with $U(t) = \exp(i\omega_C a^\dagger a t)$.
One has to keep in mind, that the state vectors $|\psi\rangle$ also transform under the unitairy transformation $|\tilde{\psi}\rangle = U^\dagger |\psi\rangle$. This will also lead to some dynamics in the parity subspaces which are not the focus of this work. We are interested in the dephasing caused by the measurement which is mainly the qubit-cavity interaction. The dephasing caused for example by the unitary transformation $U(t) = \exp(i \sum_{n=1}^{N} \frac{\omega_n'}{2} \sigma_n^z t)$ would also occur in the bare qubit system and does not change if one couples it to a cavity.

10.3 Derivation of the cavity occupation

Evtl. noch dazu nehmen also expect(a.dag a)

$$\langle a^\dagger a \rangle = tr\left[\rho_{cav} a^\dagger a\right] \tag{283}$$

Using the relation from equation 52, with $\lambda = 0$ leads to,

$$C_n^{\left[\rho_{cav} a^\dagger a\right]} \bigg|_{\lambda=0} = tr\left[\rho_{cav} a^\dagger a e^{\lambda a^\dagger} e^{-\lambda^* a}\right] \bigg|_{\lambda=0} = tr\left[\rho_{cav} a^\dagger a\right] = -\frac{\partial}{\partial \lambda^*} \frac{\partial}{\partial \lambda} C^{[\rho_{cav}]} \tag{284}$$

With $\rho_{cav} = tr_{qb}\left[\rho\right]$ is the cavity density matrix with the qubits traced out. With $\sigma_i \in \{\uparrow, \downarrow\}$ The density matrix of the full system in the qubit basis has the form:

$$\rho = \sum_{\sigma_1',\sigma_2',\sigma_1'',\sigma_2''} \rho_{\sigma_1'\sigma_2'\sigma_1''\sigma_2''} |\sigma_1'\sigma_2'\rangle\langle\sigma_1''\sigma_2''| \tag{285}$$

The partial trace can be performed the following:

$$\rho_{cav} = tr_{qb}\left[\rho\right] = \sum_{\sigma_1,\sigma_2} \langle\sigma_1\sigma_2| \left(\sum_{\sigma_1',\sigma_2',\sigma_1'',\sigma_2''} \rho_{\sigma_1'\sigma_2',\sigma_1''\sigma_2''} |\sigma_1'\sigma_2'\rangle\langle\sigma_1''\sigma_2''| \right) |\sigma_1\sigma_2\rangle \tag{286}$$

Using the orthogonality relation $\langle\sigma_1\sigma_2|\sigma_1'\sigma_2'\rangle = \delta_{\sigma_1,\sigma_1'}\delta_{\sigma_2,\sigma_2'}$ we find,

$$\rho_{cav} = \sum_{\sigma_1,\sigma_2} \rho_{\sigma_1\sigma_2,\sigma_1\sigma_2} \tag{287}$$

Therefore ρ_{cav} consists only of the diagonal elements of ρ

$$\begin{aligned} C_n^{\left[\rho_{cav}a^\dagger a\right]} &= tr\left[\rho_{cav}a^\dagger a e^{\lambda a^\dagger} e^{-\lambda^* a}\right] = tr\left[\sum_{\sigma_1,\sigma_2} \rho_{\sigma_1\sigma_2,\sigma_1\sigma_2} a^\dagger a e^{\lambda a^\dagger} e^{-\lambda^* a}\right] \\ &= \sum_{\sigma_1,\sigma_2} tr\left[\rho_{\sigma_1\sigma_2,\sigma_1\sigma_2} a^\dagger a e^{\lambda a^\dagger} e^{-\lambda^* a}\right] = \sum_{\sigma_1,\sigma_2} C_n^{\left[\rho_{\sigma_1\sigma_2,\sigma_1\sigma_2}a^\dagger a\right]} \end{aligned} \tag{288}$$

We have to find the diagonal elements of ρ to calculate $\langle a^\dagger a\rangle$. For this we can do a very similar calculation like in section 10.4.

$$\dot\rho_{ii} = -i\left[H_1, \rho_{ii}\right] + \kappa(\omega_r) D\left[a\right]\rho_{ii} \tag{289}$$

$$\frac{d}{dt} C_n^{[\rho_{ii}]} = tr\left[\dot\rho_{ii} e^{\lambda a^\dagger} e^{-\lambda^* a}\right] = \tag{290}$$

Doing exactly the same calculations but with the ansatz for diagonal terms $\rho_{ii} = |c_{ii}|^2 |\alpha_i(t)\rangle\langle\alpha_i(t)|$ where the prefactor c_{ii} is not time dependent compared to the off-diagonal terms. At first it leads to the same cavity states:

$$\dot\alpha_1(t) = \alpha_1(t)\left[-i(\omega_C + \chi 1 + \chi 2) - \frac{\kappa}{2}\right] \Rightarrow \alpha_1(t) = \alpha_1(0)\exp\left(\left[-i(\omega_C + \chi 1 + \chi 2) - \frac{\kappa}{2}\right] t\right) \tag{291}$$

$$\dot\alpha_2(t) = \alpha_2(t)\left[-i(\omega_C - \chi 1 - \chi 2) - \frac{\kappa}{2}\right] \Rightarrow \alpha_2(t) = \alpha_2(0)\exp\left(\left[-i(\omega_C - \chi 1 - \chi 2) - \frac{\kappa}{2}\right] t\right) \tag{292}$$

$$\dot\alpha_3(t) = \alpha_3(t)\left[-i(\omega_C + \chi 1 - \chi 2) - \frac{\kappa}{2}\right] \Rightarrow \alpha_3(t) = \alpha_3(0)\exp\left(\left[-i(\omega_C + \chi 1 - \chi 2) - \frac{\kappa}{2}\right] t\right) \tag{293}$$

$$\dot\alpha_4(t) = \alpha_4(t)\left[-i(\omega_C - \chi 1 + \chi 2) - \frac{\kappa}{2}\right] \Rightarrow \alpha_4(t) = \alpha_4(0)\exp\left(\left[-i(\omega_C - \chi 1 + \chi 2) - \frac{\kappa}{2}\right] t\right) \tag{294}$$

Now calculating,

$$\begin{aligned} \langle a^\dagger a\rangle &= \sum_{\sigma_1,\sigma_2} C_n^{\left[\rho_{cav}a^\dagger a\right]}\Big|_{\lambda=0} = \sum_{\sigma_1,\sigma_2} C_n^{\left[\rho_{\sigma_1\sigma_2,\sigma_1\sigma_2}a^\dagger a\right]}\Big|_{\lambda=0} = -\sum_{\sigma_1,\sigma_2} \frac{\partial}{\partial\lambda^*}\frac{\partial}{\partial\lambda} C^{\left[\rho_{\sigma_1\sigma_2,\sigma_1\sigma_2}\right]}\Big|_{\lambda=0} \\ &= -\sum_i \frac{\partial}{\partial\lambda^*}\frac{\partial}{\partial\lambda}\left(\alpha_i e^{\lambda\alpha_i^* - \lambda^*\alpha_i}\right)\Big|_{\lambda=0} = \sum_i \alpha_i(0) e^{\lambda\alpha_i^* - \lambda^*\alpha_i}|\alpha_i(t)|^2\Big|_{\lambda=0} = \sum_i \alpha_i(0)|\alpha_i(t)|^2 \end{aligned} \tag{295}$$

and $|\alpha_i(t)|^2 = \alpha_i^2(0)\exp\left(-\kappa t\right)\ \forall i$. Therefore the decay rate of the cavity is κ.

10.4 Calculation of $c_{12}(t)$

$$\dot{\rho}_{12} = -i(H_1\rho_{12} - \rho_{12}H_2) + \kappa(\omega_r)D\left[a\right]\rho_{12} \tag{296}$$

$$H_1 = (\omega_C + \chi_1 + \chi_2)a^\dagger a \tag{297}$$
$$H_2 = (\omega_C - \chi_1 - \chi_2)a^\dagger a \tag{298}$$

$$\begin{aligned}\frac{d}{dt}C_n^{[\rho_{12}]} &= tr\left[\dot{\rho}_{12}e^{\lambda a^\dagger}e^{-\lambda^* a}\right] \\ &= tr\left[(-i(\omega_C + \chi_1 + \chi_2)a^\dagger a\rho_{12} + i\rho_{12}(\omega_C - \chi_1 - \chi_2)a^\dagger a + \frac{\kappa}{2}(2a\rho_{12}a^\dagger - a^\dagger a\rho_{12} - \rho_{12}a^\dagger a)e^{\lambda a^\dagger}e^{-\lambda^* a}\right]\end{aligned} \tag{299}$$

Now we use the relations we derived in Eq. 47 to 53

$$\begin{aligned}\frac{d}{dt}C_n^{[\rho_{12}]} =& \Bigg[-i(\omega_C + \chi 1 + \chi 2)\left(\lambda^* - \frac{\partial}{\partial\lambda}\right)\frac{\partial}{\partial\lambda^*} + i(\omega_C - \chi 1 - \chi 2)\left(\lambda - \frac{\partial}{\partial\lambda^*}\right)\frac{\partial}{\partial\lambda} + \\ &\frac{\kappa}{2}\left(2\left(-\frac{\partial^2}{\partial\lambda\partial\lambda^*}\right) - \left(\lambda^* - \frac{\partial}{\partial\lambda}\right)\frac{\partial}{\partial\lambda^*} - \left(\lambda - \frac{\partial}{\partial\lambda^*}\right)\frac{\partial}{\partial\lambda}\right)\Bigg]C_n^{[\rho_{12}]}\end{aligned} \tag{300}$$

using the Ansatz $\rho_{12} = c_{12}(t)|\alpha_1\rangle\langle\alpha_2|$, $C_n^{[\rho_{12}]}$ becomes:

$$C_n^{[\rho_{12}]} = C_n^{[c_{12}(t)|\alpha_1\rangle\langle\alpha_2|]} = tr\left[c_{12}(t)|\alpha_1\rangle\langle\alpha_2|e^{\lambda a^\dagger}e^{-\lambda^* a}\right] = c_{12}(t)e^{\lambda\alpha_2^* - \lambda^*\alpha_1} \tag{301}$$

The last equality holds because the trace is invariant under cyclic permutations and $a|\alpha\rangle = \alpha|\alpha\rangle$ respectively $\langle\alpha|a^\dagger = \langle\alpha|\alpha^*$.
With this ansatz we obtain:

$$\frac{d}{dt}C_n^{[\rho_{12}]} = \frac{d}{dt}c_{12}(t)e^{\lambda\alpha_2^* - \lambda^*\alpha_1} = \dot{c}_{12}(t)e^{\lambda\alpha_2^* - \lambda^*\alpha_1} + c_{12}(t)(\lambda\dot{\alpha}_2^* - \lambda^*\dot{\alpha}_1)e^{\lambda\alpha_2^* - \lambda^*\alpha_1} \tag{302}$$

Now we can plug equation 301 and 302 into 300 and get:

$$\begin{aligned}\frac{d}{dt}C_n^{[\rho_{12}]} =& \left[\left(-i(\omega_C + \chi 1 + \chi 2) - \frac{\kappa}{2}\right)\lambda^*(-\alpha_1) + \left(-i(\omega_C - \chi 1 - \chi 2) - \frac{\kappa}{2}\right)\lambda\alpha_2^* + 2i(\chi_1 + \chi_2)(-\alpha_2^*\alpha_1)\right] = \\ &\dot{c}_{12}(t)e^{\lambda\alpha_2^* - \lambda^*\alpha_1} + c_{12}(t)(\lambda\dot{\alpha}_2^* - \lambda^*\dot{\alpha}_1)e^{\lambda\alpha_2^* - \lambda^*\alpha_1}\end{aligned} \tag{303}$$

Now we can compare coefficients and get the differential equations,

$$\dot{\alpha}_1(t) = \alpha_1(t)\left[-i(\omega_C + \chi 1 + \chi 2) - \frac{\kappa}{2}\right] \tag{304}$$
$$\dot{\alpha}_2(t) = \alpha_2(t)\left[-i(\omega_C - \chi 1 - \chi 2) - \frac{\kappa}{2}\right] \tag{305}$$
$$\dot{c}_{12}(t) = -2ic_{12}(t)\alpha_1(t)\alpha_2^*(t)(\chi 1 + \chi 2) \tag{306}$$

which we can solve.

10.5 Effective deacy rate, resonant case

To derive the effective decay rate caused by the cavity-JPM-interaction we describe the system with the Hamiltonian,

$$H_0 = \omega_C a^\dagger a + \omega_C|0\rangle\langle 0| + g_J(a|2\rangle + a^\dagger|1\rangle) - \omega_0|0\rangle\langle 0| \tag{307}$$

and solve the master equation,

$$\dot{\rho} = -i\left[H, \rho\right] + \kappa D\left[|0\rangle\langle 2|\right]\rho \tag{308}$$

Where $D\left[O\right]\rho = \frac{1}{2}(2O\rho O^{\dagger} - O^{\dagger}O\rho - \rho O^{\dagger}O)$ again is the Lindblad dissipator.
We can rewrite the Hamiltonian into the reduced basis sates $|n+1, 1\rangle, |n, 2\rangle, |n, 0\rangle$ and it gets the following form:

$$H_n = \begin{bmatrix} (n+1)\omega_C & \sqrt{n+1}g & 0 \\ \sqrt{n+1}g & (n+1)\omega_C & 0 \\ 0 & 0 & -\omega_0 \end{bmatrix} \tag{309}$$

When we write:

$$\rho = \begin{bmatrix} \rho_{11} & \rho_{12} & \rho_{10} \\ \rho_{21} & \rho_{22} & \rho_{20} \\ \rho_{01} & \rho_{02} & \rho_{00} \end{bmatrix} \tag{310}$$

We can calculate

$$\kappa D\left[|0\rangle\langle 2|\right]\rho = \frac{1}{2}(2|0\rangle\langle 2|\rho|2\rangle\langle 0| - |2\rangle\langle 2|\rho - \rho|2\rangle\langle 2|) = \begin{bmatrix} 0 & -\frac{1}{2}\rho_{12} & 0 \\ -\frac{1}{2}\rho_{21} & -\rho_{22} & -\frac{1}{2}\rho_{20} \\ 0 & -\frac{1}{2}\rho_{02} & \rho_{22} \end{bmatrix} \tag{311}$$

By calculating the commutator we can obtain the differential equations for ρ.

$$[H_n, \rho] = \begin{bmatrix} g\sqrt{n+1}(\rho_{21} - \rho_{12}) & g\sqrt{n+1}g(\rho_{22} - \rho_{11}) & \omega_0\rho_{10} + (n+1)\omega_C\rho_{10} + g\sqrt{n+1}\rho_{20} \\ g\sqrt{n+1}(\rho_{11} - \rho_{22}) & g\sqrt{n+1}(\rho_{12} - \rho_{21}) & \omega_0\rho_{20} + (n+1)\omega_0\rho_{20} + g\sqrt{n+1}\rho_{10} \\ -\omega_0\rho_{01} - (n+1)\omega_C\rho_{01} - g\sqrt{n+1}\rho_{02} & -\omega_0\rho_{02} - (n+1)\omega_C\rho_{02} - g\sqrt{n+1}\rho_{01} & 0 \end{bmatrix} \tag{312}$$

From this matrix we can obtain the following differential equations. Since we are interested in the occupation of the state $|0\rangle$ we want to calculate $\rho_{00}(t)$. Therefore the following differential equations are sufficient.

$$\dot{\rho}_{11} = -ig\sqrt{n+1}(\rho_{21} - \rho_{12}) \tag{313}$$
$$\dot{\rho_{22}} = -ig\sqrt{n+1}(\rho_{12} - \rho_{21}) - \kappa\rho_{22} \tag{314}$$
$$\dot{\rho_{00}} = \kappa\rho_{22} \tag{315}$$
$$\dot{\rho_{12}} = -ig\sqrt{n+1}(\rho_{22} - \rho_{11}) - \frac{\kappa}{2}\rho_{12} \tag{316}$$
$$\dot{\rho_{21}} = -ig\sqrt{n+1}(\rho_{11} - \rho_{22}) - \frac{\kappa}{2}\rho_{21} \tag{317}$$

To simplify this system of differential equations we can use that:

$$\frac{d}{dt}(\rho_{12} + \rho_{21}) = -\frac{\kappa}{2}(\rho_{12} + \rho_{21}) \tag{318}$$

And solve for the real part of ρ_{12}:

$$\rho_{12} + \rho_{21} = 2Re(\rho_{12} = (\rho_{12}(0) + \rho_{21}(0))e^{-\frac{\kappa}{2}t} \tag{319}$$

So we only have to find

$$Im(\rho_{12}) = \frac{\rho_{12} - \rho_{21}}{2i} \tag{320}$$

The system of differential equations reduces to:

$$\frac{d}{dt}\begin{bmatrix}\rho_{11}\\ \rho_{22}\\ Im(\rho_{12})\end{bmatrix} = \begin{bmatrix}0 & 0 & -2g\sqrt{n+1}\\ 0 & -\kappa & 2g\sqrt{n+1}\\ g\sqrt{n+1} & -g\sqrt{n+1} & -\frac{\kappa}{2}\end{bmatrix}\begin{bmatrix}\rho_{11}\\ \rho_{22}\\ Im(\rho_{12})\end{bmatrix} \tag{321}$$

If we call:

$$A = \begin{bmatrix}0 & 0 & -2g\sqrt{n+1}\\ 0 & -\kappa & 2g\sqrt{n+1}\\ g\sqrt{n+1} & -g\sqrt{n+1} & -\frac{\kappa}{2}\end{bmatrix} \tag{322}$$

The solution of this system of differential equations is:

$$\begin{bmatrix}\rho_{11}(t)\\ \rho_{22}(t)\\ Im(\rho_{12})(t)\end{bmatrix} = e^{At}\begin{bmatrix}\rho_{11}(0)\\ \rho_{22}(0)Im(\rho_{12})(0)\end{bmatrix} \tag{323}$$

Under the initial conditions, that $\rho_{11}(0) = 1$ is occupied and $\rho_{22}(0) = Im\rho_{12}(0) = 0$ are unoccupied in the beginning. If we simplify $e^{At} = X(t)$ we can solve the equation the following way:

$$\rho_{22}(t) = X_{12}(t)\rho_{11}(0) = X_{12}(t) \tag{324}$$

with $\beta = 2g\sqrt{n+1}$:

$$X_{12}(t) = \frac{\beta^2}{\kappa^2 - 4\beta^2}(e^{\frac{\sqrt{\kappa^2-4\beta^2}}{2}t} + e^{\frac{-\sqrt{\kappa^2-4\beta^2}}{2}t} - 2)e^{-\frac{\kappa}{2}t} \tag{325}$$

Going back to the differential equations 328 to 332 we see $\dot{\rho}_{00} = \kappa\rho_{22}$ and since $\rho_{00}(0) = 0$ we can find the solution for $\rho_{00}(t)$ just by integrating:

$$\rho_{00}(t) = \kappa\int_0^t d\tau\rho_{22}(\tau) = \kappa\int_0^t d\tau X_{21}(\tau) \tag{326}$$

$$= \frac{\kappa\beta^2}{\kappa^2 - 4\beta^2}\left[\frac{e^{(\sqrt{(\frac{\kappa}{2})^2-\beta^2}-\frac{\kappa}{2})t} - 1}{\sqrt{(\frac{\kappa}{2})^2-\beta^2}-\frac{\kappa}{2}} - \frac{e^{(-\sqrt{(\frac{\kappa}{2})^2-\beta^2}-\frac{\kappa}{2})t} - 1}{\sqrt{(\frac{\kappa}{2})^2-\beta^2}+\frac{\kappa}{2}} + \frac{4}{\kappa}(e^{\frac{-\kappa}{2}t} - 1)\right] \tag{327}$$

10.6 Laplace Transformation

With a Laplace Transformation it was possible to solve the differential equation for a non zero detuning.

$$\dot{\rho}_{11} = -ig\sqrt{n+1}(\rho_{21} - \rho_{12}) \tag{328}$$
$$\dot{\rho_{22}} = -ig\sqrt{n+1}(\rho_{12} - \rho_{21}) - \kappa\rho_{22} \tag{329}$$
$$\dot{\rho_{00}} = \kappa\rho_{22} \tag{330}$$
$$\dot{\rho_{12}} = -ig\sqrt{n+1}(\rho_{22} - \rho_{11}) - \frac{\kappa}{2}\rho_{12} - i\Delta\rho_{12} \tag{331}$$
$$\dot{\rho_{21}} = -ig\sqrt{n+1}(\rho_{11} - \rho_{22}) - \frac{\kappa}{2}\rho_{21} + i\Delta\rho_{21} \tag{332}$$

To simplify the calculation we split ρ_{12} into its imaginary and real part.

$$\dot{\rho_{12}}^R = \frac{1}{2}(\rho_{12} + \rho_{21}) = -\frac{\kappa}{2}\rho_{12}^R + \Delta\rho_{12}^I \tag{333}$$
$$\dot{\rho_{12}}^I = \frac{1}{2i}(\rho_{12} - \rho_{21}) = -g\sqrt{n+1}(\rho_{22} - \rho_{11}) - \frac{\kappa}{2}\rho_{12}^I - \Delta\rho_{12}^R \tag{334}$$

When we apply a Laplace Transformation to the s space with $\rho(0) = (1,0,0,0)^T$ we find the following equations.

$$\rho_{12}^{R} = \frac{\Delta}{s+\frac{\kappa}{2}}\rho_{12}^{I} \tag{335}$$

$$\rho_{22} = \frac{2\beta_n}{s+\kappa}\rho_{12}^{I} = \frac{2\beta_n}{s+\kappa}\rho_{12}^{I} \tag{336}$$

$$\rho_{11} = \frac{1}{s} - \frac{2\beta_n}{s}\rho_{12}^{I} \tag{337}$$

$$\rho_{12}^{I} = \frac{\beta_n}{s(\frac{\Delta^2}{s+\frac{\kappa}{2}} + 2\beta_n^2(\frac{1}{s}+\frac{1}{s+\kappa}))} = \frac{2\beta_n(s+\frac{\kappa}{2})(s+\kappa)}{s+\frac{\kappa}{2}+\Delta^2 s\,(s+\kappa)+\left(s+\frac{\kappa}{2}\right)^2 s\,(s+\kappa)+2\beta_n^2\left((s+\kappa)\left(s+\frac{\kappa}{2}\right)+s\left(s+\frac{\kappa}{2}\right)\right)} \tag{338}$$

Here we used the short hand notation $\beta = g\sqrt{n+1}$. In the end we are intrested in ρ_{00} which can be obtained by integrating ρ_{22}. To find ρ_{22} we just have to plug ρ_{12}^{I} into equation (336) and this will also cancel the factor $(s+\kappa)$. To do the back transformation to the time space we have to calculate the integral:

$$\rho_{kl}(t) = \frac{1}{2\pi i}\int_{\gamma-i\infty}^{\gamma+i\infty} ds\rho_{kl}(s)e^{st} \tag{339}$$

Which can easily be solved if we find the factorized form of the denominator of the function we want to integrate. If we find this form we only have to calculate the residua of the function and sum them up.
For $\Delta = 0$ the poles of ρ_{12}^{I} are:

$$s_0 = -\frac{\kappa}{2} \tag{340}$$

$$s_+ = \frac{1}{2}\left(\sqrt{\kappa^2-16\beta_n^2}-\kappa\right) \tag{341}$$

$$s_- = \frac{1}{2}\left(-\sqrt{\kappa^2-16\beta_n^2}-\kappa\right) \tag{342}$$

For this case one has to be carefull because if we set $\Delta = 0$ the factor $\left(\frac{\kappa}{2}+s\right)$ also cancels in the numerator and we are only left with:

$$\rho_{22}(s) = \frac{2\beta_n^2}{(\frac{\kappa}{2}+s)\,(4\beta_n^2+s^2+\kappa s)} = \frac{2\beta_n^2}{(s-s_0)(s-s_-)(s-s_+)} \tag{343}$$

$$\rho_{22}(t) = \sum_i Res_i(\rho_{22}(s)e^{st}) \tag{344}$$

$$= 2\beta_n^2\left(\frac{e^{-\frac{\kappa}{2}t}}{(s_0-s_+)\,(s_0-s_-)} + \frac{e^{\left(-\frac{\kappa}{2}+\frac{\sqrt{\kappa^2-16\beta_n^2}}{2}\right)t}}{\left(s_++\frac{\kappa}{2}\right)(s_+-s_-)} + \frac{e^{\left(-\frac{\kappa}{2}-\frac{\sqrt{\kappa^2-16\beta_n^2}}{2}\right)t}}{\left(s_-+\frac{\kappa}{2}\right)(s_--s_+)}\right) \tag{345}$$

And to find $\rho_{00}(t)$ we have to integrate $\rho_{00}(t) = \kappa\int_0^t \rho_{22}(\tau)d\tau$. Therefore:

$$\rho_{00}(t) == \frac{4\kappa\beta_n^2}{\kappa^2-16\beta_n^2}\left[\frac{e^{(\sqrt{(\frac{\kappa}{2})^2-4\beta_n^2}-\frac{\kappa}{2})t}-1}{\sqrt{(\frac{\kappa}{2})^2-4\beta_n^2}-\frac{\kappa}{2}} - \frac{e^{(-\sqrt{(\frac{\kappa}{2})^2-4\beta_n^2}-\frac{\kappa}{2})t}-1}{\sqrt{(\frac{\kappa}{2})^2-4\beta_n^2}+\frac{\kappa}{2}} + \frac{4}{\kappa}(e^{\frac{-\kappa}{2}t}-1)\right] \tag{346}$$

The other matrix elements of the density matrix can be calculated completely analogous.

$$\rho_{11}(t) = 1 - \frac{8\beta_n^2}{\kappa_J^2-16\beta_n^2}\left(\frac{\kappa_J+\sqrt{\kappa_J^2-16\beta_n^2}}{2}e^{\frac{-\kappa_J+\sqrt{\kappa_J^2-16\beta_n^2}}{2}t} + \frac{\kappa_J-\sqrt{\kappa_J^2-16\beta_n^2}}{2}e^{\frac{-\kappa_J-\sqrt{\kappa_J^2-16\beta_n^2}}{2}t} - \frac{\kappa_J}{2}e^{-\frac{\kappa}{2}t}\right) \tag{347}$$

$$\rho_{22}(t) = \frac{4\beta_n^2}{\kappa^2-16\beta_n^2}(e^{\frac{\sqrt{\kappa^2-4\beta_n^2}}{2}t}+e^{\frac{-\sqrt{\kappa^2-4\beta_n^2}}{2}t}-2)e^{-\frac{\kappa}{2}t} \tag{348}$$

For $\Delta \neq 0$ the poles of ρ_{12}^I are:

$$s_0 = \frac{1}{2}\left(+\frac{\sqrt{+\sqrt{\left(16g^2m+\kappa^2+4\epsilon^2\right)^2-64g^2\kappa^2m}-16g^2m+\kappa^2-4\epsilon^2}}{\sqrt{2}}-\kappa\right) \tag{349}$$

$$s_1 = \frac{1}{2}\left(-\frac{\sqrt{-\sqrt{\left(16g^2m+\kappa^2+4\epsilon^2\right)^2-64g^2\kappa^2m}-16g^2m+\kappa^2-4\epsilon^2}}{\sqrt{2}}-\kappa\right) \tag{350}$$

$$s_2 = \frac{1}{2}\left(+\frac{\sqrt{-\sqrt{\left(16g^2m+\kappa^2+4\epsilon^2\right)^2-64g^2\kappa^2m}-16g^2m+\kappa^2-4\epsilon^2}}{\sqrt{2}}-\kappa\right) \tag{351}$$

$$s_3 = \frac{1}{2}\left(-\frac{\sqrt{+\sqrt{\left(16g^2m+\kappa^2+4\epsilon^2\right)^2-64g^2\kappa^2m}-16g^2m+\kappa^2-4\epsilon^2}}{\sqrt{2}}-\kappa\right) \tag{352}$$

So the Laplace transfomed ρ_{22} takes the form:

$$\rho_{22}(s) = \frac{2\beta_n(s+\frac{\kappa}{2})(s+\kappa)}{(s-s_0)(s-s_1)(s-s_2)(s-s_2)} \tag{353}$$

To do the back transformation we again only have to calculate the residua of $\rho_{22}(s)e^{st}$ and after that we again integrate $\kappa\int_0^t \rho_{22}(\tau)d\tau$ to obtain $\rho_{00}(t)$

The terms of ρ_{00} that correspond to the poles $s_{0,1,2,3}$ are

$$\rho_{00,s_0} = \frac{1-\exp\left(-\frac{1}{4}t\left(\sqrt{2}\sqrt{-16\beta_n^2+\sqrt{256\beta_n^4+32\beta_n^2\left(4\Delta^2-\kappa^2\right)+\left(\kappa^2+4\Delta^2\right)^2}+\kappa^2-4\Delta^2}+2\kappa\right)\right)}{\sqrt{2}\sqrt{-16\beta_n^2+\sqrt{256\beta_n^4+32\beta_n^2\left(4\Delta^2-\kappa^2\right)+\left(\kappa^2+4\Delta^2\right)^2}+\kappa^2-4\Delta^2}+2\kappa} \tag{354}$$

$$\rho_{00,s_1} = \frac{1-\exp\left(\frac{1}{4}t\left(\sqrt{2}\sqrt{-16\beta_n^2-\sqrt{256\beta_n^4+32\beta_n^2\left(4\Delta^2-\kappa^2\right)+\left(\kappa^2+4\Delta^2\right)^2}+\kappa^2-4\Delta^2}-2\kappa\right)\right)}{\sqrt{2}\sqrt{-16\beta_n^2-\sqrt{256\beta_n^4+32\beta_n^2\left(4\Delta^2-\kappa^2\right)+\left(\kappa^2+4\Delta^2\right)^2}+\kappa^2-4\Delta^2}-2\kappa} \tag{355}$$

$$\rho_{00,s_2} = -\frac{1-\exp\left(-\frac{1}{4}t\left(\sqrt{2}\sqrt{-16\beta_n^2-\sqrt{256\beta_n^4+32\beta_n^2\left(4\Delta^2-\kappa^2\right)+\left(\kappa^2+4\Delta^2\right)^2}+\kappa^2-4\Delta^2}+2\kappa\right)\right)}{\sqrt{2}\sqrt{-16\beta_n^2-\sqrt{256\beta_n^4+32\beta_n^2\left(4\Delta^2-\kappa^2\right)+\left(\kappa^2+4\Delta^2\right)^2}+\kappa^2-4\Delta^2}+2\kappa} \tag{356}$$

$$\rho_{00,s_3} = -\frac{1-\exp\left(\frac{1}{4}t\left(\sqrt{2}\sqrt{-16\beta_n^2+\sqrt{256\beta_n^4+32\beta_n^2\left(4\Delta^2-\kappa^2\right)+\left(\kappa^2+4\Delta^2\right)^2}+\kappa^2-4\Delta^2}-2\kappa\right)\right)}{\sqrt{2}\sqrt{-16\beta_n^2+\sqrt{256\beta_n^4+32\beta_n^2\left(4\Delta^2-\kappa^2\right)+\left(\kappa^2+4\Delta^2\right)^2}+\kappa^2-4\Delta^2}-2\kappa}. \tag{357}$$

These terms all have the prefactor

$$A = \frac{16\beta_n^2\kappa}{\sqrt{256\beta_n^4+32\beta_n^2\left(4\Delta^2-\kappa^2\right)+\left(\kappa^2+4\Delta^2\right)^2}}. \tag{358}$$

And $\rho_{00} = A\sum_i \rho_{00,s_i}$. If we now look at these term we can see that they all have a similar form. They contain some prefactor and exponantial of the form $(1-exp(\cdots))$. If we look at the prefactors B_{s_i},

$$B_{s_i} = \frac{1}{\sqrt{2}\sqrt{-16\beta_n^2\pm\sqrt{256\beta_n^4+32\beta_n^2\left(4\Delta^2-\kappa^2\right)+\left(\kappa^2+4\Delta^2\right)^2}+\kappa^2-4\Delta^2}\pm 2\kappa} \tag{359}$$

and expand them to the 2nd order in ϵ we can simplify them. Furthermore we always have to keep in mind that $\kappa \gg \beta$.

$$B_{s_0} = \frac{1}{\sqrt{2}\sqrt{\sqrt{\left(\kappa^2-16\beta_n^2\right)^2}-16\beta_n^2+\kappa^2}+2\kappa} + \frac{2\sqrt{2}\Delta^2\left(\sqrt{\left(16\beta_n^2-\kappa^2\right)^2}-16\beta_n^2-\kappa^2\right)}{\sqrt{\left(16\beta_n^2-\kappa^2\right)^2}\sqrt{\sqrt{\left(16\beta_n^2-\kappa^2\right)^2}-16\beta_n^2+\kappa^2}\left(\sqrt{2}\sqrt{\sqrt{\left(\kappa^2-16\beta_n^2\right)^2}-16\beta_n^2+\kappa^2}+2\kappa\right)^2} \tag{360}$$

$$B_{s_1} = \frac{1}{\sqrt{2}\sqrt{-\sqrt{(\kappa^2-16\beta_n^2)^2}-16\beta_n^2+\kappa^2}-2\kappa} + \frac{2\sqrt{2}\Delta^2\left(\sqrt{(16\beta_n^2-\kappa^2)^2}+16\beta_n^2+\kappa^2\right)}{\sqrt{(16\beta_n^2-\kappa^2)^2}\sqrt{-\sqrt{(16\beta_n^2-\kappa^2)^2}-16\beta_n^2+\kappa^2}\left(\sqrt{2}\sqrt{-\sqrt{(\kappa^2-16\beta_n^2)^2}-16\beta_n^2+\kappa^2}-2\kappa\right)^2} \tag{361}$$

$$B_{s_2} = -\frac{1}{\sqrt{2}\sqrt{-\sqrt{(\kappa^2-16\beta_n^2)^2}-16\beta_n^2+\kappa^2}+2\kappa} - \frac{2\Delta^2\left(\sqrt{2}\left(\sqrt{(16\beta_n^2-\kappa^2)^2}+16\beta_n^2+\kappa^2\right)\right)}{\sqrt{(16\beta_n^2-\kappa^2)^2}\sqrt{-\sqrt{(16\beta_n^2-\kappa^2)^2}-16\beta_n^2+\kappa^2}\left(\sqrt{2}\sqrt{-\sqrt{(\kappa^2-16\beta_n^2)^2}-16\beta_n^2+\kappa^2}+2\kappa\right)^2} \tag{362}$$

$$B_{s_3} = -\frac{1}{\sqrt{2}\sqrt{\sqrt{(\kappa^2-16\beta_n^2)^2}-16\beta_n^2+\kappa^2}-2\kappa} - \frac{2\Delta^2\left(\sqrt{2}\left(\sqrt{(16\beta_n^2-\kappa^2)^2}-16\beta_n^2-\kappa^2\right)\right)}{\sqrt{(16\beta_n^2-\kappa^2)^2}\sqrt{\sqrt{(16\beta_n^2-\kappa^2)^2}-16\beta_n^2+\kappa^2}\left(\sqrt{2}\sqrt{\sqrt{(\kappa^2-16\beta_n^2)^2}-16\beta_n^2+\kappa^2}-2\kappa\right)^2} \tag{363}$$

In this form we can obtain that the denominator of the first term of the prefactor B_{s_3} will go to zero for $\Delta \ll 1$ and $\kappa \gg \beta_n$. So this term will be dominant. The next step will be to simplify the exponential of ρ_{00,s_3}.

$$\begin{aligned}
\exp_{s_3} &= 1-\exp\left(\frac{1}{4}t\left(\sqrt{2}\sqrt{-16\beta_n^2+\sqrt{256\beta_n^4+32\beta_n^2\left(4\Delta^2-\kappa^2\right)+\left(\kappa^2+4\Delta^2\right)^2}+\kappa^2-4\Delta^2}-2\kappa\right)\right) && (364)\\
&= 1-\exp\left(\frac{1}{4}t\left(\left(\sqrt{2}\sqrt{\sqrt{(\kappa^2-16\beta_n^2)^2}-16\beta_n^2+\kappa^2}-2\kappa\right)-\frac{2\Delta^2\left(\sqrt{2}\left(\sqrt{(-16\beta_n^2+\kappa^2)^2}-16\beta_n^2-\kappa^2\right)\right)}{\sqrt{(-16\beta_n^2+\kappa^2)^2}\sqrt{\sqrt{(-16\beta_n^2+\kappa^2)^2}-16\beta_n^2+\kappa^2}}\right)\right) && (365)\\
&= 1-\exp\left(\frac{1}{4}t\left(-\frac{16\beta_n^2}{\kappa}+\frac{64\Delta^2\beta_n^2}{\kappa^3\left(1-\frac{16\beta_n^2}{\kappa^2}\right)\sqrt{1-\frac{16\beta_n^2}{\kappa^2}}}\right)\right) && (366)\\
&= 1-\exp\left(-\frac{4\beta_n^2}{\kappa}t\left(1-4\frac{\Delta^2}{\kappa_J^2}\right)\right) && (367)
\end{aligned}$$

On the first line we did the expansion in Δ^2 and in the 2nd line we expanded $\sqrt{-16\beta_n^2+\kappa^2} \approx \kappa(1-8\beta_n^2/\kappa^2)$. One also has to be carefull with terms like $\sqrt{(-16\beta_n^2+\kappa^2)^2}$ which is the absolute value $|-16\beta_n^2+\kappa^2|$. Here we always have to keep in mind that $\kappa \gg \beta_n$ and therefore $|-16\beta_n^2+\kappa^2| = \kappa^2-16\beta_n^2$. It is also very important to keep in mind that because of the first expansion in $\Delta^2 \ll 1$ that the detuning has to be $\Delta^2 \ll \kappa_J$ and $\Delta^2 \ll g_J$. And since $g_J \ll \kappa_J \Rightarrow \Delta^2 \ll g_J \ll \kappa_J$

10.7 Unravelling of the density matrix

we already know:

$$\mathcal{L}_B \cdot = -i\big[H, \cdot\big] - \frac{\kappa}{2}(a^\dagger a \cdot + \cdot\, a^\dagger a)$$

$$H_B = H - i\frac{\kappa}{2}a^\dagger a$$

$$\mathcal{L}_B|\Psi\rangle\langle\Psi| = \frac{1}{i}(H_B|\Psi\rangle\langle\Psi| + |\Psi\rangle\langle\Psi|{H_B}^\dagger)$$

We want to show:

$$e^{\mathcal{L}_B t}|\Psi\rangle\langle\Psi| \overset{!}{=} e^{-iH_B t}|\Psi\rangle\langle\Psi|e^{+iH_B t}$$

Prove:

$$e^{\mathcal{L}_B t}\rho = \left(1 + \mathcal{L}_B t + \frac{(\mathcal{L}_B t)^2}{2} + \cdots\right)\rho$$

We know how $\mathcal{L}_B$ applies to ρ so we have to find out how $\mathcal{L}_B^2$ and higher order apply. Therefore:

$$\mathcal{L}_B^2\rho = \mathcal{L}_B\frac{1}{i}(H_B\rho - \rho H_B^\dagger) = -i\big[H, \frac{1}{i}(H_B\rho - \rho H_B^\dagger)\big] - \frac{\kappa}{2}\left(\frac{a^\dagger a}{i}(H_B\rho - \rho H_B^\dagger) + (H_B\rho - \rho H_B^\dagger)\frac{a^\dagger a}{i}\right)$$

To solve the first part we take into account that H and H_B commute. The 2nd part we can use that $a^\dagger a$ and H_B commute and we rewrite it:

$$\frac{\kappa}{2}\left(\frac{a^\dagger a}{i}(H_B\rho - \rho H_B^\dagger) + (H_B\rho - \rho H_B^\dagger)\frac{a^\dagger a}{i}\right) = \frac{\kappa}{2i}\left(H_B(a^\dagger a\rho + \rho a^\dagger a) - (a^\dagger a\rho + \rho a^\dagger a)H_B^\dagger\right)$$

Therefore:

$$\mathcal{L}_B^2\rho = \left(\frac{H_B}{i}\underbrace{\left(-i\big[H,\rho\big] - \frac{\kappa}{2}(a^\dagger a\rho - \rho a^\dagger a\right)}_{\mathcal{L}_B\rho} - \left(-i\big[H,\rho\big] - \frac{\kappa}{2}(a^\dagger a\rho - \rho a^\dagger a\right)\frac{H_B^\dagger}{i}\right)$$

We us now again $\mathcal{L}_B|\Psi\rangle\langle\Psi| = \frac{1}{i}(H_B|\Psi\rangle\langle\Psi| + |\Psi\rangle\langle\Psi|{H_B}^\dagger)$ and so we find:

$$\mathcal{L}_B^2\rho = \left(\frac{1}{i}\right)^2(H_B^2\rho - 2H_B\rho H_B^\dagger + \rho(H_B^\dagger)^2)$$

For higher order terms of $\mathcal{L}_B$ this pattern repeats and we find:

$$e^{\mathcal{L}_B t}\rho = \left(1 - iH_B t + \frac{(H_B t)^2}{2} + \cdots\right)\rho\left(1 - iH_B^\dagger t + \frac{(H_B^\dagger t)^2}{2} + \cdots\right) = e^{-iH_B t}\rho e^{-iH_B^\dagger t}$$

q.e.d.

10.8 Calculate density matrix for leaking Cavity which is initially in a Fock state

We solved the quantum trajectory for an initial Fock state. And the aim is to see, if we average over all stochastic variables $Y(t)$ and $N(t)$ we should get the same result as if we solved the master equation for this system.
In the Project work from summer we only calculated the master equation with an initial coherent state. So we have to solve this equation for Fock states. For coherent states we used the characteristic function ansatz. Here we can try something else.
We start with the ME:

$$\dot{\rho}(t) = -i[H,\rho] + \kappa D[a]\rho \tag{368}$$

In a rotating frame we have the Hamiltonian $H = \chi a^\dagger a \sigma^z$. In the the number basis we define:

$$\rho_{nn}(t) = \langle n|\rho(t)|n\rangle \tag{369}$$

And the bare qubit density matrix is the partial trace of the whole density matrix. Which is defined as:

$$\rho_{qb} = \sum_n \rho_{nn}(t) \tag{370}$$

$$\dot{\rho}_{nn}(t) = \langle n|\dot{\rho}(t)|n\rangle = -i\langle n|([H,\rho] + \kappa D[a]\rho)|n\rangle \tag{371}$$

By plugging in the Hamiltonian an let it operate on the left and the right $|n\rangle$ we get:

$$\dot{\rho}_{nn}(t) = -i\chi n(\sigma^z \rho_{nn}(t) - \rho_{nn}(t)\sigma^z) + \frac{\kappa}{2}(2(n+1)\rho_{n+1,n+1}(t) - 2n\rho_{nn}(t)) \tag{372}$$

the commutator $[\sigma^z, \rho_{nn}(t)]$ can be evaluated just by assuming that:

$$\rho_{nn}(t) = \begin{bmatrix} \rho_{nn}^{\uparrow\uparrow} & \rho_{nn}^{\uparrow\downarrow} \\ (\rho_{nn}^{\uparrow\downarrow})^* & \rho_{nn}^{\downarrow\downarrow} \end{bmatrix} \tag{373}$$

And it can be seen that:

$$[\sigma^z, \rho_{nn}(t)] = \begin{bmatrix} 0 & 2\rho_{nn}^{\uparrow\downarrow} \\ -2(\rho_{nn}^{\uparrow\downarrow})^* & 0 \end{bmatrix} \tag{374}$$

An other way to evaluate this commutator is that the Hamiltonian does not flip spins. Therefore the matrix elements of $\rho_{nn}(t)$ have the structure for example $\rho_{nn}^{\uparrow\downarrow} \sim |e\rangle\langle g|$ and $\rho_{nn}^{\uparrow\uparrow} \sim |e\rangle\langle e|$. So it can be seen, that the diagonal elements of $\rho_{nn}(t)$ vanish.
The master equation can be solved component wise. Since we are mostly interested in the off-diagonal parts of the density matrix we solve it for the element $\rho_{nn}^{\uparrow\downarrow}(t)$. So we find a system of linear differential equations:

$$\dot{\rho}_{nn}^{\uparrow\downarrow}(t) = -2n\rho_{nn}^{\uparrow\downarrow}(t)(i\chi + \frac{\kappa}{2}) + \kappa(n+1)\rho_{n+1,n+1}^{\uparrow\downarrow}(t) \tag{375}$$

In matrix form we can write it the following for a N dimensional Fock space:

$$\begin{bmatrix} \dot{\rho}_{00}^{\uparrow\downarrow}(t) \\ \dot{\rho}_{11}^{\uparrow\downarrow}(t) \\ \dot{\rho}_{22}^{\uparrow\downarrow}(t) \\ \vdots \\ \dot{\rho}_{nn}^{\uparrow\downarrow}(t) \\ \vdots \\ \dot{\rho}_{NN}^{\uparrow\downarrow}(t) \end{bmatrix} = \underbrace{\begin{bmatrix} 0 & \kappa & 0 & 0 & \cdots & 0 & 0 & \cdots \\ 0 & -2(i\chi+\frac{\kappa}{2}) & 2\kappa & 0 & \cdots & 0 & 0 & \cdots \\ 0 & 0 & -4(i\chi+\frac{\kappa}{2}) & 3\kappa & \cdots & 0 & 0 & \cdots \\ 0 & 0 & 0 & \ddots & \ddots & 0 & 0 & \cdots \\ 0 & 0 & 0 & 0 & 0 & -2n(i\chi+\frac{\kappa}{2}) & n\kappa & \cdots \\ 0 & 0 & 0 & 0 & 0 & 0 & \ddots & \cdots \\ 0 & 0 & 0 & 0 & 0 & 0 & 0 & -2N(i\chi+\frac{\kappa}{2}) \end{bmatrix}}_{=A} = \begin{bmatrix} \rho_{00}^{\uparrow\downarrow}(t) \\ \rho_{11}^{\uparrow\downarrow}(t) \\ \rho_{22}^{\uparrow\downarrow}(t) \\ \vdots \\ \rho_{nn}^{\uparrow\downarrow}(t) \\ \vdots \\ \rho_{NN}^{\uparrow\downarrow}(t) \end{bmatrix} \tag{376}$$

This system of differential equations can be solved with $\rho(t) = e^{At}\rho(0)$.
As an initial state we choose $|\psi\rangle = 1/\sqrt{2}(|e\rangle + |g\rangle) \otimes |m\rangle$. Therefore we have:

$$\rho^{\uparrow\downarrow}(0) = \begin{bmatrix} \rho_{00}^{\uparrow\downarrow}(0) \\ \rho_{11}^{\uparrow\downarrow}(0) \\ \rho_{22}^{\uparrow\downarrow}(0) \\ \vdots \\ \rho_{mm}^{\uparrow\downarrow}(0) \\ \rho_{m+1,m+1}^{\uparrow\downarrow}(0) \\ \vdots \\ \rho_{NN}^{\uparrow\downarrow}(0) \end{bmatrix} = \begin{bmatrix} 0 \\ 0 \\ 0 \\ \vdots \\ 1/2 \\ 0 \\ \vdots \\ 0 \end{bmatrix} \tag{377}$$

The Matrix A is an upper triangle matrix. Therefore e^{At} has also upper triangle form which will lead to a cut-off of all elements in ρ that are higher than m. This also makes physically sense because we are at zero temperature and if we start in the Fock state $|m\rangle$ we can never end up in a state higher than m. So we can reduce our system of differential equations to m dimensions. If we calculate $\rho^{\uparrow\downarrow}(t) = e^{At}\rho^{\uparrow\downarrow}(0)$ we can sum up all elements of $\rho^{\uparrow\downarrow}(t)$ to come back to the off diagonal element of $\rho_{qb}(t)$ (Eq. 370).
To solve this system of differential equations we diagonalize the matrix with the transformation matrix P. With the diagonal matrix D we get the relation $A = PDP^{-1}$. P is the matrix consisting of the eigenvectors of A. The eigenvalues of A can just be read of the diagonal of A. Therefore we get

$$P = \begin{bmatrix} 1 & -\frac{\kappa}{(2i\chi+\kappa)} & \frac{\kappa^2}{(2i\chi+\kappa)^2} & \frac{\kappa^3}{(2i\chi+\kappa)^2} & \cdots \\ 0 & 1 & -2\frac{\kappa}{(2i\chi+\kappa)} & 3\frac{\kappa^2}{(2i\chi+\kappa)^2} & \cdots \\ 0 & 0 & 1 & -3\frac{\kappa}{(2i\chi+\kappa)} & \cdots \\ 0 & 0 & 0 & 1 & \cdots \\ \vdots & \vdots & \vdots & \vdots & \cdots \end{bmatrix} = \sum_{k\geq l}^{m} (-1)^{k-l}\left(\frac{\kappa}{2i\chi+\kappa}\right)^{k-l}\binom{k}{l}|l\rangle\langle k|, \tag{378}$$

with $|l\rangle\langle k|$ is standing for the entry of column i and raw j of the matrix. Furthermore we get

$$P^{-1} = \sum_{k\geq l}^{m}\left(\frac{\kappa}{2i\chi+\kappa}\right)^{k-l}\binom{k}{l}|l\rangle\langle k| \tag{379}$$

and

$$e^{D} = \sum_{k}^{m} e^{-k(2i\chi+\kappa)t}|k\rangle\langle k|. \tag{380}$$

Calculating now $\rho^{\uparrow\downarrow}(t) = Pe^{Dt}P^{-1}\rho^{\uparrow\downarrow}(0)$ with an initial state $\rho^{\uparrow\downarrow}(0)$ that only has m dimensions leads to

$$\rho^{\uparrow\downarrow}(t) = \frac{1}{2}\sum_{l=0}^{m}\sum_{k=0}^{m}(-1)^{k-l}\left(\frac{\kappa}{2i\chi+\kappa}\right)^{m-l} e^{-kt(2i\chi+\kappa)}\binom{k}{l}\binom{m}{k}|l\rangle, \tag{381}$$

where we define $\binom{k}{l} = 0$ for $l > k$. From Eq. 370 we know that $\rho_{qb}^{\uparrow\downarrow}$ is the sum of every entry in $\rho^{\uparrow\downarrow}$. So

$$\rho_{qb}^{\uparrow\downarrow}(t) = \frac{1}{2}\sum_{l=0}^{m}\sum_{k=0}^{m}(-1)^{k-l}\left(\frac{\kappa}{2i\chi+\kappa}\right)^{m-l} e^{-kt(2i\chi+\kappa)}\binom{k}{l}\binom{m}{k} \tag{382}$$

and

$$\rho_{qb}^{\uparrow\downarrow}(t) = \frac{1}{2}\sum_{l=0}^{m}\sum_{k=0}^{m}(-1)^{k-l}\left(\frac{\kappa}{2i\chi+\kappa}\right)^{m-l} e^{-kt(2i\chi+\kappa)}\binom{k}{l}\binom{m}{k}. \tag{383}$$

Here we can split $(\kappa/(2i\chi+\kappa))^{m-l}$ into $(\kappa/(2i\chi+\kappa))^{m}((2i\chi+\kappa)/\kappa)^{l}$ and use the binomial series $(a+b)^n = \sum_{k=0}^{n} a^n b^{n-k}$ leads to

$$\rho_{qb}^{\uparrow\downarrow}(t) = \frac{1}{2}\sum_{k=0}^{m}\left(\frac{\kappa}{2i\chi+\kappa}\right)^{m}\left(\frac{2i\chi+\kappa}{\kappa}-1\right)^{k} e^{-kt(2i\chi+\kappa)}\binom{m}{k}. \tag{384}$$

Here we also used that $\binom{k}{l} = 0$ for $l > k$ this leads to a cut-off of the sum over l at k. Again using the binomial series leads to:

$$\rho_{qb}^{\uparrow\downarrow}(t) = \frac{1}{2}\left(\frac{\kappa}{2i\chi+\kappa}\right)^{m}\left(e^{-t(2i\chi+\kappa)}\frac{2i\chi}{\kappa}+1\right)^{m} \tag{385}$$

Which is the compact result for initially being in the Fock state $|m\rangle$ from the full simplified numerics:

$$\rho_{qb}^{\uparrow\downarrow} = \frac{1}{2}\left(\frac{e^{-mt(\kappa+2i\chi)}\left(e^{t(\kappa+2i\chi)}\kappa+2i\chi\right)^{m}}{(\kappa+2i\chi)^{m}}\right) \tag{386}$$

10.9 Rotating Frame

Putting a system to a rotating frame is sometimes useful to simplify the Hamiltonian and investigate for example the time evolution just caused by some specific terms of the Hamiltonian. In the specific case of section 2.1 we are interested in the time evolution caused by the dispersive shift of the cavity $\chi_n \sigma_n^z a^\dagger a$. The full Hamiltonian reads,

$$H = \omega_C a^\dagger a + \sum_{n=1}^{N} (\chi_{Q_n} a^\dagger a + \frac{\omega_{Q_n} + \chi_{Q_n}}{2}) \sigma_n^z \tag{387}$$

Defining a unitairy transformation $U(t) = \exp(i \sum_{n=1}^{N} \frac{\omega_{Q_n}+\chi_{Q_n}}{2} \sigma_n^z t) = \exp(i \sum_{n=1}^{N} \frac{\omega_n'}{2} \sigma_n^z t)$ the Hamiltonian transforms,

$$\tilde{H} = UHU^\dagger - iU\dot{U}^\dagger \tag{388}$$

evaluating first the second right hand term,

$$-iU\dot{U}^\dagger = -i \exp\left(i \sum_{n=1}^{N} \frac{\omega_n'}{2} \sigma_n^z t\right) \left(-i \sum_{n=1}^{N} \frac{\omega_n'}{2} \sigma_n^z\right) \exp\left(-i \sum_{n=1}^{N} \frac{\omega_n'}{2} \sigma_n^z t\right) \tag{389}$$

because $\left[\sigma_i^z, \sigma_j^z\right] = 0 \forall i,j$ the exponentials chancel and,

$$-iU\dot{U}^\dagger = -i \left(-i \sum_{n=1}^{N} \frac{\omega_n'}{2} \sigma_n^z\right) = -\left(\sum_{n=1}^{N} \frac{\omega_n'}{2} \sigma_n^z\right) \tag{390}$$

Evaluating the first second hand term of $\tilde{H}$ we can use the same arguments. $\left[a^\dagger a, \sigma_j^z\right] = 0$ and $\left[\sigma_i^z, \sigma_j^z\right] = 0 \forall i,j$ leads to,

$$UHU^\dagger = H \tag{391}$$

Plugging this together leads to,

$$\tilde{H} = UHU^\dagger - iU\dot{U}^\dagger = H - \left(\sum_{n=1}^{N} \frac{\omega_n'}{2} \sigma_n^z\right) \tag{392}$$

Therefore this transformation chancels simply the bare qubit term of the Hamiltonian. To get rid of the bare cavity term $\omega_C a^\dagger a$ one can repeat the same calculation with $U(t) = \exp(i\omega_C a^\dagger a t)$.
One has to keep in mind, that the state vectors $|\psi\rangle$ also transform under the unitairy transformation $|\tilde{\psi}\rangle = U^\dagger |\psi\rangle$. This will also lead to some dynamics in the parity subspaces which are not the focus of this work. We are interested in the dephasing caused by the measurement which is mainly the qubit-cavity interaction. The dephasing caused for example by the unitary transformation $U(t) = \exp(i \sum_{n=1}^{N} \frac{\omega_n'}{2} \sigma_n^z t)$ would also occur in the bare qubit system and does not change if one couples it to a cavity.

10.10 Loss of coherence through cavity-JPM dynamics

This section is a brief discussion about the expected loss of coherence of the cavity state. If we approximate our full system with an effective decay rate κ_{eff} and assume the cavity to decay through the decay channel $\sqrt{\kappa_{\text{eff}}} a$ there should be more information contained in the decaying photon than there actually is. Since a coherent state $|\alpha\rangle$ is an eigenstate of the annihilation operator a with the eigenvalue α the decaying photon in the effective model should contain information about the phase and the amplitude of the cavity. In the full system dynamics on the other side we are not able to extract this information. For this reason Govia et al. propose that the cavity is not exactly coherent after the decay of a photon through the JPM and the effective model could be approximated with the operator $B = \sum_{n=0}^{\infty} |n-1\rangle\langle n|$. To investigate the coherence of the cavity state before a photon jump and after it we define the coherency parameter for an arbitrary cavity state $|\psi\rangle$ as follows:

$$C(|\psi\rangle) = \frac{|\langle\psi|a|\psi\rangle|^2}{\langle\psi|a^\dagger a|\psi\rangle} \tag{393}$$

This coherence value C will be exactly one if $|\psi\rangle$ is an eigenstate of the operator a. In Figure 26 we show the numerical results of a coherence measurement of the full system and the effective model with the B-Operator. For this purpose we calculated the coherence value directly before and after the jump which happens randomly at the time t_J. Therefore we plot the value:

$$C(|\psi\rangle(t_J - dt) - C(|\psi\rangle(t_J + dt)) \tag{394}$$

The results can be seen in figure 26. In conclusion we can say that a decay of the coherence of the order 10^{-8} is a very small effect and can be neglected. And the approach with the B-operator is not necessary because there is no real improvement compared to the annihilation operator a where we would not have any decay of coherence.

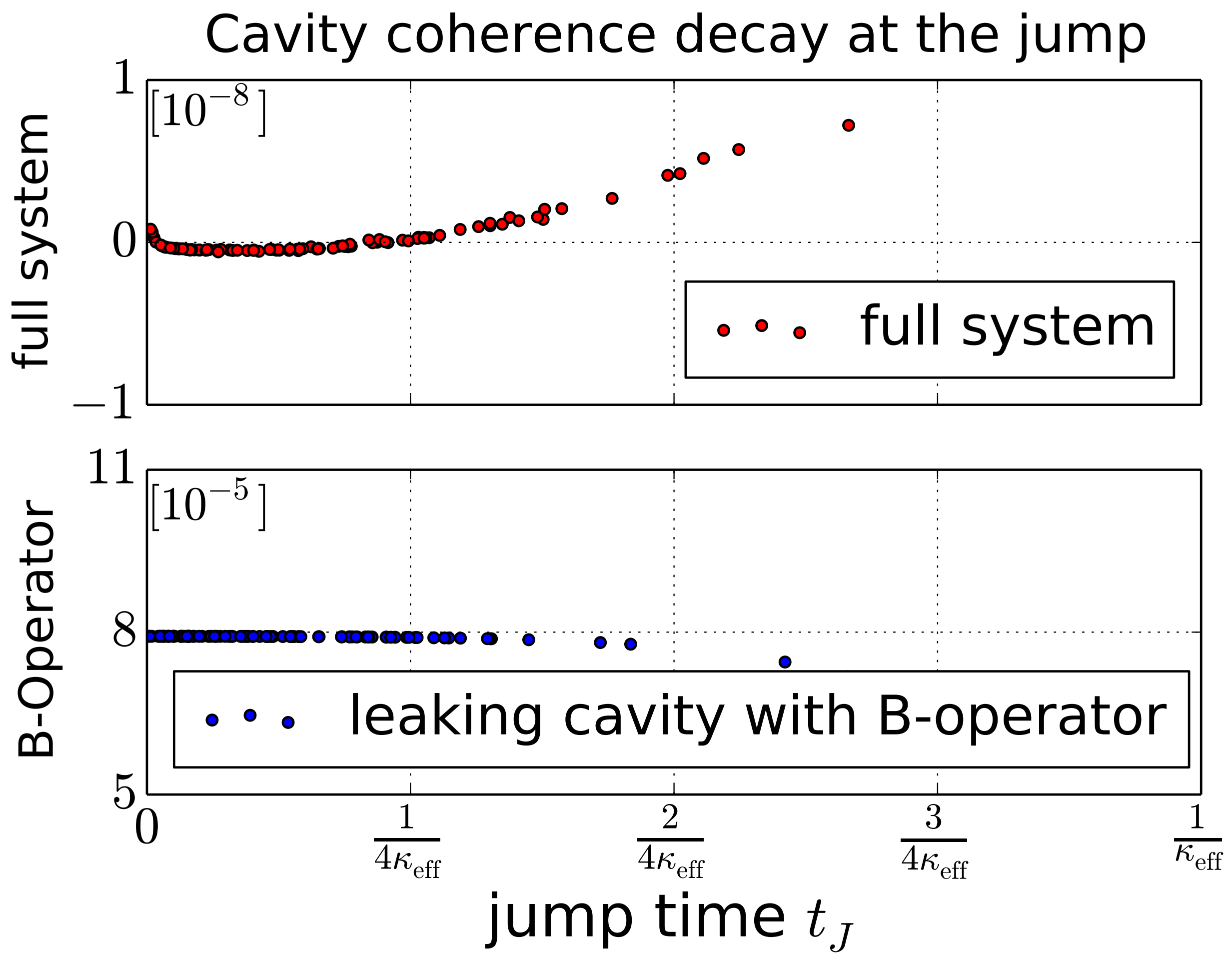

Figure 26: Comparison of the coherence decay $C(|\psi\rangle(t_J - dt) - C(|\psi\rangle(t_J + dt))$ of the full system cavity state and the effective model that decays through the channel $\sqrt{\kappa_{\text{eff}}}B$. The decay is plotted against the jump time t_J. The cavity was set to an initial amplitude $\alpha = 4$.

References

[1] L. C. G. Govia, E. J. Pritchett, C. Xu, B. L. T. Plourde, M. G. Vavilov, F. K. Wilhelm, and R. McDermott, *High-fidelity qubit measurement with a microwave-photon counter*, Physical Review A **90**, 062307 (2014).

[2] L. C. G. Govia, E. J. Pritchett, R. McDermott, and F. K. Wilhelm, *Scaleable two and four qubit parity measurement with a photon counter*, Physical Review A, **92**, 022335 (2015).

[3] S. E. Nigg, *Lecture notes on quantum information processing with superconducting circuits I*, University of Basel (Fruhjahrsemester 2015).

[4] T.C. Ralph, S.D. Bartlett, J.L. O'Brien, G.J. Pryde and H. M. Wiseman, *Quantum Non-demolition Measurements on Qubits*, Physical Review A**73**, 012113 (2006).

[5] M.A. Nielsen and I. L. Chuang. *Quantum computation and quantum information*, Cambridge university press (2010).

[6] A. Sarlette and M. Mirrahimi. *Loss-tolerant parity measurement for distant quantum bits*, arXiv preprint arXiv:1604.04490 (2016).

[7] H.M. Wiseman and G. J. Milburn, *Quantum measurement and control*, Cambridge University Press (2009).

[8] R. R. Ernst, G. Bodenhausen and A. Wokaun, *Principles of nuclear magnetic resonance in one and two dimensions (Vol. 14)*, Oxford: Clarendon Press (1987).

[9] H.J. Carmichael, *Statistical Methods in Quantum Optics 2*, Springer Science & Business Media (2009).

[10] J. Keeling, *Light-matter interactions and quantum optics*, CreateSpace Independent Publishing Platform (2014).

[11] S. J. Devitt, K. Nemoto, and W.J. Munro, *Quantum error correction for beginners*, arXiv:0905.2794 (2009).

[12] D. Gottesman, *A Class of Quantum Error-Correcting Codes Saturating the Quantum Hamming Bound*, Phys. Rev. A, 54:1862 (1996).

[13] B. Vlastakis, et al. *Deterministically encoding quantum information using 100-photon Schrödinger cat states*, Science 342.6158 (2013): 607-610.

[14] L. C. G. Govia, E. J. Pritchett, S. T. Merkel, D. Pineau and F. K. Wilhelm, Phys. Rev. A **86**, 032311 (2012).

[15] K. Jacobs, *Quantum Measurement Theory and its Applications*, Cambridge University Press (2014).

[16] H. P. Breuer and F. Petruccione, *The theory of open quantum systems*, Oxford University Press (2002).

[17] J. Govenius, Y. Matsuzaki, I. G. Savenko, and M. Möttönen, Physical Review A **92**, 042305 (2015).

[18] P. Hümbeli, Master Projektarbeit *On a proposed multi-qubit parity measurement utilizing a current biased Josephson Junction threshold detector* (2015).